PEEP Titration Guided by Esophageal Pressure Monitoring and Electrical Impedance Tomography

Arthur R van Nieuw Amerongen

Master Thesis TU Delft

Supervisors: P. Somhorst MSc and H. Endeman PhD

October 2022

Contents

1 Introduction 3

2 Electrical impedance tomography: methods to titrate PEEP and its evidence 7

3 Esophageal pressure monitoring: methods to titrate PEEP and its evidence 27

4 Filtering circulatory activity from EIT sequences: an algorithm proposal 44

5 Filtering cardiac activity from P_{es} signals: an algorithm proposal 67

6 Filtering cardiac activity from P_{es} signals acquired by a solid-state catheter: an algorithm proposal 73

7 Optimal PEEP guided by EIT versus P_{es} monitoring: a comparative study 74

8 Mechanical ventilation guided by ventilation and circulation: a research proposal 96

9 Conclusions 104

Appendices 105

A Example of filtering P_{aw} and P_{tp} 106

B Evaluation of the effect of removing high PEEP levels on the calculation of optimal PEEP and collapse **107**

Chapter 1

Introduction

Invasive mechanical ventilation is the cornerstone of respiratory failure treatment. Setting ventilator parameters is a balancing act between providing adequate oxygenation and ventilation on the one hand, and minimizing lung damage and adverse cardiovascular effects on the other hand. The application of positive end-expiratory pressure (PEEP) can improve oxygenation and minimizes lung damage by preventing alveolar collapse, but high PEEP levels can induce harmful (regional) hyperinflation and increased vascular resistance [1].

Conventionally, PEEP settings are titrated according to the ARDSnet PEEP/FiO_2 table, which makes PEEP levels depend on oxygen demand [2]. While these target values are practical for clinical use, they do not take into account the large heterogeneity of lung characteristics in mechanically ventilated patients. For example, the percentage of potentially recruitable lung is extremely variable among patients with acute respiratory distress syndrome (ARDS) [1]. Accordingly, higher PEEP application improves outcomes only in a subset of patients [3–5]. This observation demonstrates the need for personalized optimization of ventilator settings.

Advanced bed-side monitoring technologies have the potential to support choosing the right ventilation strategy. Electrical Impedance Tomography (EIT) is such a technology that assesses the distribution of ventilation and perfusion based on impedance changes measured by an electrode belt placed around the thorax [6]. This enables the evaluation of lung collapse, overdistention and recruitability, providing valuable information for PEEP titration [7, 8]. Esophageal pressure (P_{es}) monitoring is a bed-side technology that offers valuable information on the pa-

tient's respiratory mechanics. Since esophageal pressure can be considered as a surrogate of pleural pressure, this monitoring method can distinguish between the pressure drop across the lung parenchyma and across the chest wall [9]. Consequently, PEEP can be titrated such that the end-expiratory transpulmonary pressure remains positive, preventing alveolar collapse [10–12].

With EIT and P_{es} monitoring becoming more available, the question rises what place they should have in clinical decision making. Both methods provide similar information on the patient's lung physiology, but each in a different way. The aim of this thesis is to investigate the clinical implications of these differences for PEEP titration. The analysis of EIT and P_{es} recordings, however, requires advanced pre-processing to isolate respiratory information. Therefore, this thesis also aims to provide solutions for the filtering of undesired information from EIT and P_{es} recordings.

In **chapter 2** and **3**, I describe the technology behind EIT and P_{es} monitoring, as well as how these technologies can be used for PEEP titration and the available clinical evidence. These chapters are taken from the literature review I wrote as part of my graduation.

In **chapter 4**, I propose an algorithm for the suppression of circulatory information in EIT recordings. In **chapter 5**, I propose an adjusted version of the same algorithm, making it suitable to remove cardiac oscillations from P_{es} signals.

In **chapter 7**, I present data on the comparison of PEEP titration guided by EIT and P_{es} monitoring.

Finally, in **chapter 8**, I include a research proposal for a new study investigating how PEEP can be titrated not only based on respiratory information, but also on circulatory information.

References

1. Gattinoni L, Caironi P, Cressoni M, et al. Lung recruitment in patients with the acute respiratory distress syndrome. N Engl J Med 2006;354:1775–86.
2. Brower RG, Lanken PN, MacIntyre N, et al. Higher versus lower positive end-expiratory pressures in patients with the acute respiratory distress syndrome. N Engl J Med 2004;351:327–36.
3. Goligher EC, Kavanagh BP, Rubenfeld GD, et al. Oxygenation response to positive end-expiratory pressure predicts mortality in acute respiratory distress syndrome. A secondary analysis of the LOVS and ExPress trials. Am J Respir Crit Care Med 2014;190:70–6.
4. Guo L, Xie J, Huang Y, et al. Higher PEEP improves outcomes in ARDS patients with clinically objective positive oxygenation response to PEEP: a systematic review and meta-analysis. BMC Anesthesiol 2018;18:172.
5. Walkey AJ, Del Sorbo L, Hodgson CL, et al. Higher PEEP versus Lower PEEP Strategies for Patients with Acute Respiratory Distress Syndrome. A Systematic Review and Meta-Analysis. Ann Am Thorac Soc 2017;14:S297–S303.
6. Frerichs I, Amato MB, Kaam AH van, et al. Chest electrical impedance tomography examination, data analysis, terminology, clinical use and recommendations: consensus statement of the TRanslational EIT developmeNt stuDy group. Thorax 2017;72:83–93.
7. Bachmann MC, Morais C, Bugedo G, et al. Electrical impedance tomography in acute respiratory distress syndrome. Crit Care 2018;22:263.
8. Zhao Z, Chang MY, Chang MY, et al. Positive end-expiratory pressure titration with electrical impedance tomography and pressure-volume curve in severe acute respiratory distress syndrome. Ann Intensive Care 2019;9:7.

9. Akoumianaki E, Maggiore SM, Valenza F, et al. The application of esophageal pressure measurement in patients with respiratory failure. Am J Respir Crit Care Med 2014;189:520–31.

10. Talmor D, Sarge T, Malhotra A, et al. Mechanical ventilation guided by esophageal pressure in acute lung injury. N Engl J Med 2008;359:2095–104.

11. Beitler JR, Sarge T, Banner-Goodspeed VM, et al. Effect of Titrating Positive End-Expiratory Pressure (PEEP) With an Esophageal Pressure-Guided Strategy vs an Empirical High PEEP-Fio2 Strategy on Death and Days Free From Mechanical Ventilation Among Patients With Acute Respiratory Distress Syndrome: A Randomized Clinical Trial. JAMA 2019;321:846–57.

12. Sarge T, Baedorf-Kassis E, Banner-Goodspeed V, et al. Effect of Esophageal Pressure-guided Positive End-Expiratory Pressure on Survival from Acute Respiratory Distress Syndrome: A Risk-based and Mechanistic Reanalysis of the EPVent-2 Trial. Am J Respir Crit Care Med 2021;204:1153–63.

Chapter 2

Electrical impedance tomography: methods to titrate PEEP and its evidence

2.1 The technology

EIT is based on the principle of bioimpedance, which is the ability of tissue to oppose electric current flow [1]. Since air is not a good conductor of electric current, inflated lung tissue has higher impedance than deflated lung tissue. EIT measures the tidal change of thoracic impedance using an electrode belt which is placed around the chest (figure 2.1). A current with high frequency and low amplitude is applied to a pair of electrodes, while the remaining electrode pairs read the resulting voltage change. The location of the current-generating electrode pair changes sequentially along the electrode array (figure 2.2). At the end of one sequence, all electrodes have served as current injectors. This provides sufficient information to reconstruct a 2D image of the distribution of impedance across the chest [2].

EIT images are based on impedance changes relative to a reference time point. Only thorax regions that change their impedance are represented in EIT images. Accordingly, differences in gas and blood content of the thorax can be measured, while preexisting consolidated lung areas, pleural effusions or large bullae cannot be distinguished with EIT [2].

A global EIT waveform can be obtained by summing the relative impedance changes of all pixels and plotting this against time [3]. The tidal oscillation of the waveform shows close

Figure 2.1: Left image: example EIT belt. Right image: patient wearing the EIT belt around the thorax. Images from Draeger (www.draeger.com/Library/Content/EIT-Mini-Manual.pdf)

correlation with tidal volume change as measured by CT (R^2=0.92), demonstrating that EIT is able to monitor ventilation [4]. Also, the change in end-expiratory lung impedance shows strong correlation with a change in end-expiratory lung volume as measured by the nitrogen-washout method (R^2=0.95), demonstrating that EIT is able to monitor changes in aeration [5].

EIT provides diagnostic information through functional images and aggregated measures [6]. *Functional images* are created by applying mathematical operations on the pixel waveforms (i.e. pixel impedance values plotted against time). Probably the most frequently used functional image is the tidal variation image, which is created by calculating the difference between the end-inspiratory and end-expiratory impedance for each individual pixel. By visual expression of the obtained pixel values in a color scale, the tidal variation image intuitively shows which lung regions are ventilated the most. Other functional image examples include the volume-difference image, which compares aeration between two time points, and the ventilation delay image [6]. *Aggregated measures* are values that summarize functional EIT images into one or multiple number(s). Example EIT measures include the anterior/posterior ventilation ratio, the center of ventilation, the global inhomogeneity index and the coefficient of variation [6].

2.2 Methods to titrate PEEP

A literature search was done to evaluate which methods have been described to titrate PEEP using EIT. The PUBMED database was searched using the query

```
("electrical impedance tomography" OR "EIT") AND
```

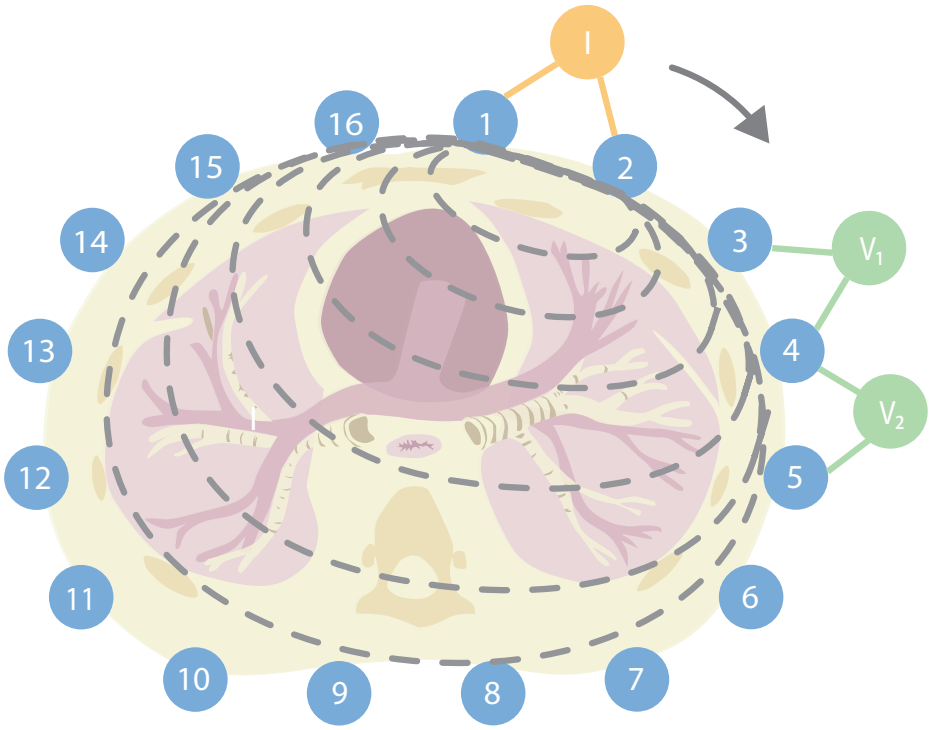

Figure 2.2: Schematic representation of electrodes and electrical current pathways through the thorax. An electrical current (I) is applied to an electrode pair. The other electrode pairs measure the resulting voltage change. The location of the current-generating electrode pair changes sequentially along the electrode array. At the end of one sequence, all electrodes have served as current injectors. Redrawn from [7]

```
("positive end-expiratory pressure" OR "PEEP")
```

The search yielded 240 publications between February 1998 and May 2022. Papers were included that suggest how to choose an 'optimal' PEEP level based on EIT measurements. A total of 52 publications mention such a suggestion, from which 21 suggestions are unique. The suggestions are listed in table 2.1.

Optimal PEEP suggestions could be categorized based on their physiological focus. Categories include collapse, balance between collapse and overdistension, tidal recruitment, dynamic hyperinflation and ventilation distribution.

2.2.1 Collapse

Lung collapse (or: derecruitment) can be monitored by EIT under the assumption that decreasing compliance with decreasing PEEP is a sign of lung collapse. While global compliance can

Focus	Parameter(s)	Abbreviation	Suggested criterium	Suggested by
Collapse	Compliance of most dependent 1/4 layer	C_{reg}	Highest compliance of most dependent 1/4 layer	[8]
	Compliance of dependent region	C_{reg}	Highest compliance of dependent region	[9]
	Stability of EELV	EELV	Stable EELV	[10–13]
Collapse vs. overdistension	Percentage collapsed and overdistended lung tissue, based on compliance	CL; OD	Lowest percentage of overdistended tissue, limiting collapsed tissue to 10%	[7]
			Lowest percentage of overdistended tissue, limiting collapsed tissue to 15%	[14–16]
	Sum of percentage collapsed and overdistend lung tissue, based on compliance	CL+OD	Lowest sum of collapsed and overdistended lung tissue	[11, 13, 15, 17–28]
	Amount of newly aerated pixels compared to ZEEP; amount of pixels not ventilating while aerated	CL; OD	Lowest amount of recruited pixels, without overdistended pixels	[29]
	Ratio of percentage collapsed and overdistended lung tissue, based on compliance	CL/OD	Lowest ratio of collapsed and overdistended lung tissue	[30]
	Percentage pixels with low tidal variation (silent spaces)	SS	Lowest percentage silent spaces	[31, 32]
			<15% silent spaces	[33]
	Percentage pixels with increased tidal variation after PEEP decrease	$d\text{TV}_{pos}$	50% of pixels having increased tidal variation after PEEP decrease	[34]
	Global compliance	C_{glob}	Highest global compliance	[15, 25]
Tidal recruitment	Standard deviation of regional ventilation delay	SD_{RVD}	Lowest standard deviation of pixel regional ventilation delay	[35]
			Onset of rise in standard deviation of pixel regional ventilation delay	[36, 37]
	Percentage of pixels being ventilated but not aerated at end-expiration (cyclic collapse)	CC	Lowest percentage of pixels being ventilated but not aerated at end-expiration	[16]
Dynamic hyperinflation	Standard deviation of regional ventilation delay	SD_{RVD}	Lowest standard deviation of pixel regional ventilation delay	[30, 38]
Ventilation distribution	Global inhomogeneity index	GI index	Lowest global inhomogeneity index	[11, 13, 30, 39]
	Center of ventilation	CoV	Lowest center of ventilation	[30]
			Center of ventilation at 50%	[20, 40, 41]
	Coefficient of variation in tidal variation	CV_{TV}	Lowest SD/mean of tidal variation of six regions	[42]
	Ratio of dependent and non-dependent tidal variation	ITV index	ITV index at 1	[11, 16, 43, 44]

Table 2.1: Suggested PEEP titration methods with the use of EIT. C: compliance; CC: cyclic collapse; CL: collapse; CoV: center of ventilation; CV: coefficient of variation; EELV: end-expiratory lung volume; GI: global inhomogeneity; glob: global; ITV: intratidal ventilation distribution; OD: overdistention; PEEP: positive end-expiratory pressure; pos: positive; reg: regional; RVD: regional ventilation delay; SD: standard deviation; SS: silent spaces; TV: tidal variation; ZEEP: zero end-expiratory pressure

be measured by the ventilator, measuring regional compliance requires regional ventilation monitoring. With EIT, regional compliance can be calculated by dividing a region's impedance change by the driving pressure:

$$\text{Compliance}_{\text{ROI}} = \frac{\Delta Z_{\text{ROI}}}{P_{\text{plateau}} - \text{PEEP}}$$

where ΔZ_{ROI} is the change in impedance of a region of interest during a tidal breath and P_{plateau} is the plateau pressure [7].

Wolf et al. [8] divided the lungs in 4 horizontal layers. Considering that collapse mainly takes place in the dorsal regions, optimal PEEP was suggested to be the PEEP level that shows best compliance in the most dependent layer. During an incremental PEEP trial, PEEP was increased until the layer's compliance did not increase anymore. Then, during a decremental PEEP trial with smaller steps, PEEP was decreased until the layer's compliance began to decrease. Similarly, Ambrisko et al. [9] divided the lungs into an anterior and posterior layer and suggested choosing the PEEP with the highest dependent lung compliance.

Alternatively, setting PEEP to minimize lung collapse can be achieved by aiming for a stable global impedance baseline. Erlandsson et al. [10] were the first to suggest a stable end-expiratory lung impedance as a criterion for optimal PEEP in order to maintain potential beneficial effects of a recruitment maneuver. The method requires visual inspection of the EELI trend during the first few breaths after PEEP change. It assumes that an upward slope indicates recruitment and a downward slope indicates derecruitment. Karsten et al. [11] argued that derecruitment most likely occurs in the dependent lung and suggested setting PEEP at the highest PEEP that shows a downward EELI slope, plus 2 cmH_2O. Eronia et al. [12] suggested to take a longer waiting period of 10 minutes after each PEEP step. EELI trend between 30 seconds and 10 minutes after PEEP change were assessed. If EELI decreased less than 10%, this PEEP level plus 2 cmH2O was suggested as optimal PEEP.

2.2.2 Collapse versus overdistention

Reversing collapse with PEEP has the important limitation that it potentially induces overdistention in other, mainly dependent lung regions [45]. Hence, choosing the PEEP level that optimizes both collapse and overdistention is widely suggested in literature. Costa et al. [7]

described a method to assess collapse and overdistention based on each pixel's compliance. It requires a decremental PEEP trial with constant driving pressure throughout the trial. Accordingly, for each PEEP step, each pixel's compliance can be calculated by dividing the tidal impedance variation with the driving pressure. The method assumes that the driving pressure is uniform across the lungs and that compliance increases towards a maximum along the trial, and decreases afterwards. Decreased compliance at PEEP levels above the maximum compliance is then interpreted as overdistention, while decreased compliance at PEEP levels below the maximum compliance is interpreted as collapse [7].

Initially, Costa et al. suggested to select the PEEP level that shows <10% collapse, regardless of the degree of overdistention [7]. Similarly, Franchineau et al. suggested minimizing overdistention while limiting collapse to <15% [14]. Karsten et al. suggested to choose PEEP with the lowest sum of collapse and overdistention, not limiting collapse to any percentage [11]. Many papers followed this approach, either by choosing the PEEP at the intersection of collapse and overdistention [13, 15, 18–26], by choosing the PEEP level above the intersection [17, 27], or by choosing the PEEP level with the lowest fraction of collapse and overdistention [29].

Bikker et al. [34] introduced a different method of PEEP titration, aiming for a balance between regions with increased compliance and regions with decreased compliance after a PEEP step. It requires PEEP steps of 15, 10, 5 and 0 cmH2O and the computation of compliance maps for each PEEP step. The compliance map of one PEEP step is subtracted from the compliance map of the lower PEEP step. Pixels with a positive change indicate less collapse at the higher PEEP level and pixels with a negative change indicate more overdistention. The optimal PEEP is suggested to be the PEEP level that shows equal amount of pixels with positive and negative difference.

Long et al. [29] introduced a method that classifies pixels for collapse and overdistention, rather than calculating the degree of collapse and overdistention for each pixel. First, the method identifies pixels that participate in ventilation and pixels that are aerated at end-expiration. Then, it defines overdistended pixels as pixels that are not or minimally ventilated, but aerated at end-expiration. Recruited pixels are defined as pixels that are newly aerated at end-expiration compared to PEEP at 2 cmH2O. Optimal PEEP was suggested as the PEEP level which can prevent significant collapse without obvious overdistention. An absolute criterium

was not provided.

Ukere et al. [46] introduced 'silent spaces' as the lung regions with impedance changes <10% of the maximum impedance during tidal ventilation. Silent spaces are indicative for both collapse and overdistention. Contrarily to the methods described by Costa et al. and Long et al, this method does not require a full decremental PEEP trial since silent spaces can be calculated without a reference measurement. Studies suggest optimal PEEP as the PEEP level that shows the lowest percentage of silent spaces [31, 32] or <15% silent spaces [33].

In their comparison with other EIT-based PEEP titration methods, Puel et al. [15] and Soulé et al. [25] mention the possibility to measure the global compliance to optimize between collapse and overdistention. Global compliance can be measured by dividing global tidal impedance variation with driving pressure. In this case, the optimal PEEP is the PEEP level with the lowest global compliance.

2.2.3 Tidal recruitment

Atelectrauma can be an important contributor to ventilator-induced injury. It is caused by repetitive opening and closing of distal airways due to ventilation at low lung volumes [47]. This tidal recruitment of alveoli is associated with higher mortality and can be avoided by providing more PEEP [48]. EIT is able to monitor the time course of regional impedance during breaths and slow inflation maneuvers. Intratidal heterogeneity of impedance changes may be a sign of tidal recruitment [49].

One way to quantify tidal recruitment with EIT is to calculate the regional ventilation delay (RVD) [49]. RVD describes the time that is required for a pixel to reach a certain impedance threshold. Usually, this threshold is set at 40% of the maximal tidal impedance. The delay is usually expressed in percentage time of the total inflation time [50]. To gain an understanding of the presence of tidal recruitment in the total lungs, the standard deviation (SD) of all single-pixel RVD values can be calculated. A higher standard deviation implies would then imply tidal recruitment [49].

Muders et al. [35] suggested to choose the PEEP level that yields the lowest SD of RVD measured using slow inflation maneuvers. In later research papers, the same group suggested to

choose the minimal PEEP level that prevents a progressive increase in SD of RVD [36, 37].

A different way to quantify tidal recruitment with EIT is to identify lung regions that are ventilated during tidal breathing but not aerated at the end of expiration. First, pixels are identified that show, at end-expiration, at least 25% of the maximal impedance change observed in the lungs. These pixels are considered to be aerated at end-expiration. Then, pixels are identified that show, during tidal breathing, at least 20% of the maximal impedance change observed in the lungs. These pixels are considered to contribute to tidal breathing. Pixels that are not aerated at end-expiration but do contribute to tidal breathing are then associated to tidal recruitment [51]. Su et al. [16] suggested to select the PEEP level that minimizes the ratio of tidal recruitment pixels and total amount of tidal breathing pixels.

2.2.4 Dynamic hyperinflation

Dynamic hyperinflation is the increase in (intrinsic) end-expiratory lung volume that may occur in patients with airflow limitation, such as chronic obstructive pulmonary disease and asthma [52]. Titrating PEEP in this condition is important, considering too low PEEP can lead to airway collapse and air trapping, while too high PEEP distends the lungs even further [53].

The RVD can be used to monitor air trapping and dynamic hyperinflation, considering these phenomena introduce heterogeneity of both temporal and spatial ventilation distribution. Kostakou et al. [38] and He et al. [30] have suggested to choose the extrinsic PEEP that yields the lowest SD of RVD.

2.2.5 Ventilation distribution

The distribution of tidal volume is often inhomogeneous in mechanically ventilated patients, especially in ARDS [54]. There can be regions hyperinflated regions, regions that are well aerated, regions that are poorly aerated and regions that are not aerated at all [55]. Lung inhomogeneity is associated with mortality, but can be partly resolved with the application of higher pressures [54]. Accordingly, PEEP titration that minimizes ventilation inhomogeneity potentially may be beneficial for mechanically ventilated patients.

One way to quantify ventilation inhomogeneity is to calculate the global inhomogeneity index (GI) [56]. This index first determines the median tidal ventilation from all pixels. Then, the variation in tidal volume distribution of the total lungs is determined by calculating the sum of of the absolute difference between the median tidal variation and each pixel's tidal variation. Finally, the variation in tidal volume distribution is normalized to the sum of all pixel's tidal variations to make the index comparable between patients:

$$\mathrm{GI}_{lung} = \frac{\sum_{x,y \in lung} |TV_{xy} - \mathrm{median}(TV_{lung})|}{\sum_{x,y \in lung} TV_{xy}}$$

where TV_{xy} is the tidal variation of pixel at row x and column y. Several papers have suggested to choose the PEEP level that yields the lowest GI [11, 13, 30, 39].

Contrarily to the GI, which does not evaluate ventilation distribution in one specific direction, the center of ventilation (CoV) expresses the ventilation distribution along the ventral-dorsal axis [57]. It is defined as the mean of the row sums weighed by the row height:

$$\mathrm{COV}\ (\%) = \frac{1}{N+1} \times \frac{\sum_{x=1}^{N} \sum_{y=1}^{N} y \times TV}{\sum_{x=1}^{N} \sum_{y=1}^{N} TV} \times 100$$

where TV_{xy} is the tidal variation of pixel at column x and row y and N is the number of pixel rows as well as the number of columns (usually 16 or 32) [20]. He et al. [30] suggested to select the PEEP level with the lowest COV (i.e. ventilation predominantly in the dependent lungs). Other papers suggest to titrate PEEP such that the COV equals 50% (i.e. equal dependent and non-dependent ventilation) [20, 40, 41]

Alternatively, the intratidal gas distribution (ITV) was conceptualized by Lowhagen et al. [58] to reveal the temporal distribution of gas during a tidal breath. Based on the global impedance curve, the inspiration is partitioned into 8 iso-volume parts. These volumes can then be dissected into specific regions of interest, such as the dependent and non-dependent lung. For example, this may reveal that the gas is initially distributed primarily to the nondependent lung and later (at higher pressures) to the dependent lung.

Blankman et al. [43] adopted the intratidal gas distribution and conceptualized the ITV-index.

Author, year	Study design	Population	Sample size	Intervention	Main findings
Zhao, 2019 [19]	Prospective vs. historical controls	Severe ARDS	EIT: n = 24 Control: n=31	Costa method vs. 2 cmH2O above LIP of PV-loop	Higher PEEP, higher compliance, lower driving pressure in EIT-group after 2 hours; better hospital survival in EIT-group (67% vs. 48%)
Hsu, 2021 [60]	RCT	Moderate to severe ARDS	EIT: n = 42 Control: n=45	Costa method vs. maximal hysteresis on PV-loop	Lower PEEP in EIT-group after intervention; lower driving pressure in EIT-group after 48 hours; better hospital survival in EIT-group (69% vs. 44%)
He., 2021 [61]	RCT	Mild to severe ARDS	EIT: n = 61 Control: n=56	Costa method vs. PEEP/FiO2 table	No difference in PEEP after intervention; no difference in 28-day mortality, ventilator-free days, length of stay

Table 2.2: Key studies comparing PEEP selection with EIT versus conventional methods. ARDS: acute respiratory distress syndrome; EIT: electrical impedance tomography; LIP: lower inflection point; PEEP: positive end-expiratory pressure; PV: pressure-volume; RCT: randomized controlled trial

This metric sums the 8 dependent volume parts and divides it by the sum of the 8 non-dependent volume parts. An ITV-index of 1 suggest equal ventilation of the dependent and non-depentent lungs. This criterium for optimal PEEP selection was suggested in several studies [11, 16, 44].

Dargaville et al. [42] divided the lung into 3 horizontal layers for both the left and right lung. Optimal PEEP was considered the PEEP that yields the lowest coefficient of variation (SD/mean) in tidal impedance variation for all 6 regions.

2.3 Evidence

In up to two thirds of mechanically ventilated patients, PEEP guided by EIT differs from PEEP guided by conventional methods [21, 23, 27, 59]. This suggests that using EIT can help finding an individualized PEEP that differs from one-size-fits-all methods such as the ARDSNet PEEP/FiO2 table. However, limited evidence exists on the question whether EIT guided PEEP delivers better clinical outcome. Table 2.2 lists the 3 studies that have evaluated clinical outcome against a control group.

All 3 studies compared conventional PEEP titration methods with the Costa method that as-

sesses collapse and overdistention [7]. Optimal EIT PEEP was the PEEP level closest to the crossing point of overdistention and collapse.

Zhao et al. [19] compared EIT guided PEEP level with PEEP at 2 cmH2O above the lower inflection point of the pressure-volume loop. PEEP was prospectively optimized in 24 severe ARDS patients, of which the outcomes were compared with retrospectively collected records of 31 severe ARDS control patients. A higher PEEP level, higher compliance and lower driving pressure was found in the EIT-group 2 hours after the intervention. The authors found a higher survival rate in the EIT-group (67% vs 48%, p=0.18), but this result was not statistically significant.

Hsu et al. [60] compared EIT guided PEEP level with the PEEP level yielding maximal hysteresis on the pressure-volume loop. Moderate to severe ARDS patients were prospectively randomized into the EIT-group (n=42) and the control-group (n=45). EIT suggested a lower PEEP. Driving pressure was lower in the EIT-group after 48 hours. The authors found a higher survival rate in the EIT-group (69% vs 44%, p=0.02).

He et al. [61] compared EIT guided PEEP level with the ARDSNet PEEP/FiO2 table. Mild to severe ARDS patients were prospectively randomized into the EIT-group (n=61) and the control-group (n=56). No difference was found in PEEP after intervention, nor in 28-day mortality.

The fact that the study by He et al. failed to show an improvement in clinical outcome could be explained by the inclusion of mild and rapidly improving ARDS [62, 63]. The studies by Zhao et al. and Hsu et al. compare EIT-guided PEEP and PEEP guided by PV-loops. The contradictory reported effects on titrated PEEP can be explained by the fact that different elements of the PV-loop are used. The lower inflection point is usually located at lower pressures than the point of maximal hysteresis. Of all 3 studies, the study by Hsu et al. is the only to show a higher survival rate with EIT guided PEEP, but its clinical applicability is limited since titration based on the point of maximal hysteresis is seldomly used. Hence, sound evidence is lacking on the clinical superiority of titrating PEEP with the use of EIT.

2.4 Discussion

Concluding, there is a wide variety of methods to titrate PEEP with the use of EIT. Most methods aim at preventing specific conditions that are potentially harmful, such as lung collapse and tidal recruitment. Other methods are less specific, such as methods that optimize the ventilation distribution.

Trying to prevent one ventilation problem carries the risk of eliciting another ventilation problem. This is especially true for minimizing lung collapse. It can be expected that a PEEP level that minimizes lung collapse in the dependent lung induces significant lung overdistention in the non-dependent lung. Simultaneous assessment of collapse and overdistention is therefore warranted. However, debate continues about how much collapse and overdistention should be permitted. It can be argued that overdistention should be avoided primarily, considering studies that suggest overdistention is more harmful than collapse [64–66]. It is unlikely that a future study will be able to prove the superiority of one trade-off over another.

The most investigated method to assess collapse and overdistention is the method described by Costa et al. [7]. This is also the only EIT method for which comparative studies have been carried out. The method comes with the limitation that collapse and overdistention are calculated relative to the highest and lowest PEEP step in a PEEP titration. Accordingly, collapse is underestimated when the lungs are not fully opened at the highest PEEP level and overdistention is underestimated when the lungs have significant overdistention at the lowest PEEP step. The Silent Spaces method does not carry this risk since its calculation can be done for each PEEP-step on its own. No evidence is available on how the Costa method and the Silent Spaces method relate to each other.

EIT has the potential to optimize multiple aspects of lung ventilation. This potential is not utilized when the clinician uses EIT only for minimizing overdistention or tidal recruitment, for example. Optimizing PEEP with EIT for multiple aspects of ventilation can be difficult as it is not always clear which condition should be prioritized. Becher et al. [67] addressed this issue by designing a protocol that combines multiple methods. First, it assesses recruitability by assessing compliance in all regions after a PEEP increase. Then, the driving pressure is halved to test for tidal recruitment (compliance loss) and overdistention (compliance win). Although

this algorithm can be considered complex, it at least provides guidance on how to use EIT for addressing multiple aspects of ventilation. This deserves more exploration in future studies.

Multiple studies compared PEEP guided by EIT with an alternative method. Only one randomized controlled trial used the conventional ARDSNet PEEP/FiO2 table as comparator, but this trial included mild ARDS patients. A similar future randomized controlled trial, but including only moderate to severe ARDS patients, could potentially demonstrate the superiority of EIT in guiding PEEP titration.

References

1. Grimnes S and Martinsen ØG. Introduction. In: *Bioimpedance and Bioelectricity Basics (Third Edition)*. Ed. by Grimnes S and Martinsen ØG. Academic Press, 2015. Chap. 1:1–7.
2. Brown BH. Electrical impedance tomography (EIT): a review. J Med Eng Technol 2003;27:97–108.
3. Bachmann MC, Morais C, Bugedo G, et al. Electrical impedance tomography in acute respiratory distress syndrome. Crit Care 2018;22:263.
4. Victorino JA, Borges JB, Okamoto VN, et al. Imbalances in regional lung ventilation: a validation study on electrical impedance tomography. Am J Respir Crit Care Med 2004;169:791–800.
5. Hinz J, Hahn G, Neumann P, et al. End-expiratory lung impedance change enables bedside monitoring of end-expiratory lung volume change. Intensive Care Med 2003;29:37–43.
6. Frerichs I, Amato MB, Kaam AH van, et al. Chest electrical impedance tomography examination, data analysis, terminology, clinical use and recommendations: consensus statement of the TRanslational EIT developmeNt stuDy group. Thorax 2017;72:83–93.
7. Costa EL, Borges JB, Melo A, et al. Bedside estimation of recruitable alveolar collapse and hyperdistension by electrical impedance tomography. Intensive Care Med 2009;35:1132–7.
8. Wolf GK, Gómez-Laberge C, Rettig JS, et al. Mechanical ventilation guided by electrical impedance tomography in experimental acute lung injury. Crit Care Med 2013;41:1296–304.

9. Ambrisko TD, Schramel J, Hopster K, Kästner S, and Moens Y. Assessment of distribution of ventilation and regional lung compliance by electrical impedance tomography in anaesthetized horses undergoing alveolar recruitment manoeuvres. Vet Anaesth Analg 2017;44:264–72.

10. Erlandsson K, Odenstedt H, Lundin S, and Stenqvist O. Positive end-expiratory pressure optimization using electric impedance tomography in morbidly obese patients during laparoscopic gastric bypass surgery. Acta Anaesthesiol Scand 2006;50:833–9.

11. Karsten J, Grusnick C, Paarmann H, Heringlake M, and Heinze H. Positive end-expiratory pressure titration at bedside using electrical impedance tomography in post-operative cardiac surgery patients. Acta Anaesthesiol Scand 2015;59:723–32.

12. Eronia N, Mauri T, Maffezzini E, et al. Bedside selection of positive end-expiratory pressure by electrical impedance tomography in hypoxemic patients: a feasibility study. Ann Intensive Care 2017;7:76.

13. Zhao Z, Lee LC, Chang MY, et al. The incidence and interpretation of large differences in EIT-based measures for PEEP titration in ARDS patients. J Clin Monit Comput 2020;34:1005–13.

14. Franchineau G, Bréchot N, Lebreton G, et al. Bedside Contribution of Electrical Impedance Tomography to Setting Positive End-Expiratory Pressure for Extracorporeal Membrane Oxygenation-treated Patients with Severe Acute Respiratory Distress Syndrome. Am J Respir Crit Care Med 2017;196:447–57.

15. Puel F, Crognier L, Soulé C, et al. Assessment of electrical impedance tomography to set optimal positive end-expiratory pressure for veno-venous ECMO-treated severe ARDS patients. J Crit Care 2020;60:38–44.

16. Su PL, Lin WC, Ko YF, Cheng KS, and Chen CW. Electrical Impedance Tomography Analysis Between Two Similar Respiratory System Compliance During Decremetal PEEP Titration in ARDS Patients. J Med Biol Eng 2021:1–7.

17. Pereira SM, Tucci MR, Morais CCA, et al. Individual Positive End-expiratory Pressure Settings Optimize Intraoperative Mechanical Ventilation and Reduce Postoperative Atelectasis. Anesthesiology 2018;129:1070–81.

18. Jang GY, Ayoub G, Kim YE, et al. Integrated EIT system for functional lung ventilation imaging. Case. 2019.

19. Zhao Z, Chang MY, Chang MY, et al. Positive end-expiratory pressure titration with electrical impedance tomography and pressure-volume curve in severe acute respiratory distress syndrome. Ann Intensive Care 2019;9:7.

20. Karsten J, Voigt N, Gillmann HJ, and Stueber T. Determination of optimal positive end-expiratory pressure based on respiratory compliance and electrical impedance tomography: a pilot clinical comparative trial. Biomed Tech (Berl) 2019;64:135–45.

21. Heines SJH, Strauch U, Poll MCG van de, Roekaerts P, and Bergmans D. Clinical implementation of electric impedance tomography in the treatment of ARDS: a single centre experience. J Clin Monit Comput 2019;33:291–300.

22. Sella N, Zarantonello F, Andreatta G, Gagliardi V, Boscolo A, and Navalesi P. Positive end-expiratory pressure titration in COVID-19 acute respiratory failure: electrical impedance tomography vs. PEEP/FiO(2) tables. Crit Care 2020;24:540.

23. Bronco A, Grassi A, Meroni V, et al. Clinical value of electrical impedance tomography (EIT) in the management of patients with acute respiratory failure: a single centre experience. Physiol Meas 2021;42.

24. Mlček M, Otáhal M, Borges JB, et al. Targeted lateral positioning decreases lung collapse and overdistension in COVID-19-associated ARDS. BMC Pulm Med 2021;21:133.

25. Soulé C, Crognier L, Puel F, et al. Assessment of Electrical Impedance Tomography to Set Optimal Positive End-Expiratory Pressure for Venoarterial Extracorporeal Membrane Oxygenation-Treated Patients. Crit Care Med 2021;49:923–33.

26. Zhao Z, Zhang JS, Chen YT, et al. The use of electrical impedance tomography for individualized ventilation strategy in COVID-19: a case report. BMC Pulm Med 2021;21:38.

27. Zee P van der, Somhorst P, Endeman H, and Gommers D. Electrical Impedance Tomography for Positive End-Expiratory Pressure Titration in COVID-19-related Acute Respiratory Distress Syndrome. Case. 2020.

28. Di Pierro M, Giani M, Bronco A, et al. Bedside Selection of Positive End Expiratory Pressure by Electrical Impedance Tomography in Patients Undergoing Veno-Venous Extracor-

poreal Membrane Oxygenation Support: A Comparison between COVID-19 ARDS and ARDS from Other Etiologies. J Clin Med 2022;11.

29. Long Y, Liu DW, He HW, and Zhao ZQ. Positive End-expiratory Pressure Titration after Alveolar Recruitment Directed by Electrical Impedance Tomography. Chin Med J (Engl) 2015;128:1421–7.

30. He H, Yuan S, Yi C, Long Y, Zhang R, and Zhao Z. Titration of extra-PEEP against intrinsic-PEEP in severe asthma by electrical impedance tomography: A case report and literature review. Medicine (Baltimore) 2020;99:e20891.

31. Taenaka H, Yoshida T, Hashimoto H, et al. Individualized ventilatory management in patients with COVID-19-associated acute respiratory distress syndrome. Respir Med Case Rep 2021;33:101433.

32. Gibot S, Conrad M, Courte G, and Cravoisy A. Positive End-Expiratory Pressure Setting in COVID-19-Related Acute Respiratory Distress Syndrome: Comparison Between Electrical Impedance Tomography, PEEP/FiO(2) Tables, and Transpulmonary Pressure. Front Med (Lausanne) 2021;8:720920.

33. Scaramuzzo G, Spadaro S, Dalla Corte F, et al. Personalized Positive End-Expiratory Pressure in Acute Respiratory Distress Syndrome: Comparison Between Optimal Distribution of Regional Ventilation and Positive Transpulmonary Pressure. Crit Care Med 2020;48:1148–56.

34. Bikker IG, Leonhardt S, Reis Miranda D, Bakker J, and Gommers D. Bedside measurement of changes in lung impedance to monitor alveolar ventilation in dependent and non-dependent parts by electrical impedance tomography during a positive end-expiratory pressure trial in mechanically ventilated intensive care unit patients. Crit Care 2010;14:R100.

35. Muders T, Hentze B, Simon P, et al. A Modified Method to Assess Tidal Recruitment by Electrical Impedance Tomography. J Clin Med 2019;8.

36. Muders T, Luepschen H, Meier T, et al. Individualized Positive End-expiratory Pressure and Regional Gas Exchange in Porcine Lung Injury. Anesthesiology 2020;132:808–24.

37. Muders T, Hentze B, Kreyer S, et al. Measurement of Electrical Impedance Tomography-Based Regional Ventilation Delay for Individualized Titration of End-Expiratory Pressure. J Clin Med 2021;10.

38. Kostakou E, Barrett N, and Camporota L. Electrical impedance tomography to determine optimal positive end-expiratory pressure in severe chronic obstructive pulmonary disease. Crit Care 2016;20:295.

39. Zhao Z, Steinmann D, Frerichs I, Guttmann J, and Möller K. PEEP titration guided by ventilation homogeneity: a feasibility study using electrical impedance tomography. Crit Care 2010;14:R8.

40. Shono A, Kotani T, and Frerichs I. Personalisation of Therapies in COVID-19 Associated Acute Respiratory Distress Syndrome, Using Electrical Impedance Tomography. J Crit Care Med (Targu Mures) 2021;7:62–6.

41. Yoshida T, Piraino T, Lima CAS, Kavanagh BP, Amato MBP, and Brochard L. Regional Ventilation Displayed by Electrical Impedance Tomography as an Incentive to Decrease Positive End-Expiratory Pressure. Am J Respir Crit Care Med 2019;200:933–7.

42. Dargaville PA, Rimensberger PC, and Frerichs I. Regional tidal ventilation and compliance during a stepwise vital capacity manoeuvre. Intensive Care Med 2010;36:1953–61.

43. Blankman P, Hasan D, Erik G, and Gommers D. Detection of 'best' positive end-expiratory pressure derived from electrical impedance tomography parameters during a decremental positive end-expiratory pressure trial. Crit Care 2014;18:R95.

44. Blankman P, Shono A, Hermans BJ, Wesselius T, Hasan D, and Gommers D. Detection of optimal PEEP for equal distribution of tidal volume by volumetric capnography and electrical impedance tomography during decreasing levels of PEEP in post cardiac-surgery patients. Br J Anaesth 2016;116:862–9.

45. Nieszkowska A, Lu Q, Vieira S, Elman M, Fetita C, and Rouby JJ. Incidence and regional distribution of lung overinflation during mechanical ventilation with positive end-expiratory pressure. Crit Care Med 2004;32:1496–503.

46. Ukere A, Marz A, Wodack KH, et al. Perioperative assessment of regional ventilation during changing body positions and ventilation conditions by electrical impedance tomography. Br J Anaesth 2016;117:228–35.

47. Slutsky AS. Lung injury caused by mechanical ventilation. Chest 1999;116:9S–15S.

48. Caironi P, Cressoni M, Chiumello D, et al. Lung opening and closing during ventilation of acute respiratory distress syndrome. Am J Respir Crit Care Med 2010;181:578–86.

49. Muders T, Luepschen H, Zinserling J, et al. Tidal recruitment assessed by electrical impedance tomography and computed tomography in a porcine model of lung injury*. Crit Care Med 2012;40:903–11.

50. Shono A and Kotani T. Clinical implication of monitoring regional ventilation using electrical impedance tomography. J Intensive Care 2019;7:4.

51. Liu S, Tan L, Moller K, et al. Identification of regional overdistension, recruitment and cyclic alveolar collapse with electrical impedance tomography in an experimental ARDS model. Crit Care 2016;20:119.

52. Calverley PM and Koulouris NG. Flow limitation and dynamic hyperinflation: key concepts in modern respiratory physiology. Eur Respir J 2005;25:186–99.

53. Brandolese R, Broseghini C, Polese G, et al. Effects of intrinsic PEEP on pulmonary gas exchange in mechanically-ventilated patients. Eur Respir J 1993;6:358–63.

54. Cressoni M, Cadringher P, Chiurazzi C, et al. Lung inhomogeneity in patients with acute respiratory distress syndrome. Am J Respir Crit Care Med 2014;189:149–58.

55. Gattinoni L, Tonetti T, and Quintel M. Regional physiology of ARDS. Crit Care 2017;21:312.

56. Zhao Z, Möller K, Steinmann D, and Guttmann J. Global and local inhomogeneity indices of lung ventilation based on electrical impedance tomography. In: *4th European Conference of the International Federation for Medical and Biological Engineering*. Ed. by Vander Sloten J, Verdonck P, Nyssen M, and Haueisen J. Springer Berlin Heidelberg:256–9.

57. Frerichs I, Hahn G, Golisch W, Kurpitz M, Burchardi H, and Hellige G. Monitoring perioperative changes in distribution of pulmonary ventilation by functional electrical impedance tomography. Acta Anaesthesiol Scand 1998;42:721–6.

58. Lowhagen K, Lundin S, and Stenqvist O. Regional intratidal gas distribution in acute lung injury and acute respiratory distress syndrome assessed by electric impedance tomography. Minerva Anestesiol 2010;76:1024–35.

59. Somhorst P, Zee P van der, Endeman H, and Gommers D. PEEP-FiO2 table versus EIT to titrate PEEP in mechanically ventilated patients with COVID-19-related ARDS. Crit Care 2022;26:272.

60. Hsu HJ, Chang HT, Zhao Z, et al. Positive end-expiratory pressure titration with electrical impedance tomography and pressure-volume curve: a randomized trial in moderate to severe ARDS. Physiol Meas 2021;42:014002.

61. He H, Chi Y, Yang Y, et al. Early individualized positive end-expiratory pressure guided by electrical impedance tomography in acute respiratory distress syndrome: a randomized controlled clinical trial. Crit Care 2021;25:230.

62. Schenck EJ, Oromendia C, Torres LK, Berlin DA, Choi AMK, and Siempos I. Rapidly Improving ARDS in Therapeutic Randomized Controlled Trials. Chest 2019;155:474–82.

63. Jimenez JV, Weirauch AJ, Culter CA, Choi PJ, and Hyzy RC. Electrical Impedance Tomography in Acute Respiratory Distress Syndrome Management. Crit Care Med 2022;50:1210–23.

64. Bellani G, Guerra L, Musch G, et al. Lung regional metabolic activity and gas volume changes induced by tidal ventilation in patients with acute lung injury. Am J Respir Crit Care Med 2011;183:1193–9.

65. Writing Group for the Alveolar Recruitment for Acute Respiratory Distress Syndrome Trial I, Cavalcanti AB, Suzumura EA, et al. Effect of Lung Recruitment and Titrated Positive End-Expiratory Pressure (PEEP) vs Low PEEP on Mortality in Patients With Acute Respiratory Distress Syndrome: A Randomized Clinical Trial. JAMA 2017;318:1335–45.

66. Gattinoni L, Quintel M, and Marini JJ. Volutrauma and atelectrauma: which is worse? Crit Care 2018;22:264.

67. Becher T, Buchholz V, Hassel D, et al. Individualization of PEEP and tidal volume in ARDS patients with electrical impedance tomography: a pilot feasibility study. Ann Intensive Care 2021;11:89.

Chapter 3

Esophageal pressure monitoring: methods to titrate PEEP and its evidence

3.1 The technology

Esophageal pressure monitoring requires the insertion of a balloon catheter in the lower third of the esophagus [1]. Changes in pleural pressure are largely transmitted through the esophageal wall, which acts as a passive membrane. Therefore, esophageal pressure can be used as a surrogate pressure for the pleural pressure in the proximity of the balloon [2].

Due to the gravitational pressure gradient, the pleural pressure in the most dependent lung is higher than the esophageal pressure, whereas the pleural pressure in the most non-dependent lung is lower. Generally, esophageal pressure is considered to correspond with the pleural pressure in the middle of the gravitational plane [2, 3]

The rationale for estimating pleural pressure is to separate the pressure applied to the respiratory system (P_{rs}) into the part that distends the lung (transpulmonary pressure, P_L), and the part that distends the chest wall (P_{cw}) [4]:

$$P_{rs} = P_L + P_{cw} \tag{3.1.1}$$

Figure 3.1: Example esophageal catheter. The balloon itself is located a few centimeters from the catheter tip. Image from CooperSurgical (coopersurgical.com/detail/esophageal-balloon-catheter-set/)

The respiratory system pressure can also be expressed as the pressure difference between the airway opening and the body surface:

$$P_{rs} = P_{aw} - P_{atm} \tag{3.1.2}$$

where P_{aw} is the airway pressure and P_{atm} is the atmospheric pressure.

Considering that the pleural cavity finds itself between the lungs and the chest wall, the transpulmonary pressure is the difference between the airway opening pressure and the pleural pressure.

$$P_L = P_{aw} - P_{pl} \tag{3.1.3}$$

Similarly, the pressure across the chest wall is the difference between the pleural pressure and the atmospheric pressure:

$$P_{cw} = P_{pl} - P_{atm} \tag{3.1.4}$$

Substituting equation (3.1.3) and (3.1.4) in (3.1.1), the pressure across the respiratory system at zero flow is

$$P_{rs} = (P_{aw} - P_{pl}) + (P_{pl} - P_{atm}) \tag{3.1.5}$$

which is similar to equation (3.1.2), but now the pleural pressure splits the respiratory system pressure into two parts that are clinically relevant.

The distribution of applied airway pressure depends on the elastance properties of both the lungs and the chest wall, which can vary significantly among patients, especially among ARDS patients [5]. Increased intra-abdominal pressure, ascites and intrathoracic edema are examples that increase the chest wall elastance [1]. As a result, different patients may experience varying transpulmonary pressures while they share the same airway pressure. This is important to consider when choosing ventilator settings, because transpulmonary pressure should be adequate to open the lungs, but should be limited at the same time to prevent harmful stress [6].

3.2 Methods to titrate PEEP

A literature search was done to evaluate which methods have been described to titrate PEEP using esophageal pressure monitoring. The PUBMED database was searched using the query

```
(optimal OR best OR select* OR titrat*) AND (PEEP OR positive
end-expiratory pressure) AND (transpulmonary OR esophageal)
```

The search yielded 263 publications between August 1970 and May 2022. Papers were included that suggested how to choose an 'optimal' PEEP level based on esophageal pressure measurements. A total of 27 publications mention such a suggestion, from which 12 suggestions are unique. The suggestions are listed in table 3.1.

Two different methods of transpulmonary pressure determination emerge from the literature. The first method is referred to as the 'absolute esophageal pressure' method and is the most often reported method. The second method is referred to as the 'elastance derived method'.

3.2.1 Absolute esophageal pressure

The absolute esophageal pressure method assumes that the esophageal pressure can be directly used as a surrogate of pleural pressure:

$$P_{pl} \approx P_{es} \tag{3.2.1}$$

Then, the transpulmonary pressure is calculated as follows:

$$P_L = P_{aw} - P_{es} \tag{3.2.2}$$

As mentioned before, the physiologic rationale for estimating the transpulmonary pressure for choosing ventilator settings is to ensure that transpulmonary pressure is high enough to maintain open lungs and low enough to prevent harmful overdistention. The most studies that propose using the absolute esophageal pressure method, aim at the first: titrating PEEP in such way that the transpulmonary pressure is zero or positive at the end of expiration [4, 7–11, 13–25, 33].

The choice of taking zero end-expiratory transpulmonary pressure as a lower cut-off is based on (sensible) observations that the amount of nonaerated tissue starts to increase significantly

Method	Target parameter	Target	Suggested by
Absolute esophageal pressure	End-expiratory transpulmonary pressure	$P_{L,EE} = 0$	[7–11]
		$P_{L,EE} \geq 0$	[12, 13]
		$0 \leq P_{L,EE} \leq 2$	[14, 15]
		$0 \leq P_{L,EE} \leq 5$	[16–18]
		$0 \leq P_{L,EE} \leq 6$	[19, 20]
		$0 \leq P_{L,EE} \leq 10$	[4, 21–25]
		$-1 \leq P_{L,EE} \leq 1$	[26]
		$-2 \leq P_{L,EE} \leq 2$	[27, 28]
		$-3 \leq P_{L,EE} \leq 3$	[29]
	Transpulmonary driving pressure	Lowest ΔP_L	[30]
Elastance ratio	Transpulmonary plateau pressure	$P_{L,PLAT} = 25$	[9, 31]
		$P_{L,PLAT} = 26$	[32]

Table 3.1: Suggested PEEP titration methods with the use of esophageal pressure monitoring. All pressures are expressed in cmH_2O. P_L: transpulmonary pressure; $P_{L,EE}$: end-expiratory transpulmonary pressure; $P_{L,PLAT}$: transpulmonary plateau pressure

when the end-expiratory transalveolar pressure becomes negative[1], i.e. when the pressure imposed on alveoli from outside is larger than the pressure inside the alveoli [34, 35]. Under the condition of zero flow, the airway pressure equals the alveolar pressure and transalveolar pressure and transpulmonary pressure are interchangeable [36]. Thus, similarly, it can be expected that lung collapse starts to increase significantly when the end-expiratory transpulmonary pressure becomes negative.

Other papers suggest an end-expiratory transpulmonary pressure of $\pm$ 1 [26], $\pm$ 2 [27, 28] or $\pm$ 3 cmH_2O [29]. These intervals are mainly chosen pragmatically to strive for an end-expiratory transpulmonary pressure close to 0. This does not hold true for the $\pm$ 2 cmH_2O interval which was based on clinical evidence as reported by Sarge et al [27], which will be discussed later.

In contrast to the lower cut-off values, the upper cut-offs vary widely. Two rationales can be distinguished. The first aims to keep the end-expiratory transpulmonary pressure as close to 0 as possible and therefore limits the pressure to a maximum of around 2 cmH_2O. The second connects the end-transpulmonary pressure to the oxygen demand, similar to the ARDSNet PEEP/FiO2 table [37], and allows the end-expiratory transpulmonary pressure to take higher values such as 6 cmH_2O [19] or 10 cmH_2O [4].

One animal study took a different approach in which the transpulmonary driving pressure determined the optimal PEEP level [30]. During a decremental PEEP trial, for each PEEP step of 1 cmH_2O the difference between end-inspiratory and end-expiratory transpulmonary pressure was calculated. The mechanical ventilator was set at volume-controlled ventilation. The PEEP level yielding the lowest driving pressure was considered optimal.

3.2.2 Elastance derived method

The elastance derived transpulmonary pressure method does not directly use the esophageal pressure as a surrogate for pleural pressure, but relies on the tidal swing of esophageal pressure to estimate the chest wall elastance and then calculates the pleural pressure [6].

Similar to the respiratory system pressure, the respiratory system elastance can be separated

[1] In their papers, Pelosi et al. [34] and Crotti et al. [35] use $P_{pl} - P_{alv}$ as the definition for transalveolar pressure and therefore report a positive transalveolar pressure instead of negative. For clarity reasons, and to adhere to the definitions by Loring et al. [36], I use $P_{alv} - P_{pl}$ as definition for transalveolar pressure.

into the elastance of the lung and the elastance of the chest wall:

$$E_{rs} = E_{lung} + E_{cw} \tag{3.2.3}$$

The elastance of the respiratory system can be expressed as the airway pressure needed to inflate the respiratory system:

$$E_{rs} = \frac{\Delta P_{aw}}{\Delta V} \tag{3.2.4}$$

where V is the inspired volume.

The elastance of the chest wall can be expressed as the pressure across the chest wall needed to inflate the thorax:

$$E_{cw} = \frac{\Delta P_{cw}}{\Delta V} \tag{3.2.5}$$

Equation (3.1.4) described the chest wall pressure as the difference between the pleural pressure and the atmospheric pressure. Under the condition that all pressures are expressed relative to atmospheric pressure, the atmospheric pressure is 0 so that

$$P_{cw} = P_{pl} \tag{3.2.6}$$

Substituting equation (3.2.6) into (3.2.5) yields

$$E_{cw} = \frac{\Delta P_{pl}}{\Delta V} \tag{3.2.7}$$

Considering that the volumes of the respiratory system and the chest wall are the same, the ratio of the chest wall pressure and the respiratory system pressure equals the ratio of the corresponding elastances:

$$\frac{\Delta P_{pl}}{\Delta P_{aw}} = \frac{E_{cw}}{E_{rs}} \tag{3.2.8}$$

which is often referred to as the elastance ratio [6].

Finally, considering that

$$\Delta P_{pl} = \Delta P_{aw} \times \frac{\Delta P_{pl}}{\Delta P_{aw}} \tag{3.2.9}$$

substituting (3.2.8) into (3.2.9) yields

$$\Delta P_{pl} = \Delta P_{aw} \times \frac{E_{cw}}{E_{rs}} \tag{3.2.10}$$

and the transpulmonary pressure can be estimated by substituting (3.2.10) in (3.1.3):

$$\Delta P_L = \Delta P_{aw} - \Delta P_{aw} \times \frac{E_{cw}}{E_{rs}} \tag{3.2.11}$$

If it is assumed that the transpulmonary pressure is zero at functional residual pressure, then the pleural pressure must be zero because no airway pressure is applied. In that case, the following representation of transpulmonary pressure is valid:

$$P_L = P_{aw} - P_{aw} \times \frac{E_{cw}}{E_{rs}} \tag{3.2.12}$$

When the difference in esophageal pressure is taken as a surrogate for the difference in pleural pressure, so that

$$E_{cw} = \frac{\Delta P_{es}}{\Delta V} \tag{3.2.13}$$

then it follows from (3.2.12) that the transpulmonary pressure can be calculated for every airway pressure if only the chest wall elastance is estimated once by measuring the esophageal

pressure at two volumes.

In healthy individuals, the elastance ratio is believed to be close to 0.5, while in ARDS patients ratios between 0.2 (high lung elastance) and 0.8 (high chest wall elastance or low lung elastance or both) have been found [6].

Two studies reported on the use of the elastance derived transpulmonary pressure. In contrast to the studies using absolute esophageal pressure, these studies assessed the transpulmonary pressure to find a PEEP that limits overdistention rather than prevents collapse.

Grasso et al. [31] evaluated the transpulmonary plateau pressure in patients that were referred to an extracorporeal membrane oxygenation (ECMO) center because conventional mechanical ventilation failed. When the transpulmonary plateau pressure was higher than 25 cmH_2O, patients received ECMO support. But when the transpulmonary plateau pressure was lower than 25 cmH_2O, PEEP was increased until the threshold of 25 cmH_2O was reached. After 30 minutes, the ECMO criteria were re-evaluated. Staffieri et al. [32] went one step further in suggesting to titrate PEEP in *all* ARDS patients based on a transpulmonary plateau pressure of 26 cmH_2O, as an alternative to the open lung approach that titrates PEEP to an airway plateau pressure of 30 cmH_2O.

3.3 Evidence

Multiple clinical studies report improved lung mechanics and oxygenation when PEEP is guided by esophageal pressure monitoring [14, 17, 20–22, 28]. This suggests that esophageal pressure monitoring can help finding an individualized PEEP that differs from one-size-fits-all methods such as the ARDSNet PEEP/FiO2 table. However, limited evidence exists on the question whether transpulmonary pressure guided PEEP leads to improved clinical outcome. Table 3.2 lists 2 randomized controlled trials that compared P_{es} guided PEEP to PEEP/FiO2 table guided PEEP.

In a single-center trial, Talmor et al. included ARDS patients with PaO2/FiO2 $\leq$ 200 mmHg [4] (EPVent 1). In both the experimental arm and the control arm, the oxygenation goal was to keep the PaO2 level between 55 and 120 mmHg. In the experimental arm, PEEP was titrated

Author, year	Study design	Population	Sample size	Intervention	Main findings
Talmor, 2008 [4]	RCT	ARDS*	P_{es}: n=30 Control: n=31	$0 \leq P_{TP,EE} \leq 10$ cmH_2O vs. lower PEEP / higher FiO2 table	Higher PaO2/FiO2 and C_{RS} at 24, 48, 72 hours in P_{es} group Lower 28-day mortality in P_{es} group (17% vs. 39%)
Beitler, 2019 [19]	RCT	Moderate to severe ARDS**	P_{es}: n=102 Control: n=98	$0 \leq P_{TP,EE} \leq 6$ cmH_2O vs. higher PEEP / lower FiO2 table	No difference in 28-day mortality (32% vs. 31%)

Table 3.2: Key studies comparing PEEP selection with P_{es} versus PEEP/FiO2 table. *: According to The American-European Consensus Conference on ARDS (PaO2/FiO2 $\leq$ 200 mmHg) [38]. **: According to the Berlin criteria [39]. ARDS: acute respiratory distress syndrome; C_{RS}: respiratory system compliance; $P_{TP,EE}$: end-expiratory transpulmonary pressure; RCT: randomized controlled trial

according to a sliding scale allowing either FiO2 level or end-expiratory transpulmonary pressure to be increased at a time. Possible end-expiratory transpulmonary pressure values ranged between 0 and 10 cmH_2O. Transpulmonary plateau pressure values were limited to 25 cmH_2O. In the control arm, PEEP was titrated according to the conventional ARDSNet PEEP/FiO2 table [40]. After 72 hours, PEEP values were significantly higher in the experimental arm (17$\pm$6 vs 10$\pm$4 cmH_2O, p<0.001). PaO2/FiO2 ratios were significantly lower in the experimental arm (280$\pm$126 vs 191$\pm$71, p<0.002). End-expiratory transpulmonary pressures were lower in the experimental arm (0.1$\pm$2.6 vs -2.0$\pm$4.7 cmH_2O, p=0.06). 28-day mortality was lower in the experimental arm (17% vs 39%, p<0.055), but this result was not statistically significant.

In a later study, the same group investigated clinical outcome in a similar patient group but with several protocol adjustments [19] (EPVent 2). In the experimental arm, PEEP was titrated according to an adjusted sliding scale with 6 cmH_2O of end-expiratory transpulmonary pressure as the upper limit. In the control arm, PEEP was titrated according to the higher PEEP/lower FiO2 table, as adopted from the ALVEOLI trial [37]. Moreover, intervention time was extended from 3 to 28 days compared to EPVent 1.

The EPVent 2 trial found no difference in 28-day mortality between the P_{es} guided arm and the control arm (33% vs 30%, p<0.88). Importantly, the resulting end-expiratory transpulmonary pressures did not differ between both arms. Therefore, the study was not able to test the hypothesis that titrating PEEP to maintain positive end-expiratory transpulmonary pressure improves clinical outcome.

In a post-hoc reanalysis of the EPVent 2 trial, Sarge et al. [27] found that 28-day and 60-day mor-

tality was lower for the P_{es} guided PEEP strategy among patients with a lower Acute Physiology and Chronic Health Evaluation-II (APACHE-II) score and higher for patients with a higher APACHE-II score. Moreover, independent of the treatment arm to which patients were allocated, mortality was lowest when PEEP titration resulted in an end-expiratory transpulmonary pressure between -2 and 2 cmH_2O. The hazard ratio for mortality was 1.10 (95% CI 1.01-1.21) for each 1 cmH_2O increase or decrease from zero end-expiratory transpulmonary pressure.

3.4 Discussion

Concluding, esophageal pressure monitoring can be used to titrate PEEP by estimating and optimizing the transpulmonary pressure. Two main methods for estimating transpulmonary pressure can be distinguished. The absolute method directly takes esophageal pressure as a surrogate for pleural pressure. The resulting transpulmonary pressure can be titrated to be close to zero at end-expiration, which is the most often suggested method in literature. The elastance derived method uses esophageal pressure to estimate the chest wall elastance, which is then used to estimate how much of the airway pressure dissipates into the lungs and the chest wall. The resulting transpulmonary pressure is titrated to be around 25 cmH_2O at end-inspiration.

There is a clear rationale why the absolute method is used to titrate transpulmonary pressure at end-expiration to limit collapse and the elastance derived method is used to titrate transpulmonary pressure at end-inspiration to limit overdistention. The pressure in the esophagus has been demonstrated to be closer to the pleural pressure of the dorsal lung, which is the place where lung collapse starts due to the gravitational gradient [3]. Alternatively, the elastance derived estimation of pleural pressure has been demonstrated to be closer to the ventral lung, the place where lung overdistention takes place first [3].

This reveals an important limitation of P_{es} monitoring as it provides information from only one location in the lungs. A positive end-expiratory transpulmonary pressure does not preclude lung collapse since the transpulmonary pressure may be negative dorsal to the esophagus. Moreover, it potentially induces harmful overdistention at the lungs ventral to the esophagus. This can be mitigated by the simultaneous limitation of plateau pressure. A commonly used

upper limit is a transpulmonary plateau pressure of 25 cmH_2O [4, 19], which could serve as a more physiologic alternative to the commonly used upper airway plateau pressure limit of 30 cmH_2O. However, especially in heterogeneous lungs, the pleural pressure at the ventral lungs may be considerably lower compared to the esophageal pressure, resulting in the underestimation of ventral transpulmonary plateau pressure.

Gulati et al. [9] demonstrated that the two estimation methods cannot be used interchangeably. The estimation of pleural pressure differed as much as 10 cmH_2O and the PEEP levels recommended by both methods seemed unrelated. Importantly, the study also showed that chest wall and respiratory system elastances could vary unpredictably with changes in PEEP. The elastance derived method assumes that the chest wall and respiratory system elastance are constant at different pressures and that the ratio between the elastances is constant. The data presented by Gulati et al. suggest that these assumptions are not valid, which could explain the lack of correlation between both method's recommended PEEP level.

Available evidence on clinical outcome is limited to the absolute esophageal pressure method. The most important limitations of the EPVent 1 trial are the fact that the study was underpowered for testing clinical outcome, that the study stopped early when a positive effect of P_{es} guided PEEP was noticed, and that there was a high proportion of surgical patients. The most important limitation of the EPVent 2 trial is the fact that both interventions resulted in similar end-expiratory transpulmonary pressure so that the hypothesis could not be tested.

The post-hoc reanalysis of the EPVent 2 trial did show better survival for more severely ill patients and patients in whom the resulting transpulmonary pressure was between -2 and 2 cmH_2O. However, there are several reasons to interpret these results with caution. First, the reanalysis was done after trial completion. Secondly, the clinical implication of the fact that the end-expiratory transpulmonary pressure did not differ between both treatment arms should be questioned. It is valuable to know that an end-expiratory transpulmonary pressure close to 0 is associated with lower mortality, but that does not directly support the use of P_{es} monitoring since the effect was found in both treatment arms. Still, the finding that patients with a higher APACHE-II score benefitted from P_{es} guided PEEP is a strong suggestion that P_{es} monitoring should be indicated for specific patient subgroups. Future prospective clinical trials should therefore attempt to establish the patient population that most likely benefits from P_{es}

monitoring.

References

1. Akoumianaki E, Maggiore SM, Valenza F, et al. The application of esophageal pressure measurement in patients with respiratory failure. Am J Respir Crit Care Med 2014;189:520–31.
2. Umbrello M and Chiumello D. Interpretation of the transpulmonary pressure in the critically ill patient. Ann Transl Med 2018;6:383.
3. Yoshida T, Amato MBP, Grieco DL, et al. Esophageal Manometry and Regional Transpulmonary Pressure in Lung Injury. Am J Respir Crit Care Med 2018;197:1018–26.
4. Talmor D, Sarge T, Malhotra A, et al. Mechanical ventilation guided by esophageal pressure in acute lung injury. N Engl J Med 2008;359:2095–104.
5. Chiumello D, Carlesso E, Cadringher P, et al. Lung stress and strain during mechanical ventilation for acute respiratory distress syndrome. Am J Respir Crit Care Med 2008;178:346–55.
6. Gattinoni L, Vagginelli F, Chiumello D, Taccone P, and Carlesso E. Physiologic rationale for ventilator setting in acute lung injury/acute respiratory distress syndrome patients. Crit Care Med 2003;31:S300–4.
7. Piraino T and Cook DJ. Optimal PEEP guided by esophageal balloon manometry. Respir Care 2011;56:510–3.
8. Rodriguez PO, Bonelli I, Setten M, et al. Transpulmonary pressure and gas exchange during decremental PEEP titration in pulmonary ARDS patients. Respir Care 2013;58:754–63.
9. Gulati G, Novero A, Loring SH, and Talmor D. Pleural pressure and optimal positive end-expiratory pressure based on esophageal pressure versus chest wall elastance: incompatible results*. Crit Care Med 2013;41:1951–7.

10. Chiumello D, Cressoni M, Carlesso E, et al. Bedside selection of positive end-expiratory pressure in mild, moderate, and severe acute respiratory distress syndrome. Crit Care Med 2014;42:252–64.

11. Alvey NJ, Hlaing M, Piccoli J, Kukreja N, and Tran TT. Positive end-expiratory pressure titration via esophageal balloon monitoring in a morbidly obese patient undergoing laparoscopic nephrectomy. Can J Anaesth 2020;67:1086–7.

12. Bikker IG, Blankman P, Specht P, Bakker J, and Gommers D. Global and regional parameters to visualize the 'best' PEEP during a PEEP trial in a porcine model with and without acute lung injury. Minerva Anestesiol 2013;79:983–92.

13. Loring SH, Pecchiari M, Della Valle P, Monaco A, Gentile G, and D'Angelo E. Maintaining end-expiratory transpulmonary pressure prevents worsening of ventilator-induced lung injury caused by chest wall constriction in surfactant-depleted rats. Crit Care Med 2010;38:2358–64.

14. Pirrone M, Fisher D, Chipman D, et al. Recruitment Maneuvers and Positive End-Expiratory Pressure Titration in Morbidly Obese ICU Patients. Crit Care Med 2016;44:300–7.

15. Fumagalli J, Santiago RRS, Teggia Droghi M, et al. Lung Recruitment in Obese Patients with Acute Respiratory Distress Syndrome. Anesthesiology 2019;130:791–803.

16. Obi ON, Mazer M, Bangley C, et al. Obesity and Weaning from Mechanical Ventilation-An Exploratory Study. Clin Med Insights Circ Respir Pulm Med 2018;12:1179548418801004.

17. Bergez M, Fritsch N, Tran-Van D, et al. PEEP titration in moderate to severe ARDS: plateau versus transpulmonary pressure. Ann Intensive Care 2019;9:81.

18. Sy E, Rao J, Zacharias S, Ronco JJ, and Lee JS. Esophageal Balloon-Directed Ventilator Management for Postpneumonectomy Acute Respiratory Distress Syndrome. Case Rep Crit Care 2021;2021:6678080.

19. Beitler JR, Sarge T, Banner-Goodspeed VM, et al. Effect of Titrating Positive End-Expiratory Pressure (PEEP) With an Esophageal Pressure-Guided Strategy vs an Empirical High PEEP-Fio2 Strategy on Death and Days Free From Mechanical Ventilation Among Patients With Acute Respiratory Distress Syndrome: A Randomized Clinical Trial. JAMA 2019;321:846–57.

20. Boesing C, Graf PT, Schmitt F, et al. Effects of different positive end-expiratory pressure titration strategies during prone positioning in patients with acute respiratory distress syndrome: a prospective interventional study. Crit Care 2022;26:82.

21. Yang Y, Li Y, Liu SQ, et al. Positive end expiratory pressure titrated by transpulmonary pressure improved oxygenation and respiratory mechanics in acute respiratory distress syndrome patients with intra-abdominal hypertension. Chin Med J (Engl) 2013;126:3234–9.

22. Baedorf Kassis E, Loring SH, and Talmor D. Mortality and pulmonary mechanics in relation to respiratory system and transpulmonary driving pressures in ARDS. Intensive Care Med 2016;42:1206–13.

23. Wang B, Wu B, and Ran YN. A clinical study on mechanical ventilation PEEP setting for traumatic ARDS patients guided by esophageal pressure. Technol Health Care 2019;27:37–47.

24. Wu X, Zheng R, and Zhuang Z. Effect of transpulmonary pressure-guided positive end-expiratory pressure titration on lung injury in pigs with acute respiratory distress syndrome. J Clin Monit Comput 2020;34:151–9.

25. Scaramuzzo G, Spadaro S, Dalla Corte F, et al. Personalized Positive End-Expiratory Pressure in Acute Respiratory Distress Syndrome: Comparison Between Optimal Distribution of Regional Ventilation and Positive Transpulmonary Pressure. Crit Care Med 2020;48:1148–56.

26. Eichler L, Truskowska K, Dupree A, Busch P, Goetz AE, and Zöllner C. Intraoperative Ventilation of Morbidly Obese Patients Guided by Transpulmonary Pressure. Obes Surg 2018;28:122–9.

27. Sarge T, Baedorf-Kassis E, Banner-Goodspeed V, et al. Effect of Esophageal Pressure-guided Positive End-Expiratory Pressure on Survival from Acute Respiratory Distress Syndrome: A Risk-based and Mechanistic Reanalysis of the EPVent-2 Trial. Am J Respir Crit Care Med 2021;204:1153–63.

28. Liou J, Doherty D, Gillin T, et al. Retrospective Review of Transpulmonary Pressure Guided Positive End-Expiratory Pressure Titration for Mechanical Ventilation in Class II and III Obesity. Crit Care Explor 2022;4:e0690.

29. Spina S, Capriles M, De Santis Santiago R, et al. Development of a Lung Rescue Team to Improve Care of Subjects With Refractory Acute Respiratory Failure. Respir Care 2020;65:420–6.

30. Scaramuzzo G, Ball L, Pino F, et al. Influence of Positive End-Expiratory Pressure Titration on the Effects of Pronation in Acute Respiratory Distress Syndrome: A Comprehensive Experimental Study. Front Physiol 2020;11:179.

31. Grasso S, Terragni P, Birocco A, et al. ECMO criteria for influenza A (H1N1)-associated ARDS: role of transpulmonary pressure. Intensive Care Med 2012;38:395–403.

32. Staffieri F, Stripoli T, De Monte V, et al. Physiological effects of an open lung ventilatory strategy titrated on elastance-derived end-inspiratory transpulmonary pressure: study in a pig model*. Crit Care Med 2012;40:2124–31.

33. Bikker IG, Leonhardt S, Reis Miranda D, Bakker J, and Gommers D. Bedside measurement of changes in lung impedance to monitor alveolar ventilation in dependent and non-dependent parts by electrical impedance tomography during a positive end-expiratory pressure trial in mechanically ventilated intensive care unit patients. Crit Care 2010;14:R100.

34. Pelosi P, Goldner M, McKibben A, et al. Recruitment and derecruitment during acute respiratory failure: an experimental study. Am J Respir Crit Care Med 2001;164:122–30.

35. Crotti S, Mascheroni D, Caironi P, et al. Recruitment and derecruitment during acute respiratory failure: a clinical study. Am J Respir Crit Care Med 2001;164:131–40.

36. Loring SH, Topulos GP, and Hubmayr RD. Transpulmonary Pressure: The Importance of Precise Definitions and Limiting Assumptions. Am J Respir Crit Care Med 2016;194:1452–7.

37. Brower RG, Lanken PN, MacIntyre N, et al. Higher versus lower positive end-expiratory pressures in patients with the acute respiratory distress syndrome. N Engl J Med 2004;351:327–36.

38. Bernard GR, Artigas A, Brigham KL, et al. The American-European Consensus Conference on ARDS. Definitions, mechanisms, relevant outcomes, and clinical trial coordination. Am J Respir Crit Care Med 1994;149:818–24.

39. Force ADT, Ranieri VM, Rubenfeld GD, et al. Acute respiratory distress syndrome: the Berlin Definition. JAMA 2012;307:2526–33.

40. Acute Respiratory Distress Syndrome N, Brower RG, Matthay MA, et al. Ventilation with lower tidal volumes as compared with traditional tidal volumes for acute lung injury and the acute respiratory distress syndrome. N Engl J Med 2000;342:1301–8.

Chapter 4

Filtering circulatory activity from EIT sequences: an algorithm proposal

4.1 Introduction

Electrical Impedance Tomography (EIT) is a noninvasive, radiation-free continuous monitoring technique that measures the distribution of ventilation and perfusion based on impedance changes [1]. Clinically, chest EIT is used for mechanical ventilation monitoring, heart activity and lung perfusion monitoring, and pulmonary function testing [1].

The monitoring of mechanical ventilation with EIT is significantly affected by cardiac and perfusion related impedance changes. Most EIT devices provide low-pass filtering to remove the higher frequent cardiac and perfusion impedance changes. Multiple papers describe the use of frequency filtering as a separation technique [2–5]. However, these methods do not take into account the occasional spectral overlap of respiratory harmonics and cardiac frequencies. Removing these harmonics results in loss of detail, which ultimately affects the outcomes of complex EIT analyses [6].

More complex separation techniques involve principle component analysis [6], singular value decomposition [7] and a combination of principle component analysis and independent component analysis [8]. While these methods are in fact promising, they are rather complex and computationally expensive. This can be explained by the fact that they primarily focus on

perfusion imaging, requiring to preserve the perfusion component rather than the respiratory component. A simple yet effective method primarily aimed at ventilation monitoring is lacking.

The aim of the current study is to design and evaluate an automated filtering method based on empirical mode decomposition (EMD) for the offline attenuation of circulation related impedance changes in both global and pixel EIT measurements.

4.2 Algorithm development

4.2.1 Subjects and signal acquisition

Data used in this study are part of a previous study in which ventilation distribution was optimized in mechanically ventilated COVID-19 patients with the use of EIT monitoring [9]. The patients were fully sedated with continuous intravenous infusion of propofol, midazolam or opiates, or a combination of drugs. All patients were ventilated in pressure-control mode and spontaneous inspiratory efforts were prevented with increased sedation or neuromuscular blockade. The Dräger Pulmovista 500 was used for the EIT measurements. A decremental positive end-expiratory pressure (PEEP) trial was performed according to the following procedure:

1. Start measuring at the PEEP level initially chosen by the attending clinician according to the PEEP-FiO_2 table ($PEEP_{base}$)[10].

2. Increase PEEP until it is 10 cmH_2O above $PEEP_{base}$ without changing the difference between the set peak inspiratory pressure and PEEP ($PEEP_{high}$). Only proceed under conditions of normotension (MAP $\geq$ 60 mmHg) and normal oxygen saturation ($SpO_2 \geq 88\%$). Otherwise, reduce PEEP to re-establish these conditions.

3. Reduce PEEP in steps of 2 cmH_2O every 30 seconds until the EIT device shows evident collapse in comparison to $PEEP_{high}$.

4. Reduce PEEP with 2 cmH_2O to confirm a further increase in collapse ($PEEP_{low}$).

5. Calculate the relative amount of collapse and overdistention for each PEEP step according to the Costa method [11]. Set PEEP at the lowest PEEP step above the intersection of relative overdistention and collapse.

The EIT data were downloaded from the monitors and stored for analysis. Sampling rate was 20 Hz and spatial resolution was 32 by 32 pixels.

4.2.2 Exploration of the EIT signal

Figure 4.1 showcases a global impedance trace during a decremental PEEP trial. The upper graph shows the global impedance trace from the complete measurement. During the first 80 seconds, PEEP is increased from a clinically set PEEP level to 24 cmH_2O. This results in an overall increase of the impedance values. Then, PEEP is reduced in steps of 2 cmH_2O, resulting in a decrease of the impedance values. Finally, at around 560 seconds PEEP is increased to the 'optimal' PEEP level which balances between lung collapse and overdistention.

The middle graph shows three different PEEP-steps, with PEEP changing at t = 345 and t = 380. Again, a baseline shift can be noticed when PEEP changes, indicating a change in lung aeration.

The lower graph of figure 4.1 shows 4 complete tidal breaths during one PEEP step. Notably, the impedance traces of the individual breaths do not completely overlap. This is contrary to expectations if one would consider that the patient's ventilation is completely passive: any spontaneous inspiratory effort was prevented by sedation, followed by a neuromuscular blockade if required. This suggests interference from a signal other than ventilation.

Exploring the frequency domain can help identify the different signals that make up the main signal. A power spectral density estimates to which degree each frequency is represented by the signal (i.e. 'power'). Figure 4.2 shows such power spectral density for the global impedance shown in the middle graph of figure 4.1. In this particular case, respiratory activity and circulatory activity can be clearly distinguished. Peak A corresponds to the respiratory rate (0.5 Hz, 30 breaths per minute). Peak B is a double of peak B and therefore most likely represent the second harmonic of the respiratory (1.0 Hz, 60 breaths per minute). Peak C is at 1.4 Hz, corre-

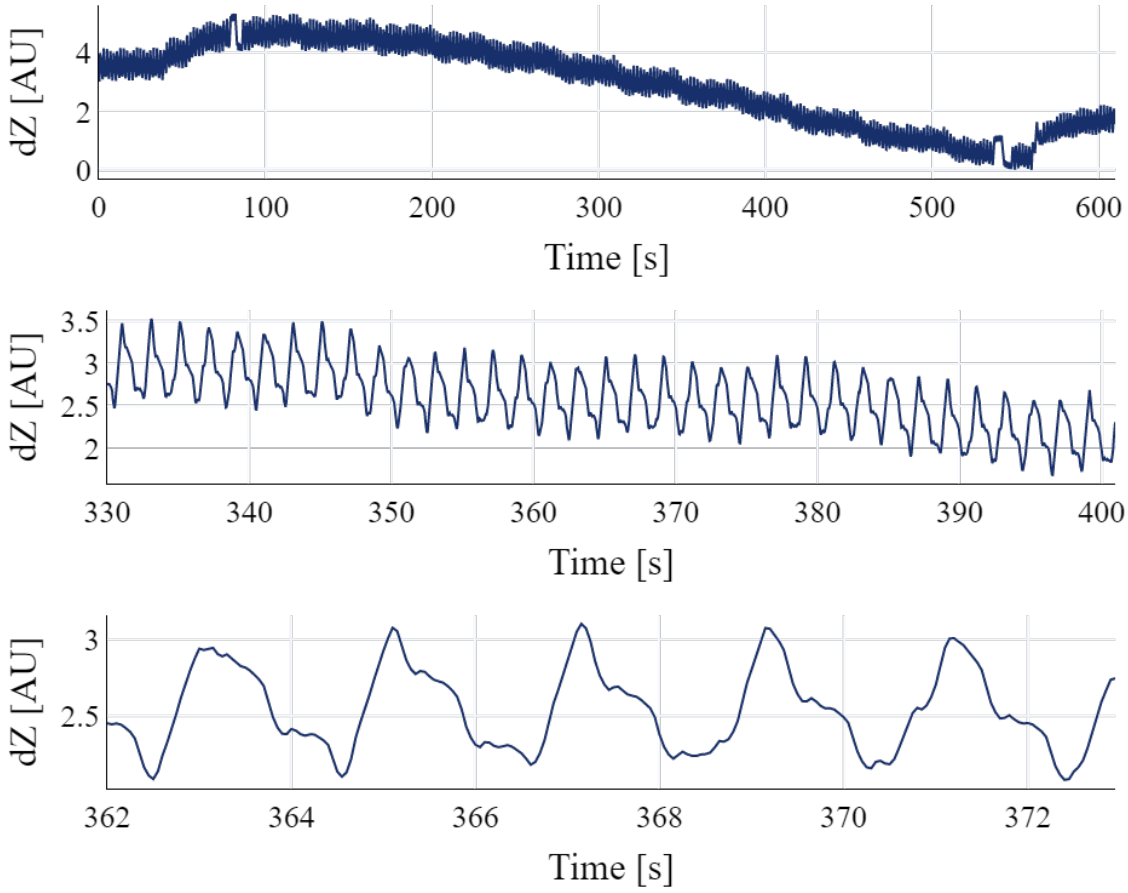

Figure 4.1: Upper graph: Global impedance trace of a typical decremental PEEP trial. During the first 80 seconds, PEEP is increased from a clinically set PEEP level to 24 cmH_2O. This results in an overall increase of the impedance values. Then, PEEP is reduced in steps of 2 cmH_2O. This results in an decrease of the impedance values. Finally, at around 560 seconds PEEP is increased to the 'optimal' PEEP level which balances between lung collapse and overdistention. **Middle graph:** Zoomed-in view of the same recording as in the upper graph. Tidal breaths can now be distinguished. Each peak corresponds to end-inspiration and each trough corresponds to end-expiration. At around t = 345 seconds and t = 380 seconds, the end-expiratory impedance value can be seen decreasing, indicating a decrease of aeration after PEEP change. **Lower graph:** Zoomed-in view of the same recording as in the middle graph. Although the patient is mechanically ventilated and fully sedated, the tidal breaths do not look exactly the same each time due to an interfering signal, most likely lung perfusion. **Abbreviations:** *AU*: arbitrary unit; *dZ*: impedance change; *PEEP*: positive end-expiratory pressure; *s*: seconds

sponding an oscillation at 84 beats per minute. It is plausible that this oscillation represents the lung perfusion.

Figure 4.3 demonstrates that the presence of circulatory activity can vary widely across the EIT image. Pixel A is located in the right dorsal lung, while pixel B is located in the left ventral lung. Although the tidal impedance variation does not seem to differ much, pixel A shows considerably more circulatory activity than pixel B. Identifying end-inspiration impedance and end-expiration impedance is very challenging at pixel A, as well as calculating measures that look after temporal aspects of ventilation, such as the regional ventilation delay [12]. The power

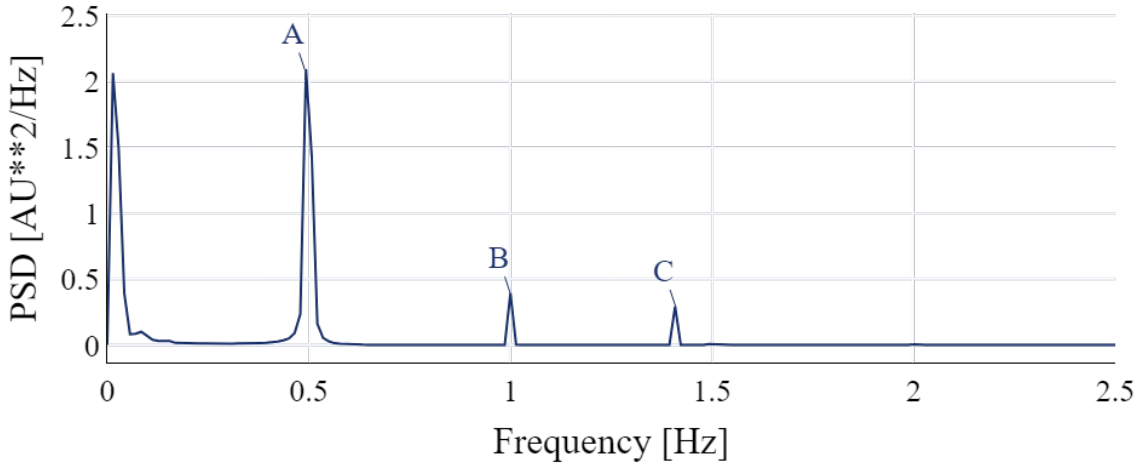

Figure 4.2: Power spectral density of the global impedance as presented in the middle graph of figure 4.1. Peak A corresponds to the respiratory rate (0.5 Hz, 30 breaths per minute). Peak B is a double of peak B and therefore most likely represent the second harmonic of the respiratory rate (1.0 Hz, 60 breaths per minute). Peak C most likely corresponds to the heart rate (1.4 Hz, 84 breaths per minute). **Abbreviations:** *AU*: arbitrary unit of impedance change; *Hz*: Hertz; *PSD*: power spectral density.

spectral density in figure 4.3 confirms the difference in the frequency content of the signals at pixel A and B. It also demonstrates that the power of circulatory activity and respiratory activity can be very close to each other, complicating automatic detection of these frequencies.

4.2.3 Frequency filtering

Most EIT devices provide the option to filter out high frequencies by applying a low-pass filter. For example, the Dräger Pulmovista 500 offers the option to filter out all frequencies above 0.83 Hz (50 bpm). This is a reasonable cut-off value, since most often respiratory rate will be less than 50 breaths per minute. However, heart rate can be very close to 50 bpm. Depending on the filter properties, a 50 bpm low-pass filter may not completely suppress nearby frequencies such as 60 bpm or 70 bpm, which can be considered normal heart rate values.

Moreover, removing all frequencies higher than 50 bpm results in the suppression of the second harmonic of all frequencies above 25 bpm. The importance of preserving harmonics is illustrated in figure 4.4. In the upper graph, the unfiltered global impedance trace is compared with a filtered version using a lowpass filter of 0.83 Hz (50 bpm). The filtered signal is a smooth sinusoidal-like curve which may acceptably approach the respiratory signal. However, if the global impedance trace is specifically filtered for heart rate with a 1.25 Hz (75 bpm) lowpass filter, it appears that the respiratory component carries more detail (figure 4.4, middle graph).

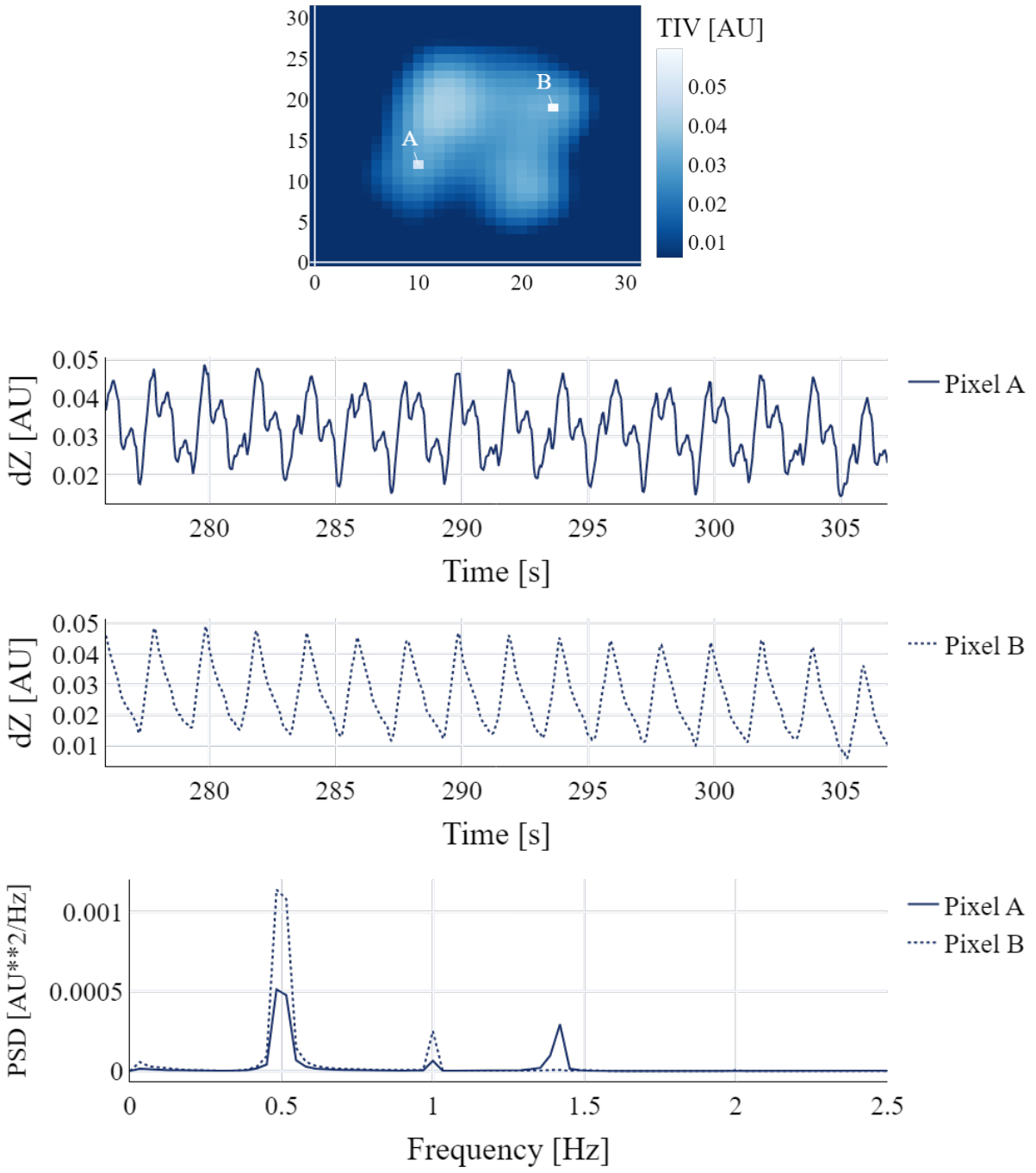

Figure 4.3: Image at top: Tidal impedance variation map, showing the tidal impedance variation (TIV) for every individual pixel. The TIV is the impedance gain during one breath. **Upper graph:** Impedance trace of pixel A. High frequent oscillations can be seen interfering with the lower frequent tidal ventilation. **Middle graph:** Impedance trace of pixel B. The higher frequent oscillations as seen at pixel A are significantly less dominant at pixel B. **Lower graph:** Comparison of frequency spectrum for both pixels. Assuming respiratory rate is at 0.5 Hz, pixel A has less respiratory activity than pixel B. Contrarily, assuming heart rate is at 1.4 Hz, pixel B has considerably more circulatory activity than pixel B. **Abbreviations:** *AU*: arbitrary unit; *dZ*: impedance change; *Hz*: Hertz; *PSD*: power spectral density; *s*: seconds; *TIV*: tidal impedance variation

Comparing both filtered signals reveals that the steep inspiratory rise and the inflection point at expiration are missing in the 0.83 Hz (50 bpm) filtered signal. This information is apparently

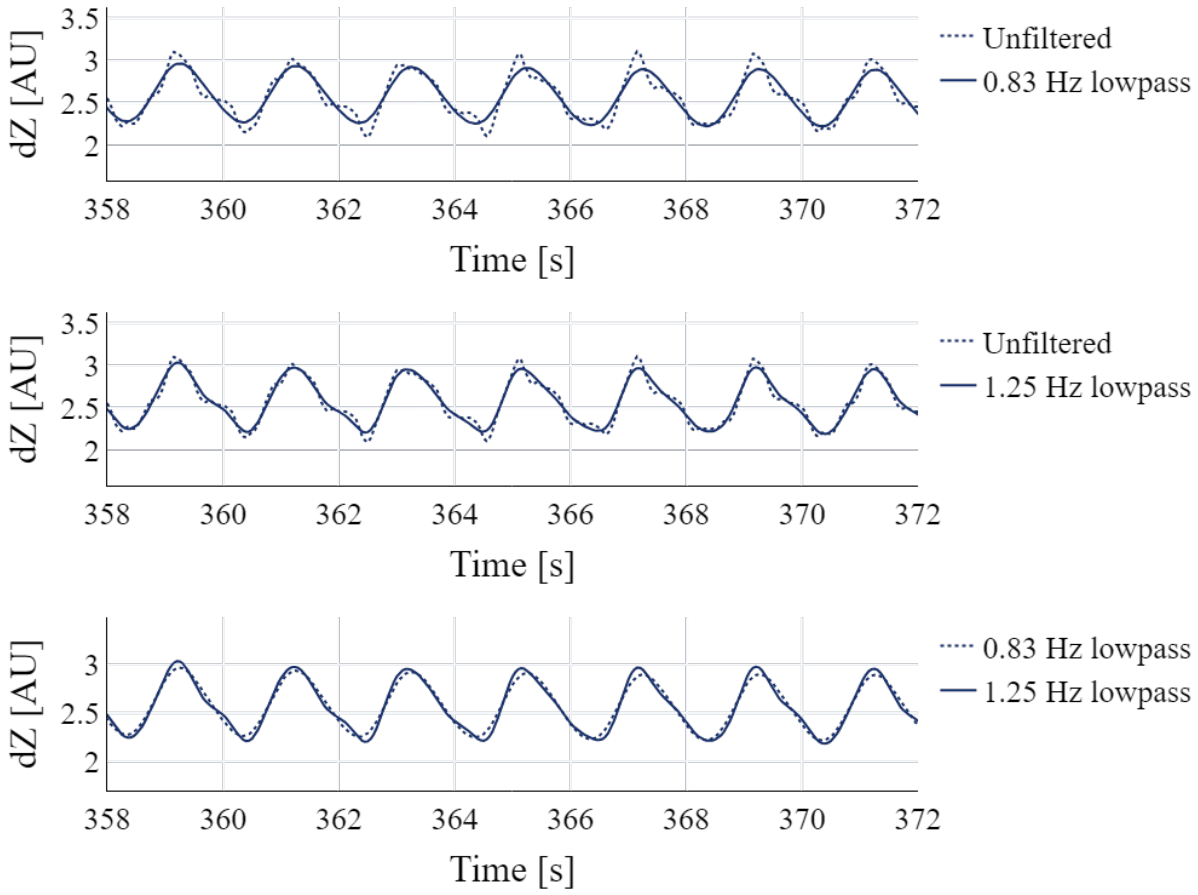

Figure 4.4: Upper graph: Unfiltered global impedance trace compared with filtered global impedance trace with the use of a 0.83 Hz (50 bpm) lowpass filter. **Middle graph:** Unfiltered global impedance trace compared with filtered global impedance trace with the use of a 1.25 Hz (75 bpm) lowpass filter. **Lower graph:** Global impedance trace filtered with a 0.83 Hz (50 bpm) filter compared to a global impedance trace filtered with a 1.25 Hz (75 bpm) filter. The 0.83 Hz filter results in the loss of respiratory information, such as the sharp rise during inspiration and the inflection point during experiation. **Abbreviations:** *AU*: arbitrary unit; *dZ*: impedance change; *Hz*: Hertz; *s*: seconds

stored in the 0.83-1.25 Hz frequency bin, the bin holding the second harmonic of the respiratory rate (figure 4.4, lower graph).

This example shows that it is possible to remove circulatory information while preserving respiratory information, if only the heart rate value is known. Heart rate monitoring is not always available, however, and heart rate may vary with time. Moreover, specific frequency filtering requires input of the clinician, which is especially labor intensive when the heart rate varies over time.

4.2.4 Requirements of the new filtering algorithm

Concluding, the following requirements are relevant for designing a new filtering algorithm:

1. The filter should specifically aim at suppressing circulatory activity.
2. The filter should be robust to changing respiratory rate and heart rate.
3. The filter should aim at preserving ventilatory information, at least the second harmonic of the respiratory frequency.
4. Application of the filter to all pixels should be possible, including pixels with low respiratory power and high circulatory power.
5. The filter should be fully automatic, not requiring any user input.

4.2.5 Empirical mode decomposition

Empirical mode decomposition is a filtering method that, with adjustments, may meet the aforementioned requirements. EMD filtering [13] is a time-domain process that separates a signal into groups of frequencies that belong to each other through a process called sifting. The sifting process contains the following steps:

1. Find all minima and maxima in the signal.
2. Create envelopes by interpolating between the minima and maxima. One envelope is created through the minima and one through the maxima.
3. Calculate the middle values of both envelopes.
4. Subtract the middle values from the original signal.
5. Check if the residual is an IMF:
   (a) Difference between the amount of minima and maxima is 0 or at most 1
   (b) The mean value of the residual is near zero.
6. If the residual is an IMF, subtract the IMF from the original signal and attempt to extract more IMF's by repeating step 1-5 until no new IMF can be extracted anymore.

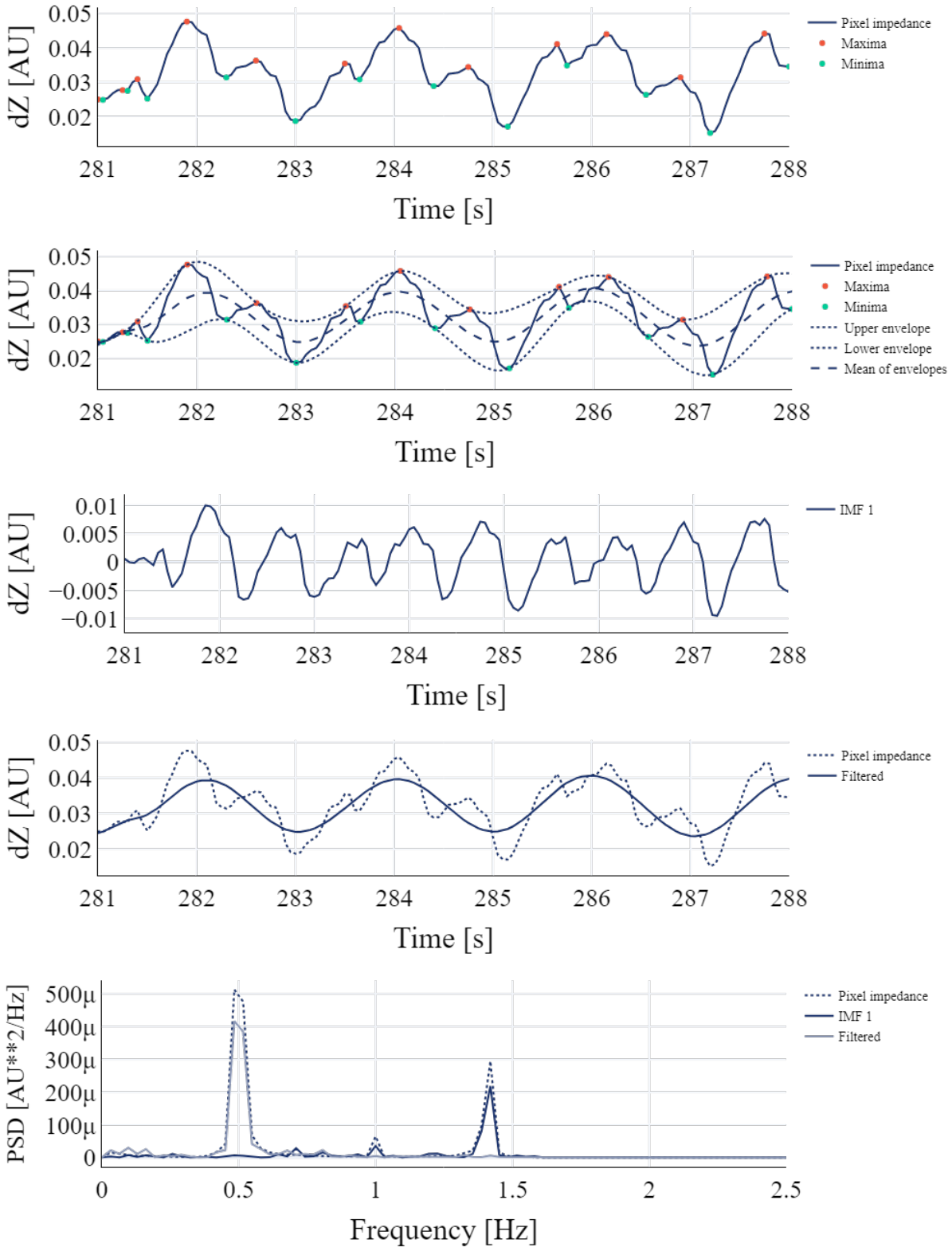

Figure 4.5: Example of EMD filtering by estimating only the first IMF and subtracting it from the original signal. The original signal represents pixel A from figure 4.3. From top to bottom: **Graph 1:** Determination of minima and maxima **Graph 2:** Calculation of envelopes and mean of envelopes **Graph 3:** First IMF obtained by subtracting the mean envelope from the original signal **Graph 4:** Filtering the signal by subtracting IMF 1 from the original signal **Graph 5:** Frequency analysis of the original signal, IMF 1 and the filtered signal **Abbreviations:** *AU*: arbitrary unit; *dZ*: impedance change; *EMD*: empirical mode decomposition; *Hz*: Hertz; *IMF*: intrinsic mode function; *s*: seconds; *PSD*: power spectral density

Figure 4.5 shows the estimation of the first IMF for pixel A from figure 4.3. IMF 1 shows a pattern that could plausibly represent the circulatory activity, which is confirmed by the IMF's main frequency being 1.4 Hz (84 bpm). Note that this example is a simplification: for clarity purposes, the EMD algorithm was adjusted such that not *all* minima and maxima were marked for finding the first IMF. The result can be observed in the frequency spectrum: the second harmonic of the respiratory rate (1 Hz) was included in the IMF. To apply EMD for the separation of respiratory and circulatory activity, the detection of minima and maxima needs to be more stringent.

Figure 4.6 demonstrates the separation of a global impedance tracing into 4 IMFs. Per definition, the first IMF contains the highest frequencies and the last IMF contains the lowest frequencies. IMF 1 contains high frequencies that do not resemble a breathing pattern. IMF 2 does resemble respiratory activity. Accordingly, the signal can be filtered by subtracting IMF 1 from the original signal.

EMD has several important characteristics that make it promising for filtering EIT signals. Unlike frequency filtering through Fourier analysis, EMD does not require the signal to originate from a linear system [13]. A system is linear if it obeys the superposition principle, i.e. if the underlying system is adheres to additivity ($F(x_1 + x_2) = F(x_1) + F(x_2)$) and homogeneity ($F(ax) = aF(x)$). In the case of thorax impedance, it is unclear whether these conditions hold true. Complex interactions exist between the lung ventilation and circulation. Like many physiological processes, these interactions may be linear only within a range of physiological conditions.

Secondly, EMD does not require the to be stationary [13]. A signal is stationary if the mean, variance and autocorrelation do not change over time. Frequency filtering through Fourier analysis requires stationarity, as it assumes that a signal can be described by a set of sinusoids. Non-stationary elements may be lost when a signal is transformed to time domain after frequency filtering. EIT measurements during a PEEP titration, for example, are clearly not stationary as a PEEP change will lead to a shift in baseline impedance. Filtering small time intervals that approach stationarity is a solution, but can still be problematic at transitions (such as PEEP change).

However, EMD is sensitive to temporal changes in frequency contents. This is a limitation for

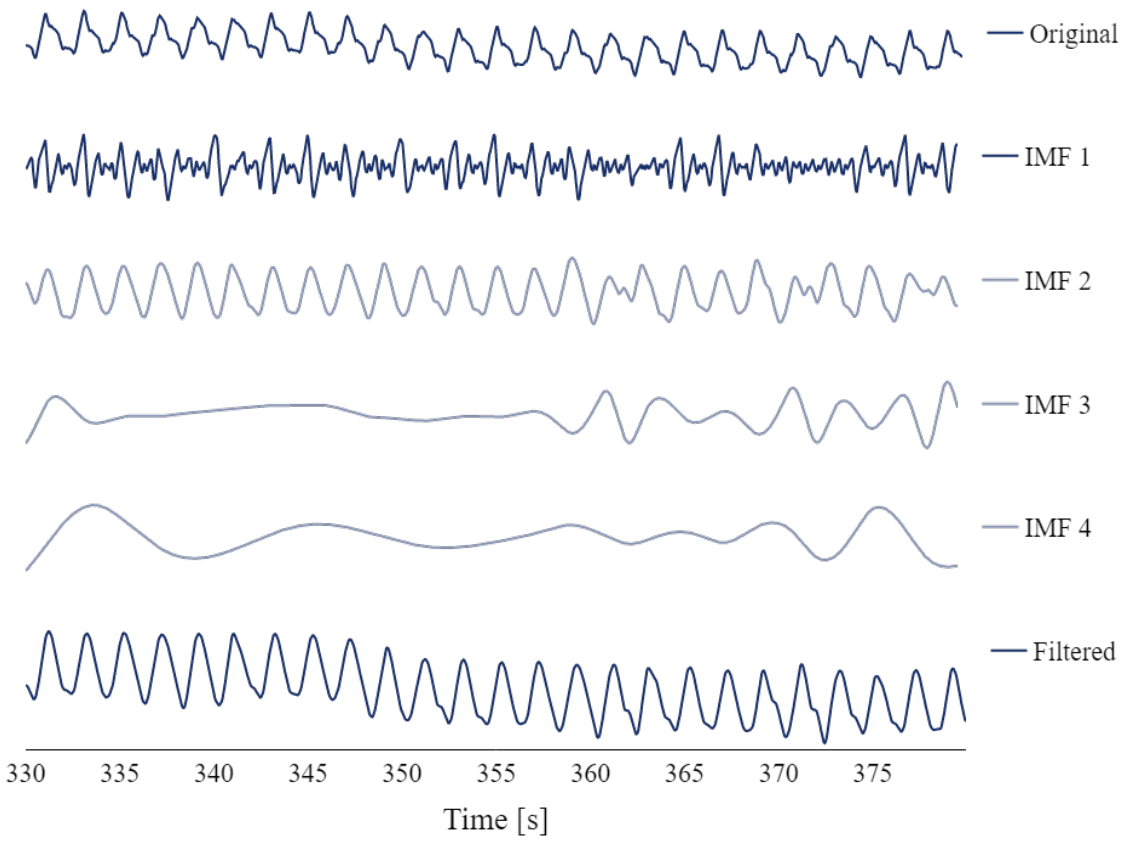

Figure 4.6: EMD filtering of the global impedance trace (from 4.1). The original signal is separated into 4 IMFs with decreasing frequency. The filtered signal is obtained by subtracting IMF 1 from the original signal. All other IMFs (gray-colored) presumably belong to respiratory activity. At t = 355 seconds, mode-mixing occurs at all IMFs, resulting in increased circulatory activity in the filtered signal. Abbreviations: *EMD*: empirical mode decomposition; *Hz*: Hertz; *IMF*: intrinsic mode function; *s*: seconds

its application to EIT recordings, as illustrated in figure 4.6. At t = 355 seconds, most IMFs start showing a different pattern. The breathing pattern in IMF 2 is interrupted by oscillations with a higher frequency. Similarly, IMF 3 changes from a near-flat line to a breathing pattern. Apparently, the higher IMFs get contaminated with circulatory activity. The filtered signal shows an increase of circulatory activity from t = 355 seconds as a result. This is phenomenon is called mode-mixing, which is inherent to EMD's adaptive nature [14].

Moreover, this application of EMD requires the visual inspection of IMFs to determine which IMFs contain circulatory activity. Accordingly, it requires user input to select the IMFs that need to be subtracted from the original signal. Adjustments to EMD are required to solve the issue of mode-mixing and the requirement of user input.

4.2.6 *Masked* empirical mode decomposition

One suggested solution to mode-mixing is the application of a mask to the signal before estimation of the IMF [15]. Considering mode-mixing is elicited by temporal changes in frequency contents, the goal of applying masks is to alter the signal in such way that there is a constant 'baseline' frequency. This can be achieved by adding a sinusoid with a known frequency (i.e. mask) to the original signal. After estimation of the first IMF, the mask can be subtracted from the filtered signal. Then, the next IMF can be estimated by the addition of a new, lower frequent mask. The masked EMD algorithm involves the following steps:

1. Make a masking sinusoid with a known frequency: $s(n)$
2. Add the mask to the signal ($x_n(n)$): $x_m(n) = x(n) + s(n)$
3. Estimate the first IMF of $x_m(n)$: $\text{IMF}_{i,m}(n)$
4. Subtract the mask from the IMF: $\text{IMF}_i(n) = \text{IMF}_{i,m}(n) - s(n)$
5. Subtract the unmasked IMF from the original signal and repeat all steps until no new IMF can be extracted anymore.

Figure 4.7 demonstrates masked EMD on a global impedance trace. In this case, the first mask was chosen at the Nyquist frequency (0.5*20 Hz) to make sure the highest frequencies are captured in the first IMF. The next IMFs were each masked at half the frequency of the preceding mask. Thus, the mask frequencies were 10, 5, 2.5, 1.25, 0.625, 0.3125 Hz. Accordingly, each masked IMF contains frequencies that are equal to or below the corresponding mask frequency. Hence, when heart rate is at 1.4 Hz (84 bpm), the circulatory activity should be represented by the first 3 IMFs. The lower graph of figure 4.7 indeed shows that subtracting the first 3 IMFs from the original signal results in a stably filtered respiratory signal that preserves details such as the expiratory inflection point.

Still, it is uncertain which IMFs will represent circulatory activity as long as the heart rate is not known. The user will need to visually inspect the IMFs and then choose which IMFs should be subtracted from the original signal. Moreover, a significant change in either respiratory rate or heart rate will result in a different allocation of respiratory and circulatory activity into

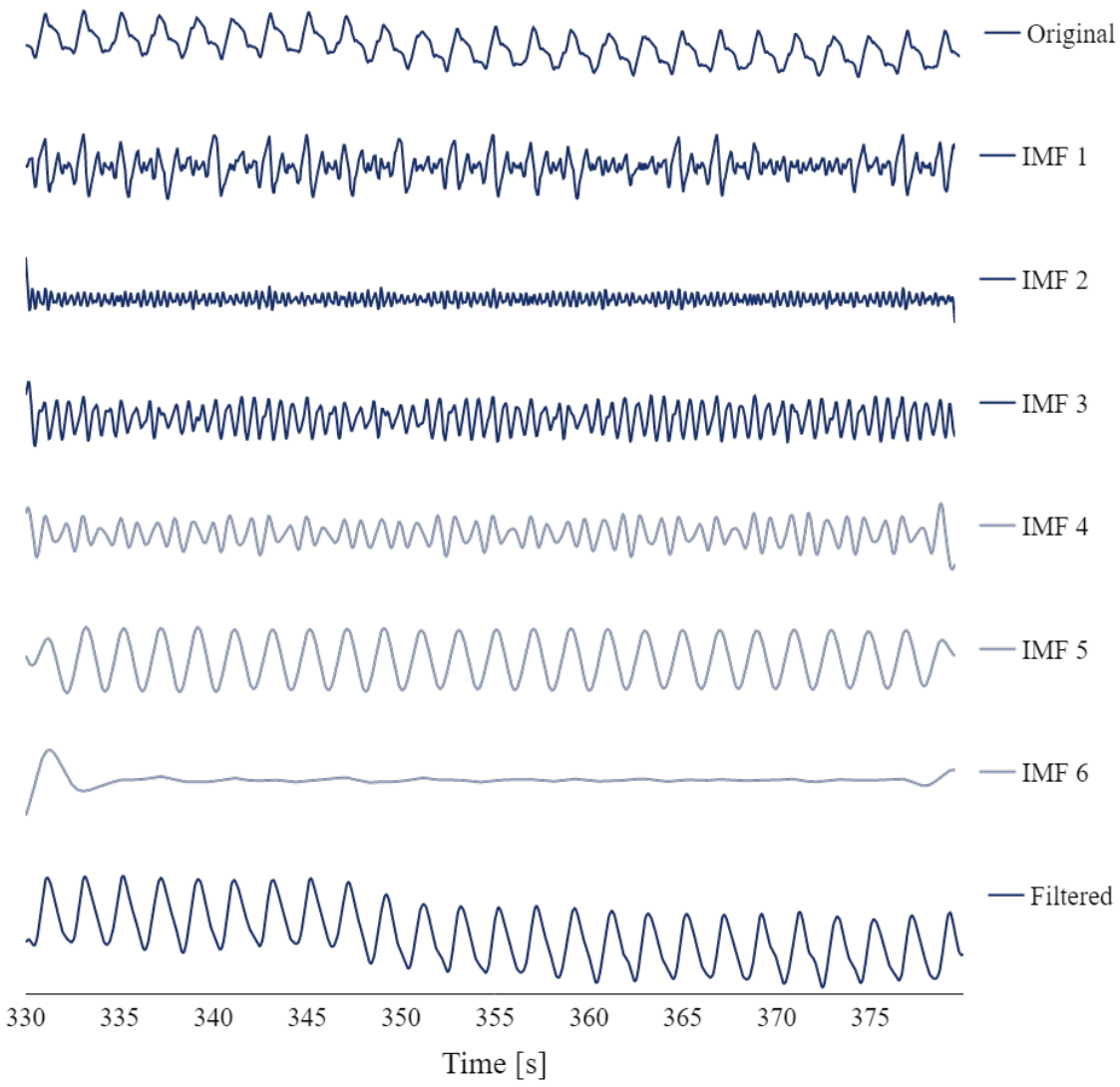

Figure 4.7: Masked EMD filtering of the global impedance trace (from 4.1). The original signal is separated into multiple IMFs (only first 6 are shown) with decreasing frequency. The filtered signal is obtained by subtracting IMF 1-3 from the original signal. The other IMFs (gray-colored) presumably belong to respiratory activity. Abbreviations: *EMD*: empirical mode decomposition; *Hz*: Hertz; *IMF*: intrinsic mode function; *s*: seconds

the IMFs. One subset of IMFs marked as circulatory activity might be valid for the first few seconds of the measurement but not for the last seconds of the measurement. Thirdly, a heart rate that is very close to a mask's frequency will likely result in the unpredictable dispersion of the circulatory activity into multiple IMFs. Finally, it remains difficult to manually select the right IMFs when masked EMD filtering is applied to impedance traces of pixels with very low respiratory or circulatory power.

4.2.7 *Automated* masked empirical mode decomposition

Here, I suggest a modification to masked EMD that aims to address the aforementioned issues.

Preferably, the masks are designed such that the circulatory information *always* ends up in specific IMFs. This would allow automatic IMF selection, not requiring any visual inspection. This can be achieved by using masks that are based on heart rate. Given that the heart rate is known *a priori*, a mask can be applied at the heart rate's frequency. Accordingly, the corresponding IMF will be a signal at the frequency of heart rate and above.

However, Fosso et al. demonstrated that this introduces mode-mixing of lower frequencies into the masked IMF. A mask with frequency f_m results in an IMF with frequencies not only larger than f_m, but also between $0.67 f_m$ and f_m [16]. In other words, if a signal is masked with a 1 Hz sinusoid, the resulting IMF will also contain frequencies between 0.67 and 1 Hz. Accordingly, to get the optimal mask frequency, the heart rate should be divided by 0.67.

Heart rate can be obtained by exploiting the property of global impedance traces that the respiratory power exceeds circulatory power in magnitude considerably. Thus, the respiratory rate can be identified as the largest peak in the frequency spectrum. Then, by removing this frequency together with its second harmonic, heart rate can be identified by the remaining largest peak. This approach has the advantage that heart rate is now *a priori* information when filtering challenging pixels.

1. Divide the global impedance waveform into segments of 180 seconds with 15 seconds overlap.
2. Multiply the overlapping ends with a half-length Hanning window, such that the first 15 seconds gradually increase from 0% power to 100% power and the final 15 seconds gradually decrease from 100% power to 0% power.
3. Estimate the power spectral density of each segment using Welch's method (Hann window, 20 seconds per segment, 50% overlap).
4. Determine respiratory frequency (*RF*) by finding the frequency with the highest power.
5. Apply a notch filter at frequency *RF* Hz with bandwidth 0.2 Hz, and a notch filter at

frequency 2*RF with bandwidth 0.2 Hz.

6. Determine cardiac frequency (CF) by finding the frequency with the highest power at $>$ 0.67 Hz (40 beats per minute)

   (a) Find the frequency with the second highest power at > 0.67 Hz.

   (b) Calculate the ratio between the power of the highest and second highest frequency.

   If ≥ 2, continue to step 6. The frequency with highest power clearly stands out and likely must be cardiac frequency.

   If < 2, repeat step 4 and 5 with the exception that only one notch filter at frequency RF is applied at step 4. The highest frequency does not stand out against other frequency peaks. Likely, the heart rate was unintendedly removed at step 4 as heart rate is likely a double of the respiration rate.

7. Divide CF by 0.67 to obtain a ground mask frequency (GMF) that precludes mode mixing of cardiac activity with respiratory activity.

8. Construct masks with frequencies $\left[2^2, 2^1, 2^0\right] * GMF$

9. Multiply the original signal with the first mask and extract the first intrinsic mode function (IMF). Subtract the IMF from te original signal. Repeat this proces by masking the residual and extracting the next IMF, until the first 3 IMFs have been extracted.

10. Filter the segment by subtracting the sum of the 3 IMFs from the original signal.

11. Repeat step 7-9 for all segments. Combine all segments through addition of the overlapping parts.

12. Repeat the filtering for all pixels.

4.3 Evaluation of performance

All signal processing was programmed in Python 3.9. Empirical mode decomposition was implemented using the EMD package version 0.5.2 [17].

Figure 4.8 shows an example of an automatically filtered global impedance trace, which was obtained without providing any user input. Heart rate was detected automatically. As intended,

all cardiac activity ends up in the first 3 IMFs, while the respiratory activity is represented by the following IMFs. Note that it is not necessary to calculate IMF 4 and 5; they are shown for clarity reasons. Compared to the non-automated masked EMD (figure 4.7), the IMFs are more stable in frequency and amplitude. Especially IMF 4 in figure 4.8 suffers considerably less from an interfering (likely cardiac) oscillation compared to IMF 4 in figure 4.7. This suggests that the automated masked method is able to better separate the original frequencies.

The frequency domain analysis (figure 4.9) confirms that the first 3 IMFs are almost completely free of the first two harmonics of respiratory activity. The frequency spectrum of the filtered signal shows the second harmonic of respiratory activity at similar amplitude compared to the frequency spectrum of the original signal, indicating that respiratory activity was preserved in the filtered signal.

Figure 4.10 and 4.11 demonstrate that filtering pixel impedance traces yields similar results. The same masks are used as for the global impedance filtering. There is no need to design new masks since the frequencies of circulatory activity are the same at any place in the thorax. Again, it can be observed that cardiac activity is collected in the first 3 IMFs and that the respiratory harmonics are preserved in the filtered signal.

4.4 Discussion

The filter proposed in this chapter is able to separate circulatory activity from respiratory activity in EIT datasets in a fully automatic way using an adjusted empirical mode decomposition algorithm.

The algorithm satisfies to the prespecified requirements. Suppression of circulatory activity is achieved through the separation of the signal into multiple frequency bands using empirical mode decomposition. The filter is robust to changing respiratory rate and heart rate through the application of masks and the segmentation of the recording into short segments. Ventilatory information is preserved by precise selection of the decomposed signals. The algorithm can be used for both filtering global and pixel impedance traces, as the ventilatory frequency and the circulatory frequency are determined based on the global impedance trace, where separation

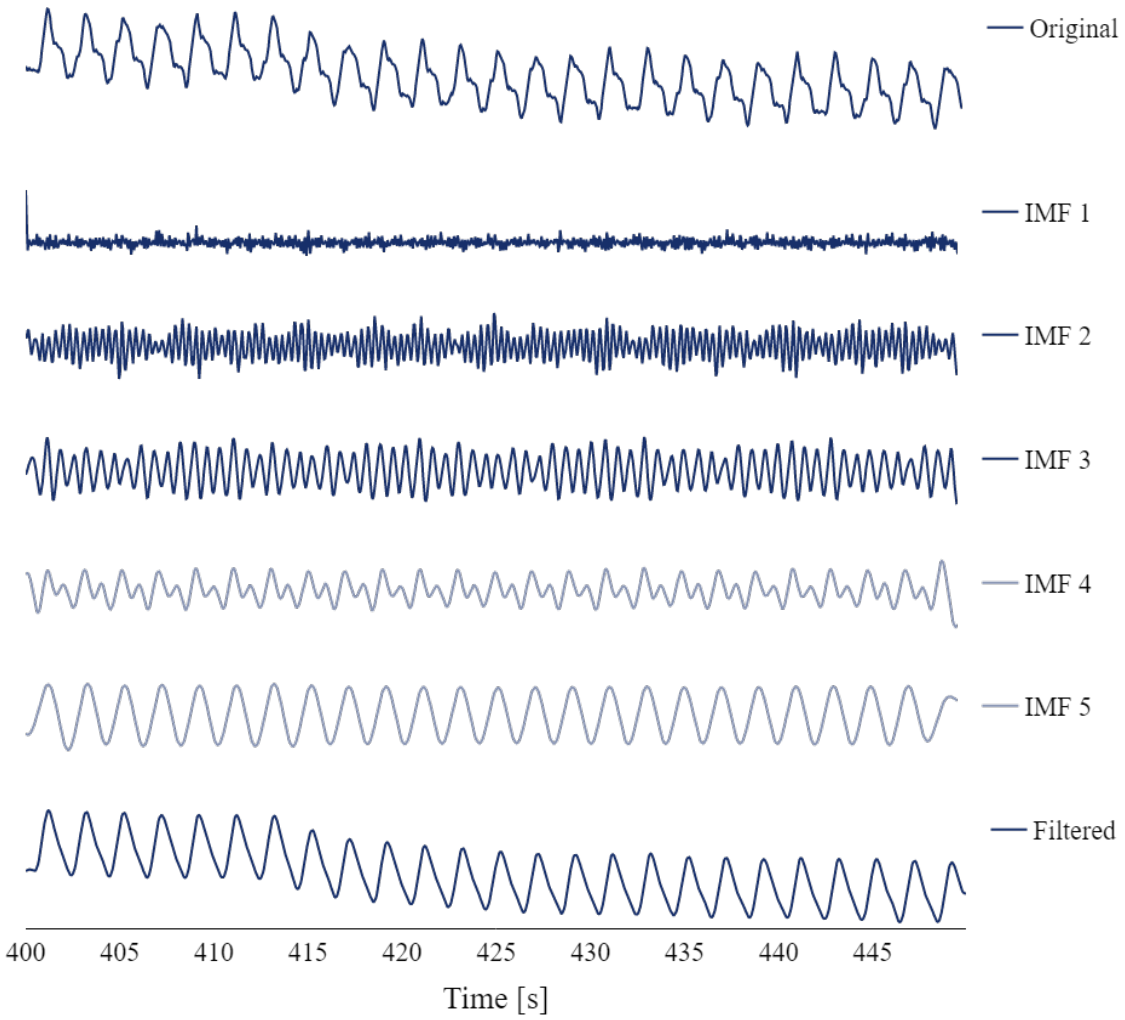

Figure 4.8: Automated masked EMD filtering of a global impedance trace. The original signal is separated into 3 IMFs specifically designed to find cardiac acitivity. Subtracting these IMFs from the original signal results in the lower filtered signal. For clarity reasons, two of the next IMFs are also shown, which likely represent the respiratory activity. These IMFs do not need to be calculated to obtain the filtered signal. Abbreviations: *EMD*: empirical mode decomposition; *IMF*: intrinsic mode function; *s*: seconds

of these frequencies is robust. The filter is fully automatic, as the user does not need to provide the cardiac frequency or select the frequency bands.

Still, there are several weaknesses to the algorithm. EMD is a complex algorithm requiring relatively much calculation power [18], although this has been debated [19]. The currently proposed algorithm has not been validated for computation power against standard filtering algorithms such as fast fourier transform filtering, yet. Second, the automatic detection of cardiac and respiratory frequency works best for longer periods of measurement time, complicating real-time filtering. Thus, implementation of the algorithm in an EIT device will only benefit the analysis of already measured recordings, while it will not enable filtering of the live-view

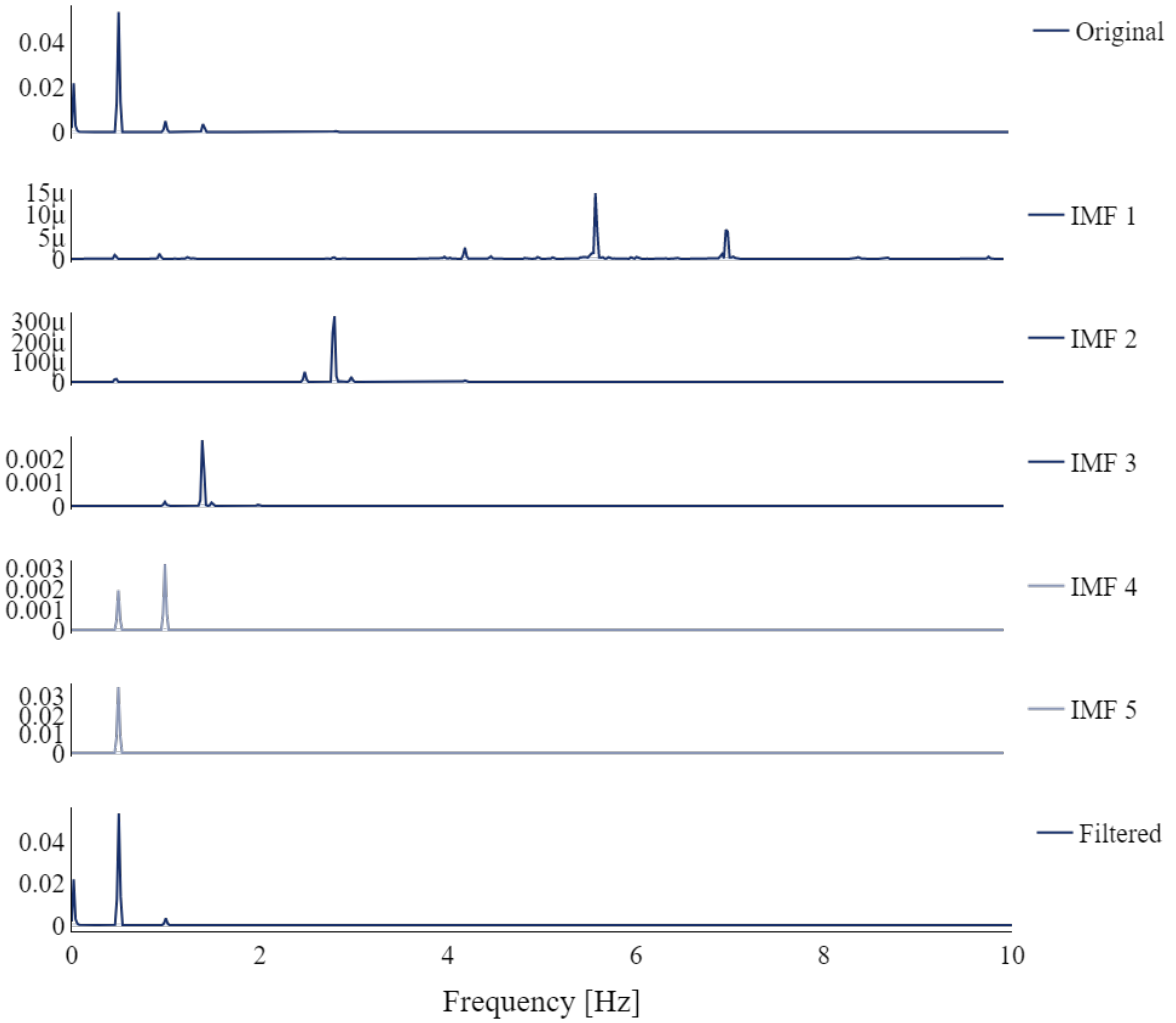

Figure 4.9: Frequency analysis of original signal, IMFs and filtered signal after automated masked EMD filtering of a global impedance trace. The y-axis represents the power of the signal (arbitrary units). Abbreviations: *EMD*: empirical mode decomposition; *Hz*: Hertz; *IMF*: intrinsic mode function.

of impedance changes, yet. The first step to making it a real-time algorithm requires making the cardiac frequency detection independent of the respiratory frequency detection. The latter frequency is normally too low to reliably detect within several seconds. The possibility of obtaining an electrocardiogram from the EIT electrodes should be investigated in the future. Third, the algorithm removes the most high frequencies, as it subtracts all 3 first IMFs which per definition contain these frequencies. This implies that, if present in the original signal, subtle changes of the respiratory activity still can be lost. This can lead to distorted results in EIT analyses, where, for example, the exact starting point of expiration must be determined. Finally, in this report, the performance of the algorithm is discussed based on only one measurement. A thorough validation is required to establish that circulatory activity can be sufficiently removed and that respiratory activity can be sufficiently preserved in a wide range of combinations of

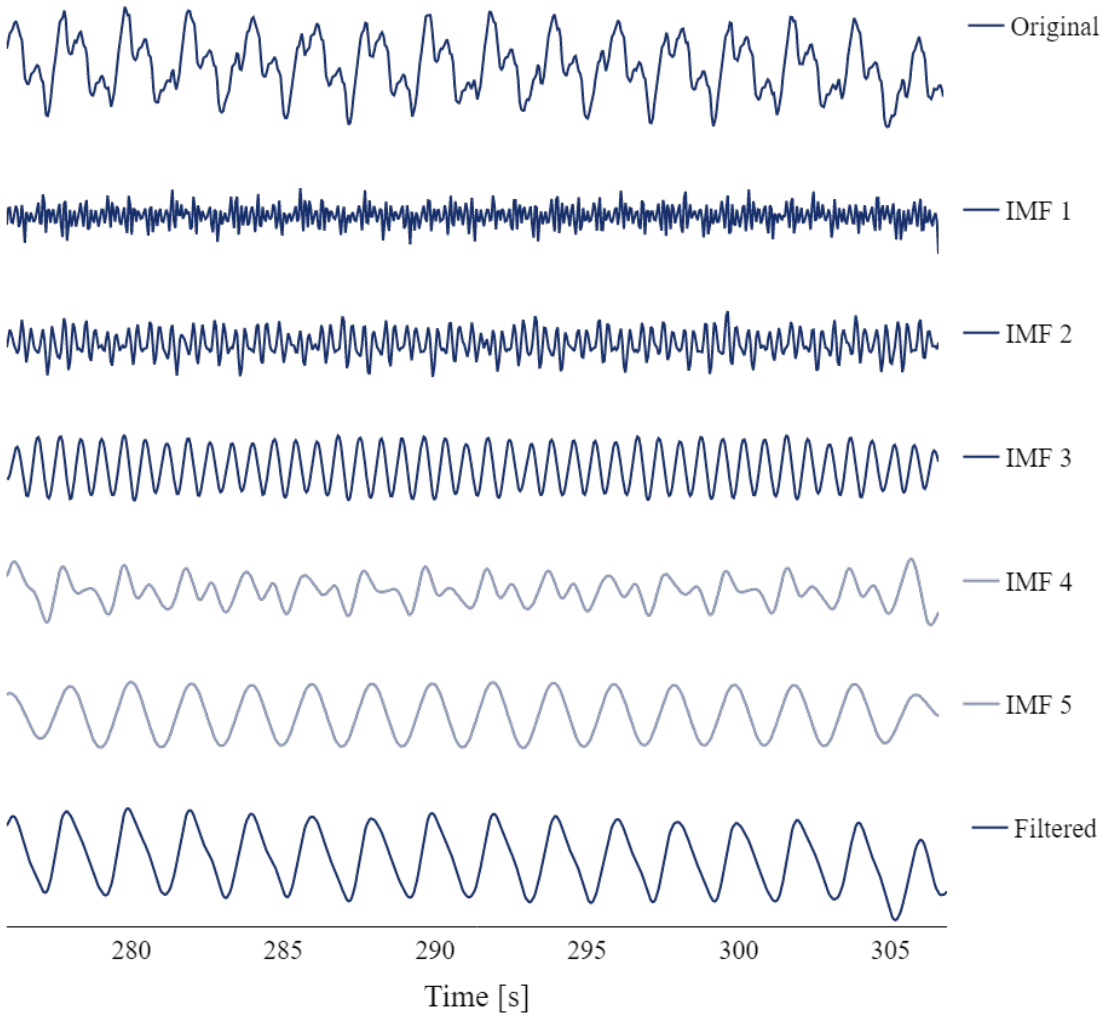

Figure 4.10: Automated masked EMD filtering of a pixel impedance trace. The original signal is separated into 3 IMFs specifically designed to find cardiac acitivity. Subtracticting these IMFs from the original signal results in the lower filtered signal. For clarity reasons, two of the next IMFs are also shown, which likely represent the respiratory activity. These IMFs do not need to be calculated to obtain the filtered signal. Abbreviations: *EMD*: empirical mode decomposition; *IMF*: intrinsic mode function; *s*: seconds

respiratory and circulatory frequencies. Test data could be obtained through simulation or by making new combinations of filtered respiratory signals and filtered circulatory signals from different patients.

Concluding, automated masked empirical mode decomposition can be used to remove circulatory activity from EIT recordings. Submission of the algorithm to a wide range of respiratory and circulatory frequencies is required to validate whether the removal of circulatory activity works under all conditions.

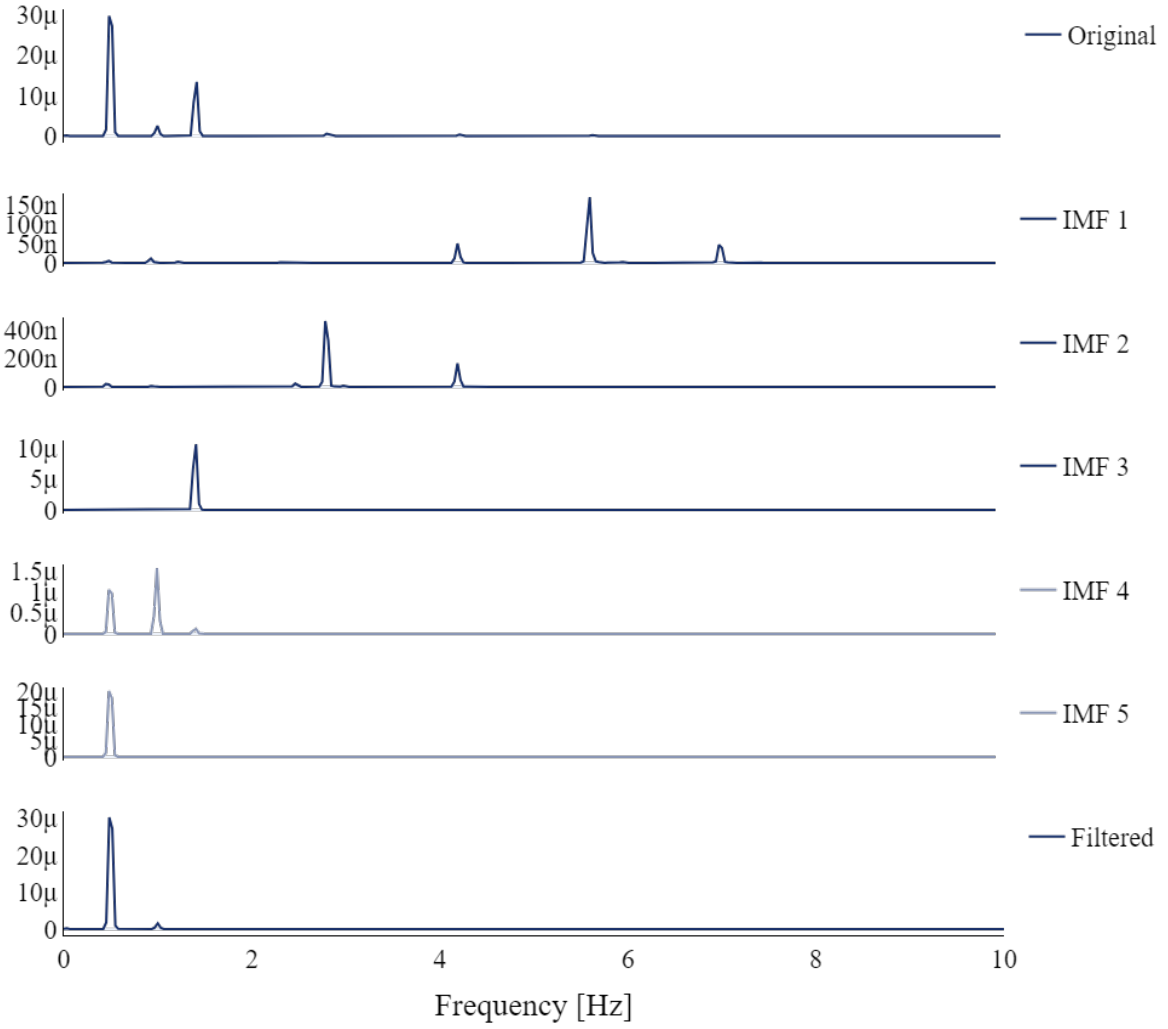

Figure 4.11: Frequency analysis of original signal, IMFs and filtered signal after automated masked EMD filtering of a pixel impedance trace. The y-axis represents the power of the signal (arbitrary units). Abbreviations: *EMD*: empirical mode decomposition; *Hz*: Hertz; *IMF*: intrinsic mode function.

References

1. Frerichs I, Amato MB, Kaam AH van, et al. Chest electrical impedance tomography examination, data analysis, terminology, clinical use and recommendations: consensus statement of the TRanslational EIT developmeNt stuDy group. Thorax 2017;72:83–93.
2. Zadehkoochak M, Blott BH, Hames TK, and George RF. Pulmonary perfusion and ventricular ejection imaging by frequency domain filtering of EIT (electrical impedance tomography) images. Clin Phys Physiol Meas 1992;13 Suppl A:191–6.
3. Leathard AD, Brown BH, Campbell J, Zhang F, Morice AH, and Tayler D. A comparison of ventilatory and cardiac related changes in EIT images of normal human lungs and of lungs with pulmonary emboli. Physiol Meas 1994;15 Suppl 2a:A137–46.
4. Dunlop S, Hough J, Riedel T, Fraser JF, Dunster K, and Schibler A. Electrical impedance tomography in extremely prematurely born infants and during high frequency oscillatory ventilation analyzed in the frequency domain. Physiol Meas 2006;27:1151–65.
5. Frerichs I, Pulletz S, Elke G, et al. Assessment of changes in distribution of lung perfusion by electrical impedance tomography. Respiration 2009;77:282–91.
6. Deibele JM, Luepschen H, and Leonhardt S. Dynamic separation of pulmonary and cardiac changes in electrical impedance tomography. Physiol Meas 2008;29:S1–14.
7. Kerrouche N, McLeod CN, and Lionheart WR. Time series of EIT chest images using singular value decomposition and Fourier transform. Physiol Meas 2001;22:147–57.
8. Jang GY, Jeong YJ, Zhang T, et al. Noninvasive, simultaneous, and continuous measurements of stroke volume and tidal volume using EIT: feasibility study of animal experiments. Sci Rep 2020;10:11242.

9. Somhorst P, Zee P van der, Endeman H, and Gommers D. PEEP-FiO2 table versus EIT to titrate PEEP in mechanically ventilated patients with COVID-19-related ARDS. Crit Care 2022;26:272.

10. Brower RG, Lanken PN, MacIntyre N, et al. Higher versus lower positive end-expiratory pressures in patients with the acute respiratory distress syndrome. N Engl J Med 2004;351:327–36.

11. Costa EL, Borges JB, Melo A, et al. Bedside estimation of recruitable alveolar collapse and hyperdistension by electrical impedance tomography. Intensive Care Med 2009;35:1132–7.

12. Muders T, Luepschen H, Zinserling J, et al. Tidal recruitment assessed by electrical impedance tomography and computed tomography in a porcine model of lung injury*. Crit Care Med 2012;40:903–11.

13. Huang NE, Shen Z, Long SR, et al. The Empirical Mode Decomposition and the Hilbert Spectrum for Nonlinear and Non-Stationary Time Series Analysis. Proceedings: Mathematical, Physical and Engineering Sciences 1998;454:903–95.

14. Xu B, Sheng Y, Li P, Cheng Q, and Wu J. Causes and classification of EMD mode mixing. Vibroengineering PROCEDIA 2019;22.

15. Deering R and Kaiser JF. The use of a masking signal to improve empirical mode decomposition. In: *Proceedings. (ICASSP '05). IEEE International Conference on Acoustics, Speech, and Signal Processing, 2005.* Vol. 4:iv/485–iv/488 Vol. 4.

16. Fosso OB and Molinas M. EMD Mode Mixing Separation of Signals with Close Spectral Proximity in Smart Grids. In: *2018 IEEE PES Innovative Smart Grid Technologies Conference Europe (ISGT-Europe)*:1–6.

17. Quinn AJ, Lopes-Dos-Santos V, Dupret D, Nobre AC, and Woolrich MW. EMD: Empirical Mode Decomposition and Hilbert-Huang Spectral Analyses in Python. J Open Source Softw 2021;6.

18. Wu LC, Chen HH, Horng JT, et al. A novel preprocessing method using Hilbert Huang transform for MALDI-TOF and SELDI-TOF mass spectrometry data. PLoS One 2010;5:e12493.

19. Wang YH, Yeh CH, Young HWV, Hu K, and Lo MT. On the computational complexity of the empirical mode decomposition algorithm. Physica A: Statistical Mechanics and its Applications 2014;400:159–67.

Chapter 5

Filtering cardiac activity from P_{es} signals: an algorithm proposal

5.1 Introduction

The analysis as described in chapter 7 requires a filtering algorithm for esophageal pressure (P_{es}) signals. The current chapter describes a proposal for the filtering of these recordings. Knowledge of the concepts as discussed in chapter 4 is assumed.

5.2 The algorithm

The algorithm for filtering P_{es} is largely based on the previously proposed algorithm for filtering EIT recordings. There are, however, two important differences to consider:

1. Cardiac oscillations can have considerably less power relative to the respiratory oscillations in P_{es} signals compared to EIT signals. Hence, the original algorithm's automatic detection of the cardiac frequency is sufficiently robust for P_{es} filtering. It was therefore decided to rely on user input for obtaining cardiac frequency.

2. The merging of individually filtered segments results in, causes sudden jumps in signal amplitude at the time points where two segments follow each other. This phenomenon

has recently been described in literature as the boundary problem [1]. In the current P_{es} filtering algorithm, this problem is mitigated by extending the segments before filtering, and de-extending the segments before merging the filtered segments [1].

The algorithm involves the following steps:

1. Divide the complete recording into segments of 180 seconds with 15 seconds overlap.
2. Extend the segment by adding a time-mirrored version of the segment at the start and end of the segment.
3. Convert the signal to frequency domain through Fourier analysis. Visually inspect the frequency spectrum and determine the cardiac frequency.
4. Divide the cardiac frequency by 0.67 to obtain the ground mask frequency (*GMF*) that precludes mode mixing of cardiac activity with respiratory activity.
5. Construct masks with frequencies $\left[2^2, 2^1, 2^0\right] * GMF$
6. Multiply the original signal with the first mask and extract the first intrinsic mode function (IMF). Subtract the IMF from te original signal. Repeat this proces by masking the residual and extracting the next IMF, until the first 3 IMFs have been extracted.
7. Filter the segment by subtracting the sum of the 3 IMFs from the original signal.
8. De-extend the segment by removing the extensions at the start and end of the segment.
9. For each segment, multiply the overlapping ends with a half-length Hanning window, such that the first 15 seconds gradually increase from 0% power to 100% power and the final 15 seconds gradually decrease from 100% power to 0% power.
10. Repeat the filtering process for each segment.
11. Combine all segments through addition of the overlapping parts.

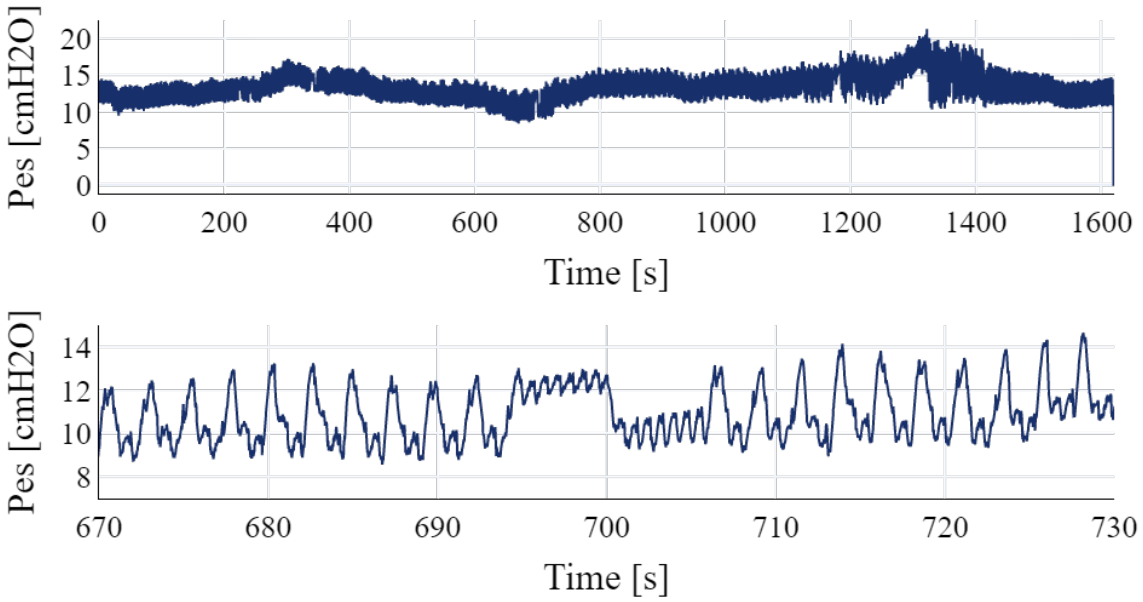

Figure 5.1: Upper graph: Raw P_{es} recording of a complete decremental PEEP trial. **Lower graph:** Magnification of the same recording as in the upper graph, showing respiratory cycles with interfering cardiac oscillations. At t=685 seconds, an inspiratory hold maneuver is performed followed by an expiratory hold maneuver. **Abbreviations:** P_{es}: esophageal pressure; *s*: seconds.

5.3 Results and discussion

All signal processing was programmed in Python 3.9. Empirical mode decomposition was implemented using the EMD package version 0.5.2 [2].

Figure 5.1 shows the tracing of a P_{es} recording from the dataset described in chapter 4. The recording involves a complete decremental PEEP trial. The lower graph shows a short segment of the recording, including an inspiratory hold followed by an expiratory hold.

The upper graph in figure 5.2 shows a part of the filtering process (step 9). Two segments are displayed, with an overlapping time of 15 seconds. The amplitude of the signal can be seen decreasing at the end of the first segment, and increasing at the start of the second segment, such that the sum of relative power of both signals is always 100%.

The lower graph in figure 5.2 shows the filtering results. The fast cardiac oscillations appear to be largely suppressed. The pressure during the inspiratory and expiratory hold can be used as reference data, since oscillations during holds can only be attributed to cardiac activity. Indeed, the filtered trace remains stable during the holds, confirming that cardiac activity is targeted by the filter. However, at the end of the normal expirations, pressure surges can be observed.

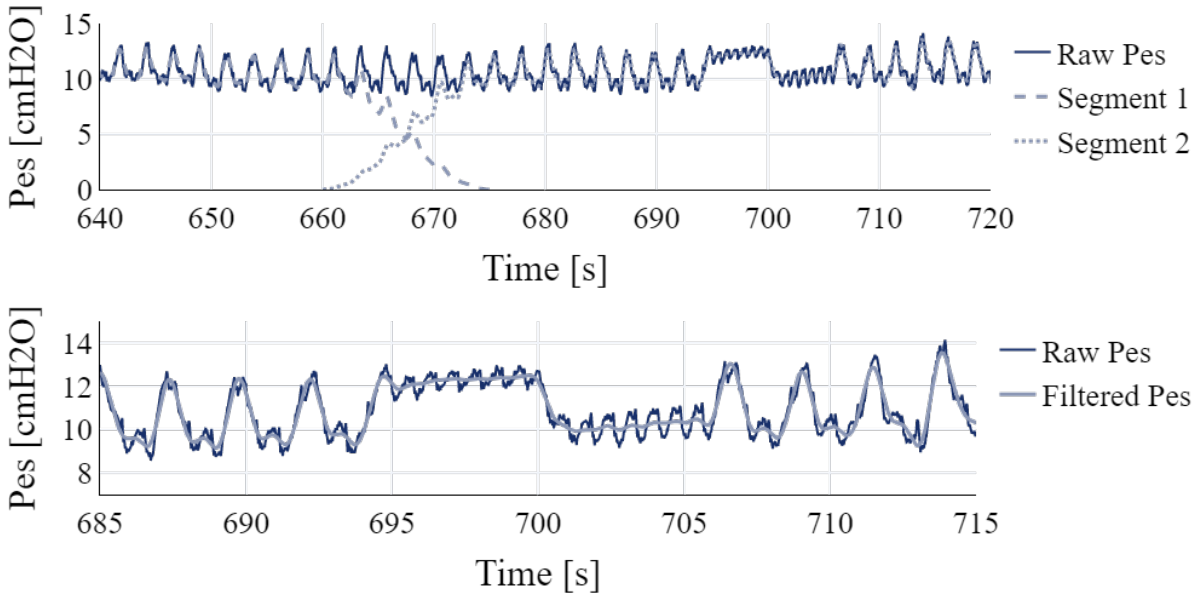

Figure 5.2: Upper graph: Raw P_{es} recording cut into 2 segments with 15 second overlap. The amplitude of the signal can be seen decreasing at the end of the first segment, and increasing at the start of the second segment, such that the sum of relative power of both signals is always 100%. **Lower graph:** Raw and filtered P_{es} recording. **Abbreviations:** P_{es}: esophageal pressure; *s*: seconds.

The filter is not able to suppress this activity completely. Meanwhile, respiratory details such as the steepness of inspiration and expiration seem to be preserved.

Importantly, the filtered signal can be seen taking the average line through the cardiac oscillations. This behaviour is inherent to the principle of EIT, as it approaches all IMFs as sinusoid-like signals. Hence, even the bias component of a signal is considered as a sinusoid and is therefore hidden in a different IMF (with higher IMF number). If this approach is valid, it would imply that cardiac activity provides both a positive and a negative pressure swing. However, it could be possible that cardiac activity only provides positive pressure swings. The respiratory component of P_{es} should then cross the minima of the cardiac oscillations. Physiologic data on this phenomenon is lacking and should be investigated in the future.

5.4 Future work

A thorough validation is required to establish that the cardiac oscillations can be sufficiently removed and that respiratory activity can be sufficiently preserved in a wide range of combinations of respiratory and cardiac frequencies. Test data could be obtained through simulation or by making new combinations of filtered respiratory signals and extracted cardiac oscillations

from different patients.

Real-time implementation of the algorithm into a device requires the automisation of cardiac frequency detection and the shortening of segments. Both require *a priori* information on heart rate. This could be achieved by either using cardiac information from preceding segments or by making use of an external measurement, such as the electrocardiogram.

5.5 Conclusion

This chapter described a proposal for the filtering of P_{es} recordings. The algorithm is able to suppress cardiac oscillations at large. Validation on a wide range of respiratory and cardiac frequencies and conversion to a real-time algorithm is required before its use in a clinical setting.

References

1. Stallone A, Cicone A, and Materassi M. New insights and best practices for the successful use of Empirical Mode Decomposition, Iterative Filtering and derived algorithms. Scientific Reports 2020;10:15161.
2. Quinn AJ, Lopes-Dos-Santos V, Dupret D, Nobre AC, and Woolrich MW. EMD: Empirical Mode Decomposition and Hilbert-Huang Spectral Analyses in Python. J Open Source Softw 2021;6.

Chapter 6

Filtering cardiac activity from P_{es} signals acquired by a solid-state catheter: an algorithm proposal

Chapter 7

Optimal PEEP guided by EIT versus P_{es} monitoring: a comparative study

7.1 Introduction

Invasive mechanical ventilation is the cornerstone of respiratory failure treatment. Setting ventilator parameters is a balancing act between providing adequate oxygenation and ventilation on the one hand, and minimizing lung damage and adverse cardiovascular effects on the other hand. The application of positive end-expiratory pressure (PEEP) can improve oxygenation and minimizes lung damage by preventing alveolar collapse, but high PEEP levels can induce harmful (regional) hyperinflation and increased vascular resistance [1].

Conventionally, PEEP settings are titrated according to the ARDSnet PEEP/FiO_2 table, which makes PEEP levels depend on oxygen demand [2]. While these target values are practical for clinical use, they do not take into account the large heterogeneity of lung characteristics in mechanically ventilated patients. For example, the percentage of potentially recruitable lung is extremely variable among patients with acute respiratory distress syndrome (ARDS) [1]. Accordingly, higher PEEP application improves outcomes only in a subset of patients [3–5]. This observation demonstrates the need for personalized optimization of ventilator settings.

Advanced bed-side monitoring technologies have the potential to support choosing the right ventilation strategy. Electrical Impedance Tomography (EIT) assesses the distribution of venti-

lation based on impedance changes measured by an electrode belt placed around the thorax [6]. This enables the evaluation of lung collapse, overdistention and recruitability, providing valuable information for PEEP titration [7, 8]. Esophageal pressure (P_{es}) monitoring offers valuable information on the patient's respiratory mechanics. Since esophageal pressure can be considered as a surrogate of pleural pressure, this monitoring method can be used to estimate the pressure drop across the lung parenchyma (transpulmonary pressure, P_{tp}) [9].

With EIT and P_{es} monitoring becoming more available, the question rises what place they should have in clinical decision making. Both methods provide similar information on the patient's lung physiology, but each in a different way. In the context of PEEP titration, EIT is most often used to find the PEEP level that yields the lowest difference between relative percentage of alveolar collapse and overdistention [8]. P_{es} monitoring is often used to find the PEEP level that yields an end-expiratory transpulmonary pressure ($P_{tp,EE}$) close to zero [10]. While both approaches theoretically aim at minimizing alveolar collapse and overdistention, it is not clear whether they result in identically suggested PEEP levels. Moreover, while there is evidence that a $P_{tp,EE}$ (measured at the esophageal level) close to zero is beneficial to clinical outcome [11], its implication for the total lung ventilation distribution is unknown.

This study aims to evaluate the differences between EIT and P_{es} monitoring in guiding PEEP titration by finding answers to the following research questions:

1. How does the EIT guided PEEP level compare to the P_{es} guided PEEP level?
2. What is the ventilation distribution at the optimal P_{es} guided PEEP?
3. What is the transpulmonary pressure at the optimal EIT guided PEEP?

7.2 Methods

7.2.1 Study design

This is a retrospective analysis of a cohort study conducted between March 1 and June 2020 the intensive care unit of the Erasmus MC, Rotterdam. Data from this cohort has been presented

earlier in studies comparing ARDSnet FiO_2-PEEP table guided PEEP with EIT guided PEEP [12, 13].

Patients were originally included that met the following criteria:

- Aged $\geq$ 16 years
- PCR positive COVID-19
- Moderate to severe ARDS according to the Berlin criteria [14]
- Intubated and on controlled mechanical ventilation

Two criteria were added for including patients in the current retrospective analysis:

- Availability of an EIT recording and a P_{es} measurement obtained during a decremental PEEP trial following admission to the ICU
- The patient is in supine position during the decremental PEEP trial

A decremental positive end-expiratory pressure (PEEP) trial was performed guided by EIT measurements obtained with the Pulmovista 500, Dräger, Germany. Simultaneously, P_{es} was recorded using the Adult Esophageal Balloon Catheter by CooperSurgical, USA. P_{es} monitoring was intended only for research purposes and did not have clinical implications for setting the PEEP.

The PEEP trial involved the following steps:

1. Start measuring at the PEEP level initially chosen by the attending clinician according to the PEEP-FiO_2 table ($PEEP_{base}$)[2].
2. Increase PEEP until it is 10 cmH_2O above $PEEP_{base}$ without changing the difference between the set peak inspiratory pressure and PEEP ($PEEP_{high}$). Only proceed under conditions of normotension (MAP $\geq$ 60 mmHg) and normal oxygen saturation ($SpO_2 \geq 88\%$). Otherwise, reduce PEEP to re-establish these conditions. Perform an end-inspiratory and end-expiratory hold at $PEEP_{high}$.

3. Reduce PEEP in steps of 2 cmH_2O every 30 seconds until the EIT device shows evident collapse in comparison to $PEEP_{high}$.

4. Reduce PEEP with 2 cmH_2O to confirm a further increase in collapse ($PEEP_{low}$). Perform an end-inspiratory and end-expiratory hold at $PEEP_{low}$.

5. Calculate the relative amount of collapse and overdistention for each PEEP step according to the Costa method [15]. Set PEEP at the lowest PEEP step above the intersection of relative overdistention and collapse ($PEEP_{set}$).

Each PEEP change was accompanied by a 1:1 change in the peak inspiratory pressure, with the aim to keep driving pressure constant.

The EIT and P_{es} data were downloaded from the monitor and stored for analysis. EIT sampling rate was 20 Hz and spatial resolution was 32 by 32 pixels. P_{es} sampling rate was 50 Hz.

7.2.2 Outcome measures

The primary outcome measure was mean difference of EIT guided PEEP and P_{es} guided PEEP.

EIT guided PEEP was defined as the first PEEP level before reaching the crossing point of collapse and overdistention. P_{es} guided PEEP was defined as the first PEEP level during decremental PEEP titration that yields any $P_{tp,EE}$ between -2 and 2 cmH_2O.

Secondary outcome measures included: relative percentage collapse and overdistention at P_{es} guided PEEP; $P_{tp,EE}$ at EIT guided PEEP; collapse and overdistention at $P_{tp,EE}$ = 0 cmH_2O; percentage of maximal collapse at the lungs dorsal and ventral to the esophageal level at $P_{tp,EE}$ = 0 cmH_2O.

7.2.3 Data processing

EIT: data selection

The EITdiag research software by Dräger was used to segment and reconstruct the EIT data. Global impedance traces were visually inspected to find one segment of 10 consecutive breaths

having stable end-expiratory lung impedance (EELI) for each PEEP step.

EIT: collapse and overdistention

Collapse and overdistention were calculated according to the method introduced by Costa et al [15]. This method is based on the assumption that a loss of compliance can be either attributed to alveolar collapse or alveolar overdistention. Along a PEEP trial, each pixel has an own compliance profile. Usually, at a high PEEP level, a pixel's compliance is low due to overdistention. Then, when PEEP is lowered, the overdistention starts to resolve and the compliance increases. At a certain PEEP level, the compliance reaches an optimum after which it decreases again when airways and alveoli start to collapse. In other words, a low compliance before the optimum is reached, can be attributed to overdistention. Likewise, a low compliance after the optimum is reached, can be attributed to collapse.

Hence, the first step of the method involves the calculation of each pixel's compliance at every PEEP step:

$$\text{Compliance}_{\text{pixel, PEEP-step}} = \frac{\Delta Z}{P_{\text{plateau}} - \text{PEEP}} \tag{7.2.1}$$

where ΔZ is the average tidal impedance variation of the PEEP step. Considering driving pressure was assumably constant throughout the PEEP trial, this element could be omitted from calculation so that

$$\text{Compliance}_{\text{pixel, PEEP-step}} = \Delta Z \tag{7.2.2}$$

Then, the best compliance throughout the PEEP trial was determined for every pixel:

$$\text{Best compliance}_{\text{pixel}} = \max \begin{pmatrix} \text{Compliance}_{\text{pixel, PEEP-step=0}} \\ \text{Compliance}_{\text{pixel, PEEP-step=1}} \\ \vdots \\ \text{Compliance}_{\text{pixel, PEEP-step=n}} \end{pmatrix} \tag{7.2.3}$$

Knowing each pixel's compliance profile, the extent of overdistention can be determined by calculating the amount of compliance loss relative to the best compliance *before* the optimum is reached:

$$\text{Overdistention}_{\text{pixel, PEEP-step}}(\%) =$$

$$\begin{cases} (1 - \frac{\text{Compliance}_{\text{pixel, PEEP-step}}}{\text{Best compliance}_{\text{pixel}}}) \times 100 & \text{if } \text{PEEP}_{\text{PEEP-step}} > \text{PEEP}_{\text{Best compliance}} \\ 0 & \text{if otherwise} \end{cases} \tag{7.2.4}$$

Likewise, the extent of collapse can be determined by calculating the amount of compliance loss relative to the best compliance *after* the optimum is reached:

$$\text{Collapse}_{\text{pixel, PEEP-step}}(\%) =$$

$$\begin{cases} (1 - \frac{\text{Compliance}_{\text{pixel, PEEP-step}}}{\text{Best compliance}_{\text{pixel}}}) \times 100 & \text{if } \text{PEEP}_{\text{PEEP-step}} < \text{PEEP}_{\text{Best compliance}} \\ 0 & \text{if otherwise} \end{cases} \tag{7.2.5}$$

To obtain one collapse and overdistention value for all pixels at a PEEP step, the individual pixel collapse and overdistention values can be cumulated:

$$\text{Cumulated collapse}_{\text{PEEP-step}} = \sum_{\text{pixel}=1}^{m} \text{Collapse}_{\text{pixel, PEEP-step}(\%)} \tag{7.2.6}$$

where m is the amount of pixels that contribute to ventilation. In this study, the device's classification of ventilated pixels was used.

However, this approach would allow pixels with low tidal ventilation, such as those representing the most peripheral lung fields, to have a high impact on the total collapse number. Physiologically, a relative compliance loss at the central lung fields yields much more loss of ventilated lung tissue than the same relative compliance loss at the peripheral lung fields. Hence, a more physiological cumulated collapse can be calculated by weighing each pixel's collapse percentage with the pixel's best compliance value:

$$\text{Cumulated Collapse}_{\text{PEEP-step}}(\%) = \frac{\sum_{\text{pixel}=1}^{m}(\text{Collapse}_{\text{pixel, PEEP-step}(\%)} \times \text{Best compliance}_{\text{pixel, PEEP-step}})}{\sum_{\text{pixel}=1}^{m} \text{Best compliance}_{\text{pixel, PEEP-step}}} \tag{7.2.7}$$

Similarly, cumulated overdistention is calculated as

$$\text{Cumulated Overdistention}_{\text{PEEP-step}}(\%) = \frac{\sum_{\text{pixel}=1}^{m}(\text{Overdistention}_{\text{pixel, PEEP-step}(\%)} \times \text{Best compliance}_{\text{pixel, PEEP-step}})}{\sum_{\text{pixel}=1}^{m} \text{Best compliance}_{\text{pixel, PEEP-step}}} \tag{7.2.8}$$

EIT: distribution of collapse

The collapse maps were divided into a part dorsal to the esophageal level and a part ventral to the esophageal level. First, pixel rows participating to ventilation were identified based on the the device's classification of ventilated pixels. The rows were each assigned an ascending row number, with the most dorsal row assigned number 0. Secondly, the number of the row representing esophageal level was defined as the nearest integer to the amount of rows times 0.4. The value of 0.4 was conveniently based on visual inspection of available CT-scans from included patients. Thirdly, the part dorsal to the esophageal level was defined as the pixel rows under the esophageal level row, including the esophageal level row itself. The part ventral to the esophageal level was defined as the pixel rows above the esophageal level. Fourth, all pixel's collapse values were cumulated for both the dorsal and ventral parts. Finally, the cumulated collapse values were divided by the total amount of collapse observed during the PEEP trial, enabling inter-patient comparisons.

P_{es}: data selection

Raw esophageal pressure (P_{es}) and airway pressure (P_{aw}) recordings were used for analysis. A custom user interface was developed to facilitate the segmentation of 5 consecutive stable breaths for each PEEP step. Segmentation was done independently by two reviewers and results were compared after completion to reach agreement. Moreover, the inspiratory and expiratory holds were segmented for the highest and lowest PEEP step.

P_{es}: estimation of end-expiratory P_{tp}

Transpulmonary pressure ($P_{tp,EE}$) was estimated according to the absolute esophageal pressure theory [16]:

$$P_{tp} = P_{aw} - P_{es} \tag{7.2.9}$$

Both the P_{aw} and P_{es} recordings were contaminated by cardiac artifacts, however. This could potentially impact end-inspiratory and end-expiratory pressure values.

The P_{es} recordings were filtered using the empirical mode decomposition (EMD) algorithm as proposed in chapter 5. In short, the method involves the segmentation of the signal in short segments of 180 seconds. The segments are filtered individually after which they are combined again. The filtering involves the detection of heart rate through visual inspection of the frequency spectrum. The heart rate value is then used to design masking signals that enable EMD to specifically extract the cardiac artifacts from the recording. Finally, the cardiac artifacts are subtracted from the recording, leaving a signal with predominantly respiratory activity.

The P_{aw} recordings were initially filtered using the same method, but it was concluded that the filtering resulted in a significant loss of details (appendix A). This would have led to an underestimation of end-inspiratory pressure and an overestimation of end-expiratory pressure. Not filtering P_{es} and P_{aw} individually, but filtering the estimated P_{tp} trace resulted in similar loss of important details.

Since the P_{aw} recordings were considerably less contaminated by cardiac artifacts than the P_{es} recordings, it was decided to filter only the P_{es} recordings. This raised a synchronization issue, as it was found that the the moment of end-expiration differed between P_{es} and P_{aw} as a result of the P_{es} filtering. Subtracting P_{es} from P_{aw} would then lead to a biased $P_{tp,EE}$. For this reason, it was decided to determine end-expiratory values for P_{aw} and P_{es} separately first, to average these values per PEEP-step and, finally, to subtract the values to obtain $P_{tp,EE}$.

P_{es}: accounting for incomplete expiration

The patients were ventilated with pressure controlled ventilation. This ventilation mode has the limitation that the expiration does not necessarily reach a zero-flow state. As long as there is airflow during expiration, the alveolar pressure is higher compared to the airway pressure. Using the airway pressure to calculate transpulmonary pressure would, in this case, result in the underestimation of end-expiratory transpulmonary pressure.

The information provided by the end-expiratory holds at $PEEP_{high}$ and $PEEP_{low}$ was used to address this issue. An end-expiratory hold involves the closure of the expiratory valve of the ventilator for multiple seconds. When the flow equals zero, P_{aw} will rise to the intrinsic PEEP level [17]. Intrinsic PEEP, or auto-PEEP, is the pressure that exists in the alveoli at end-expiration and is mainly determined by (a combination of) flow limitation, expiration time, expiratory time constant and resistance of the respiratory system [18].

To derive the intrinsic end-expiratory pressure levels from the holds for all patients automatically, a sliding window was applied to evaluate the standard deviation at any point during the holds. The sliding window had a length of 1 second and a step size of 20 milliseconds. The time interval with the lowest standard deviation of P_{aw} was then used as a starting point for the calculation of intrinsic end-expiratory P_{aw} and P_{es}.

The average of P_{aw} and P_{es} during the time interval was considered as the total end-expiratory P_{aw} and P_{es}, respectively. From tidal breathing curves at the same PEEP level, the extrinsic end-expiratory P_{aw} and P_{es} were determined. Then, intrinsic end-expiratory P_{aw} and P_{es} were calculated by subtracting extrinsic P_{aw} and P_{es} from total end-expiratory P_{aw} and P_{es}:

For $PEEP_{high}$ and $PEEP_{low}$:

$$P_{\text{aw, intrinsic}} = P_{\text{aw, total}} - P_{\text{aw, extrinsic}} \tag{7.2.10}$$

$$P_{\text{es, intrinsic}} = P_{\text{es, total}} - P_{\text{es, extrinsic}} \tag{7.2.11}$$

Linear interpolation was used to estimate the intrinsic P_{aw} and P_{es} for each PEEP step by using the intrinsic P_{aw} and P_{es} at $PEEP_{high}$ and $PEEP_{low}$ as reference pressures:

$$\hat{P}_{\text{aw, intrinsic, PEEP-step}} =$$

$$P_{\text{aw, intrinsic, PEEP}_{\text{high}}} + \frac{(P_{\text{aw, intrinsic, PEEP}_{\text{low}}} - P_{\text{aw, intrinsic, PEEP}_{\text{high}}})(\text{PEEP}_{\text{PEEP-step}} - \text{PEEP}_{\text{high}})}{\text{PEEP}_{\text{low}} - \text{PEEP}_{\text{high}}} \tag{7.2.12}$$

$$\hat{P}_{\text{es, intrinsic, PEEP-step}} =$$

$$P_{\text{es, intrinsic, PEEP}_{\text{high}}} + \frac{(P_{\text{es, intrinsic, PEEP}_{\text{low}}} - P_{\text{es, intrinsic, PEEP}_{\text{high}}})(\text{PEEP}_{\text{PEEP-step}} - \text{PEEP}_{\text{high}})}{\text{PEEP}_{\text{low}} - \text{PEEP}_{\text{high}}} \tag{7.2.13}$$

The interpolated intrinsic end-expiratory pressures were added to the extrinsic end-expiratory pressures obtained from the tidal breathing curves, resulting in a total end-expiratory pressure for each PEEP step:

For each PEEP-step between $PEEP_{high}$ and $PEEP_{low}$:

$$P_{\text{aw, total}} = P_{\text{aw, extrinsic}} + \hat{P}_{\text{aw, intrinsic}} \tag{7.2.14}$$

$$P_{\text{es, total}} = P_{\text{es, extrinsic}} + \hat{P}_{\text{es, intrinsic}} \tag{7.2.15}$$

Finally, end-expiratory transpulmonary pressure was obtained for every PEEP-step by subtracting total end-expiratory P_{es} from total end-expiratory P_{aw}:

$$P_{tp,EE} = P_{\text{aw, total}} - P_{\text{es, total}} \tag{7.2.16}$$

7.2.4 Statistical analysis

Data were presented as median [25th-75th percentile] or count (percentage). The Wilcoxin Signed-Rank test was used for non-parametric paired testing of the difference between EIT guided PEEP and P_{es} guided PEEP, as well as collapse and overdistention differences between EIT guided PEEP and P_{es} guided PEEP. Bias and limits of agreement (LOA) with mean bias +/- 2 standard deviation for EIT guided PEEP versus P_{es} guided PEEP were calculated following the Bland-Altman approach. Univariate linear regression was used to assess the explanatory value of patient characteristics for differences in EIT and P_{es} guided PEEP levels. A p-value

of ≤ 0.05 was considered to be statistically significant. Statistical analysis was performed in RStudio (Version 4.2.1, 2022).

Calculation of end-expiratory transpulmonary pressures revealed that only a subset of patients had reached a $P_{tp,EE}$ between -2 and 2 cmH_2O during the decremental PEEP trial. Hence, in a post-hoc analysis, patient characteristics and respiratory mechanics were compared between patients reaching $-2 \leq P_{tp,EE} \leq 2$ cmH_2O and patients not reaching $-2 \leq P_{tp,EE} \leq 2$ cmH_2O. The groups were compared by means of the Wilcoxin rank-sum test for non-parametric independent testing. A p-value of ≤ 0.05 was considered to be statistically significant.

7.3 Results

7.3.1 Patient characteristics

26 mechanically ventilated patients with COVID-19 ARDS were included in this retrospective cohort study. Patients had a median age of 60 [54–66] years and a body mass index (BMI) of 29.5 [26.2-36.0] kg/m^2. Median APACHE IV score at ICU admission was 51 [47-72] and median time since intubation was 4 [1-8] days (table 7.1).

Only a subset of patients (n=20, 77%) reached a $P_{tp,EE}$ between -2 and 2 cmH_2O during the decremental PEEP trial. Gender, BMI, age, 28 day mortality, SOFA score, time since intubation and time since onset symptoms were not different in the patients reaching the $P_{tp,EE}$ target and patients not reaching the target, while median APACHE IV did differ (50 [46-51] vs. 76 [71-78] respectively, p=0.005), as well as the highest D-dimer in the first 7 days of admission (2.9 [1.8-5.6] vs. 9.8 [4.8-29.4] (mg/L)) (table 7.1).

7.3.2 PEEP guided by EIT and P_{es} monitoring

Median EIT guided PEEP was 15 [14-18] cmH_2O and median P_{es} guided PEEP was 12 [10-16] cmH_2O (figure 7.1). Median difference between EIT guided PEEP and P_{es} guided PEEP was 4 [2-5] cmH_2O, which was statistically significant (p=0.008).

Univariate regression analysis table revealed no statistical significant relationship between the

	Totaal (n=26)	Not within $-2 \leq P_{tp,EE} \leq 2$ (n=10)	Within $-2 \leq P_{tp,EE} \leq 2$ (n=16)	P-value (not within $-2 \leq P_{tp,EE} \leq 2$ vs. within $-2 \leq P_{tp,EE} \leq 2$)
Male gender	22 (85%)	10 (100%)	12 (75%)	0.25
BMI (kg/m2)	29.5 [26.2-36.0]	29.5 [26.4-35.2]	29.5 [26.4-36.0]	0.98
Age (y)	60 [54-66]	62 [55-66]	60 [50-66]	0.65
28 day mortality	6 (23%)	3 (30%)	3 (19%)	0.85
APACHE IV score	51 [47-72]	74 [67-78]	49 [46-51]	0.002*
SOFA score	8.0 [6.0-10.0]	8.5 [7.2-10.8]	7.0 [6.0-9.2]	0.24
D-dimer at admission (mg/L)	1.5 [1.0-2.6]	2.4 [1.2-5.2]	1.3 [1.0-2.2]	0.19
Highest D-dimer in first 7 days (mg/L)	3.5 [2.6-8.2]	7.9 [3.8-29.4]	2.7 [1.6-4.0]	0.006*
Time since intubation (d)	4 [1-8]	2 [1-5]	4 [2-12]	0.21
Time since onset symptoms (d)	12 [8-16]	11 [8-14]	12 [10-18]	0.36

Table 7.1: Patient characteristics. Data is presented as n (%) or median [interquartile range]. * p-value $<$ 0.05.

difference in suggested PEEP between EIT and P_{es}, and the explanatory variables BMI and APACHE IV score (table 7.2).

7.3.3 Collapse and overdistention at optimal PEEP

At EIT guided PEEP, relative collapse and overdistention were 7.2% [5.0%-9.3%] and 12.2% [9.7%-13.9%], respectively. At P_{es} guided PEEP, collapse and overdistention were 15.6% [8.9%-21.1%] and 3.7% [0.0%-14.1%], respectively. Relative collapse was higher at P_{es} guided PEEP (median difference 7.6% [3.4%-14.0%], p$<$0.001). Relative overdistention was lower at P_{es} guided PEEP (median difference -6.4% [-11.5%–2.5%] , p=0.03) (figure 7.2).

7.3.4 End-expiratory transpulmonary pressure at EIT guided PEEP

At EIT guided PEEP, $P_{tp,EE}$ was 4.1 [3.2-5.9] cmH_2O for patients reaching $-2 \leq P_{tp,EE} \leq 2$ cmH_2O and 6.2 [5.7-6.8] cmH_2O for patients not reaching $-2 \leq P_{tp,EE} \leq 2$ cmH_2O. The distributions in the two groups differed statistically significant (p=0.009).

Variable	Coefficient	SE	R^2	p-value
BMI	0.069	0.145	0.012	0.641
APACHE IV score	0.019	0.039	0.013	0.632

Table 7.2: Results of univariate linear regression analyses for the difference of suggested PEEP between EIT and Pes (response), and BMI and APACHE IV score (explanatory variables). **Abbreviations:** *APACHE*: Acute Physiology and Chronic Health Evaluation; *BMI*: body mass index; *EIT*: electrical impedance tomography; P_{es}: esophageal pressure.

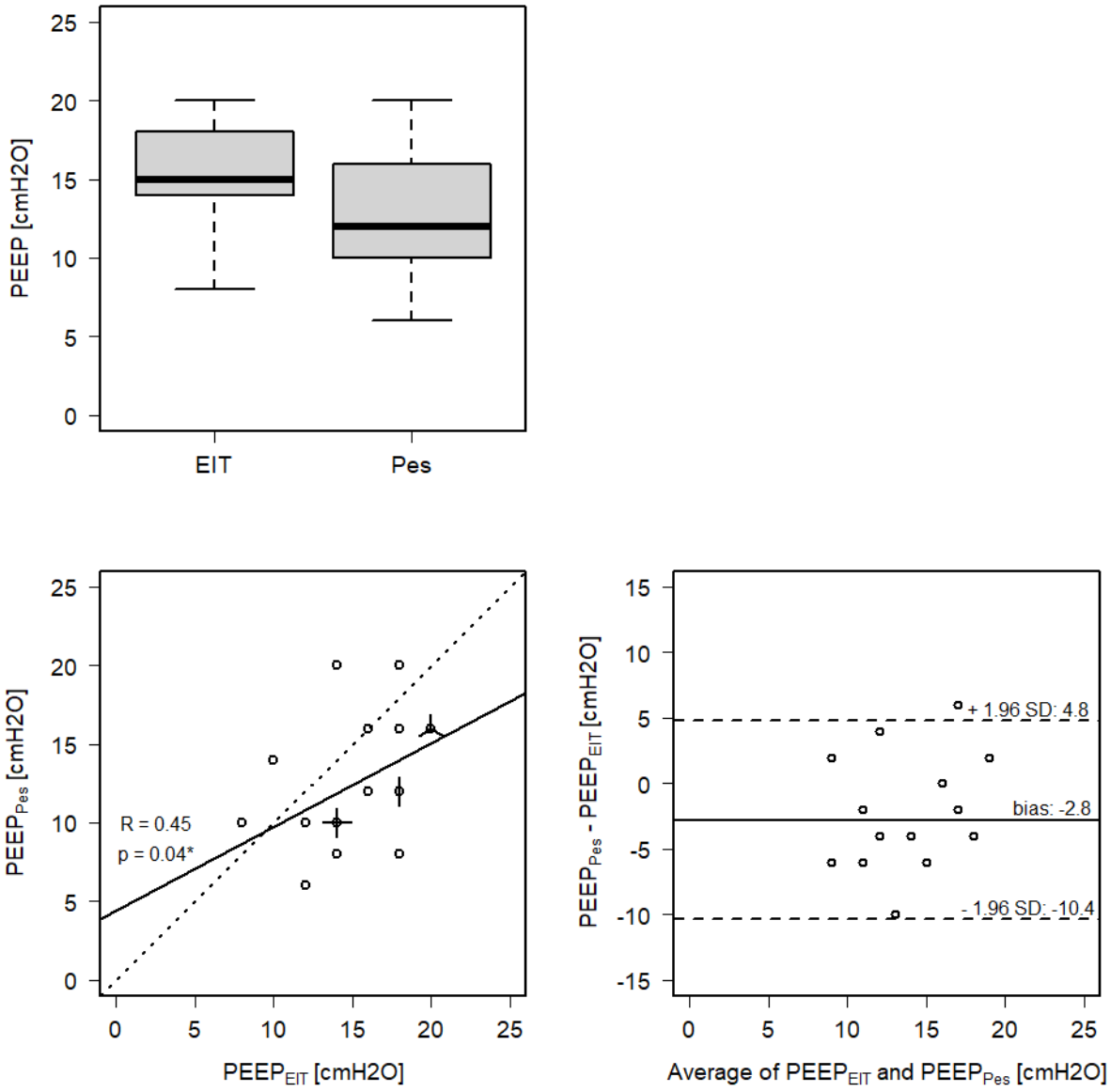

Figure 7.1: Left upper graph: Distribution of PEEP values suggested by EIT and P_{es}. **Left under graph:** Sunflower plot of PEEP values suggested by EIT and P_{es}. Each leave represents one data point. Dotted line: identity line. Solid line: estimated linear regression line. * denotes statistical significance. **Right under graph:** Bland Altman plot assessing PEEP differences between EIT and P_{es} throughout the range of average observed PEEP values. **Abbreviations:** *EIT*: electrical impedance tomography; *PEEP*: positive end-expiratory pressure; *P_{es}*: esophageal pressure.

7.3.5 Ventilation distribution at $P_{tp,EE}$ = 0 cmH_2O

A total of 14 patients reached a $P_{tp,EE}$ of 0 cmH_2O, requiring a median PEEP level of 11 [8-14] cmH_2O. Maximal observed relative collapse during the PEEP trial was 25.2% [21.0%-34.8%]. Under the condition of $P_{tp,EE}$ = 0 cmH_2O, the lungs were collapsed at 80% [43%-100%] of the

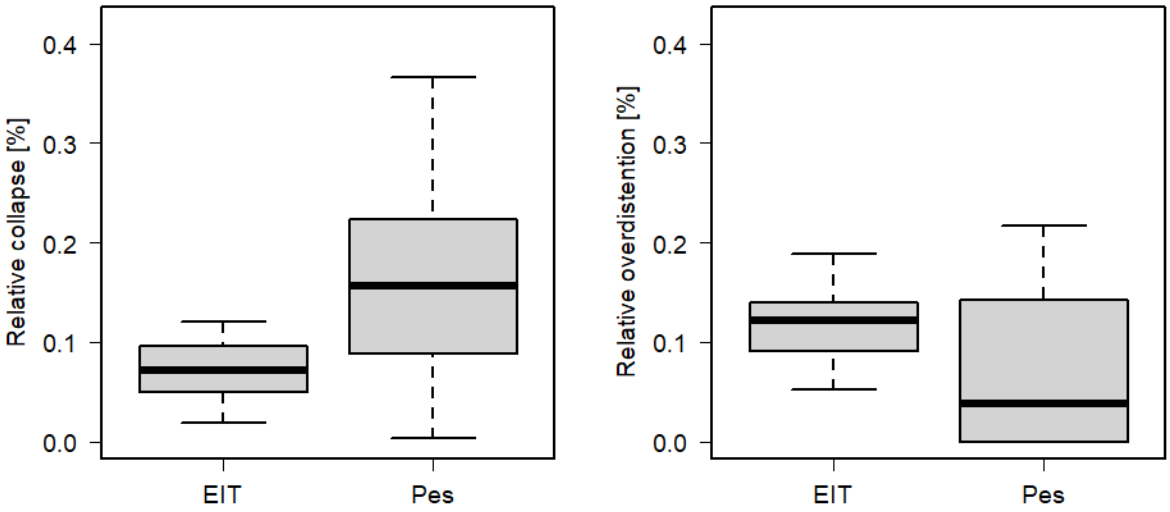

Figure 7.2: Left graph: Distribution of relative collapse values suggested by EIT and P_{es}. **Right graph:** Distribution of relative overdistention values suggested by EIT and P_{es}. **Abbreviations:** *EIT*: electrical impedance tomography; P_{es}: esophageal pressure.

maximal collapse reached during the PEEP trial. At the same PEEP level, collapse located dorsal to the presumed esophageal level attributed to 54% [33%-67%] of the maximal collapse, whereas 16% [4%-19%] of the maximal collapse was located ventral to the esophageal level. Upon visual inspection, the esophageal level separated the lungs into collapsed lungs and non-collapsed lungs in 10 out of 14 cases (71%) (figure 7.3).

Maximal observed relative overdistention during the PEEP trial was 37.5% [33.6%-46.9%]. Under the condition of $P_{tp,EE}$ = 0 cmH_2O, the lungs were overdistended at 10% [0%-18%] of the maximal collapse reached during the PEEP trial.

7.4 Discussion

The primary finding of this study is that PEEP titration guided by EIT yields higher PEEP levels compared to PEEP titration guided by P_{es} monitoring. EIT-guided PEEP levels were associated with lower alveolar collapse and higher alveolar overdistention.

Titration of PEEP with EIT and P_{es} are based on different rationales. EIT monitors the distribution of ventilated lung volumes. As such, optimal PEEP is defined as the PEEP level that produces the most homogeneous lung ventilation, expressed in terms of alveolar collapse and

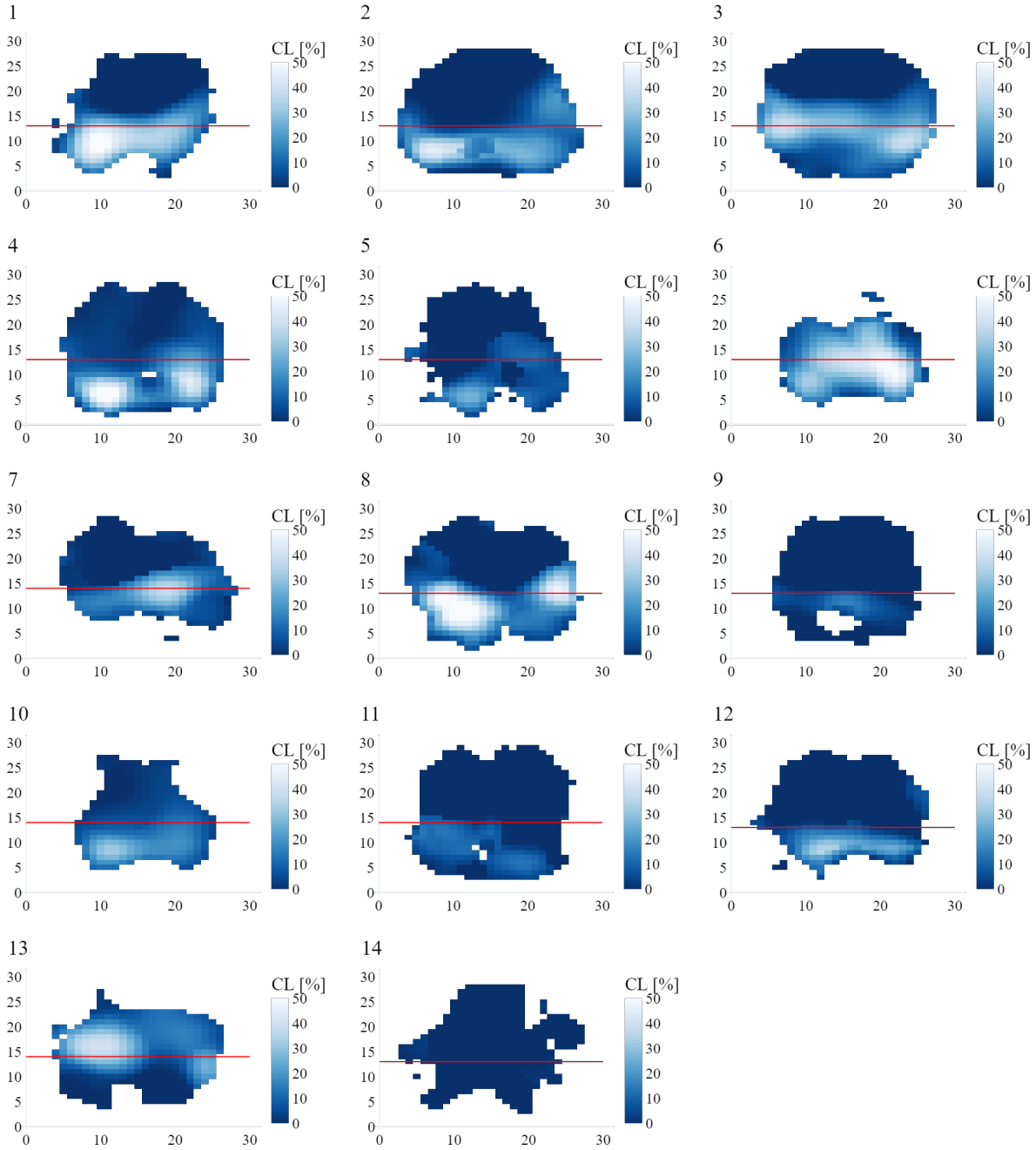

Figure 7.3: Distribution maps of relative collapse at zero end-expiratory transpulmonary pressure. Red line: presumed esophageal level. **Abbreviations:** *CL*: relative collapse

overdistention. Meanwhile, P_{es} monitoring is a technology assessing lung mechanics. It is used to optimize the transpulmonary pressure at the end of expiration. As such, P_{es} guided PEEP is primarily aimed at preventing collapse. Thus, it is reasonable to expect differences in suggested PEEP values between both strategies.

However, contradictory to the P_{es} strategy's primary aim, the current study demonstrates that the P_{es} guided PEEP yields even more alveolar collapse compared to EIT guided PEEP. More-

over, the detailed exploration of ventilation distribution showed that half of the total collapse encountered during the PEEP trial is present at zero $P_{tp,EE}$. Hence, significant collapse should be expected when aiming $P_{tp,EE}$ close to zero.

At the same time, P_{es} guided PEEP produced less overdistention on average. This can be seen as an advantage, as multiple studies suggest that alveolar overdistention may be more harmful than collapse [19–21]. Still, while overdistention was lower on average, individual overdistention percentages varied widely. Only knowing that $P_{tp,EE}$ is titrated close to zero apparently does not guarantee the absence of alveolar overdistention.

The variation in collapse and overdistention percentages was considerably larger at P_{es} guided PEEP compared to EIT guided PEEP. Hence, $P_{tp,EE}$ seemingly does not directly predict ventilation distribution. This was also reflected in the varying difference between EIT and P_{es} guided PEEP levels. The degree of difference could possibly be explained by inter-patient differences, but in this study BMI and APACHE IV scores lacked explanatory power. Assessment of lung weight from CT-scans in a future study could possibly confirm whether individual lung heterogeneity may explain varying differences between both strategy's advised PEEP level.

Alternatively, the heterogeneity in collapse and overdistention values at $P_{tp,EE}$ close to zero may have been induced by measurement errors. The filling pressure of the esophageal balloon can significantly shift the baseline of recorded P_{es} values [22]. This makes P_{es} monitoring vulnerable to user-induced errors.

In the current study, the $P_{tp,EE}$ target was set at $-2 \leq P_{tp,EE} \leq 2$ cmH_2O. This choice was based on the clinical evidence provided by Sarge et al. [11], indicating that $-2 \leq P_{tp,EE} \leq 2$ cmH_2O is associated with reduced mortality. Interestingly, not all patients in the current study reached this target during the decremental PEEP trial. Subgroup analysis revealed that patients not reaching the target had higher APACHE IV scores and higher D-dimer levels. It is likely that the increased severity of illness and increased lung perfusion anomalies led to early desaturation, necessitating the premature termination of the decremental PEEP trial.

It has been well recognized that the esophageal pressure is only a surrogate for local pleural pressure adjacent to the esophageal balloon [23]. The gravitational gradient along the dorsal-ventral axis introduces a gradient of pleural pressures, with the dorsal pleural pressure being

higher. Hence, dorsal transpulmonary pressure is lower and will become negative first. The current study corresponds to this by showing that in most patients, the esophageal level delineated the separation between collapsed and non-collapsed lung tissue at zero $P_{tp,EE}$, indicating a negative transpulmonary pressure dorsal to the esophagus.

While evidence of clinical outcome points towards a target of $-2 \leq P_{tp,EE} \leq 2$ cmH_2O, the current study shows that this target is associated with significant heterogeneity of lung ventilation. Equal amount of collapse and overdistention required an average increase of 4 cmH_2O PEEP. Considering regional inhomogeneity in tidal volume distribution is an important determinant of ventilator induced lung-injury [24], there is a clear physiological rationale for titrating PEEP a few cmH_2O above zero $P_{tp,EE}$, although it conflicts with the clinical evidence. Meanwhile, it must be noted that the clinical evidence originates from a post-hoc analysis, not investigating the clinical implications of a $P_{tp,EE}$ at few cmH_2O above zero.

The results of the current study contradict the findings by Scaramuzzo et al. [25] that EIT and P_{es} guided PEEP are uncorrelated and yield similar PEEP levels, on average. An important difference between this study and the current study is the use of Silent Spaces to assess regional ventilation distribution with EIT. Silent Spaces are defined as pixels not or minimally contributing to ventilation [26]. The advantage of this method is that it does not require a complete decremental PEEP trial, as Silent Spaces can be assessed at any PEEP level independently from other PEEP levels. Meanwhile, the method treats all lung regions equally, while the Costa method used in the current study weighs the magnitude of collapse and overdistention for each pixel based on its best observed compliance. Thus, theoretically, the Costa method is better at finding the PEEP level with the highest gain in ventilated lung regions.

Another important difference between both studies is the more diverse study population investigated by Scaramuzzo et al., which included both pulmonary ARDS and extrapulmonary ARDS patients. They found that EIT suggested a lower PEEP level specifically in pulmonary ARDS and a higher PEEP in extrapulmonary ARDS, while PEEP titration with P_{es} monitoring was less able to differentiate between ARDS origin. This would imply that the potential for lung recruitability may determine the magnitude of difference between EIT and P_{es} guided PEEP. This has not been investigated in the current study and should be addressed in future studies.

This study demonstrates that EIT and P_{es} are not interchangeable for titrating PEEP. However, while it has been suggested that both methods do not correlate before [25], the current study does show a correlation but with a seemingly systematic offset between EIT guided PEEP and P_{es} guided PEEP. This knowledge, together with the understanding that P_{es} only allows assessment of transpulmonary pressure at the esophageal level, does suggest that both strategies may be used independently if only the ventilation targets are slightly modified: if homogeneous ventilation distribution is the goal, this would require to titrate $P_{tp,EE}$ several cmH_2O positive. Conversely, if limiting overdistention is the primary goal while allowing considerable collapse, this would require titrating PEEP several cmH_2O below the point of equal collapse and overdistention. Obviously, with regard to clinical outcome, these findings are only hypothesis generating, deserving investigation in future studies.

7.4.1 Limitations

This study has several limitations. First, the study protocol did not prespecify the current analysis. EIT and P_{es} recordings were not obtained with the primary aim to compare both techniques. This may have impacted the accuracy of the measurements.

Second, relating to the retrospective nature of the study, not all patients reached the target of $-2 \leq P_{tp,EE} \leq 2$ cmH_2O. If the target would have been protocolized, probably more effort was spent by the clinician to reach the target. Requiring to leave out this subgroup of patients from the EIT and P_{es} comparison may have impacted results. The finding that patients not reaching $-2 \leq P_{tp,EE} \leq 2$ cmH_2O had higher $P_{tp,EE}$ at optimal EIT PEEP, underscores this possibility.

Third, patients were ventilated in pressure controlled mode, requiring expiratory holds to assess zero-flow respiratory mechanics. These holds were only assessed at the highest and lowest PEEP level. Intrinsic end-expiratory pressures had to be estimated for the intermediate steps through interpolation. A linear relationship between PEEP level and auto-PEEP was assumed. However, airway resistance may be related exponentially with set PEEP, as one study suggests [27]. A future study should apply holds at every PEEP step or use volume controlled ventilation.

Fourth, the highest and lowest PEEP level varied between patients. This potentially impacts

the assessment of collapse and overdistention, as these are calculated relative to the highest and lowest PEEP step, respectively. However, appendix B highlights that collapse values differed minimally when applying a $PEEP_{high}$ cut-off of 24 cmH_2O. The choice of not applying this cut-off in the current analysis is based on the aim of making the results match clinical practice.

Fifth, information on airway pressure was not included in the estimation of collapse and overdistention with EIT. Instead, driving pressure was assumed to be constant throughout the PEEP trial. This resembles clinical practice, as EIT devices are often not connected to an airway pressure sensor. However, considering that airway pressure does not remain constant at varying PEEP levels, the static driving pressure may have been overestimated, impacting the calculation of collapse and overdistention.

Sixth, EIT was used to assess ventilation distribution at $P_{tp,EE}$ guided PEEP levels. While changes in ventilation correlate well with changes in impedance [28], sound evidence of the validity of collapse and overdistention assessed through the Costa method is lacking.

Finally, the present study only included COVID-19 patients, questioning the generalizability of the current results. Although respiratory mechanics of COVID-19 ARDS resemble non-COVID-19 ARDS [29], a more diverse distribution of ARDS origin could have enabled unraveling why differences in EIT and P_{es} guided PEEP levels vary between patients.

7.4.2 Conclusion

Concluding, PEEP titration guided by EIT and P_{es} yield different levels of PEEP. EIT guided PEEP results in higher PEEP levels compared to P_{es} guided PEEP. Optimal P_{es} PEEP yields more collapse and less overdistention compared to optimal EIT PEEP. Zero end-expiratory transpulmonary is not sufficient to reach the more homogeneous ventilation distribution observed at optimal EIT PEEP.

References

1. Gattinoni L, Caironi P, Cressoni M, et al. Lung recruitment in patients with the acute respiratory distress syndrome. N Engl J Med 2006;354:1775–86.
2. Brower RG, Lanken PN, MacIntyre N, et al. Higher versus lower positive end-expiratory pressures in patients with the acute respiratory distress syndrome. N Engl J Med 2004;351:327–36.
3. Goligher EC, Kavanagh BP, Rubenfeld GD, et al. Oxygenation response to positive end-expiratory pressure predicts mortality in acute respiratory distress syndrome. A secondary analysis of the LOVS and ExPress trials. Am J Respir Crit Care Med 2014;190:70–6.
4. Guo L, Xie J, Huang Y, et al. Higher PEEP improves outcomes in ARDS patients with clinically objective positive oxygenation response to PEEP: a systematic review and meta-analysis. BMC Anesthesiol 2018;18:172.
5. Walkey AJ, Del Sorbo L, Hodgson CL, et al. Higher PEEP versus Lower PEEP Strategies for Patients with Acute Respiratory Distress Syndrome. A Systematic Review and Meta-Analysis. Ann Am Thorac Soc 2017;14:S297–S303.
6. Frerichs I, Amato MB, Kaam AH van, et al. Chest electrical impedance tomography examination, data analysis, terminology, clinical use and recommendations: consensus statement of the TRanslational EIT developmeNt stuDy group. Thorax 2017;72:83–93.
7. Bachmann MC, Morais C, Bugedo G, et al. Electrical impedance tomography in acute respiratory distress syndrome. Crit Care 2018;22:263.
8. Zhao Z, Chang MY, Chang MY, et al. Positive end-expiratory pressure titration with electrical impedance tomography and pressure-volume curve in severe acute respiratory distress syndrome. Ann Intensive Care 2019;9:7.

9. Akoumianaki E, Maggiore SM, Valenza F, et al. The application of esophageal pressure measurement in patients with respiratory failure. Am J Respir Crit Care Med 2014;189:520–31.

10. Gattinoni L, Vagginelli F, Chiumello D, Taccone P, and Carlesso E. Physiologic rationale for ventilator setting in acute lung injury/acute respiratory distress syndrome patients. Crit Care Med 2003;31:S300–4.

11. Sarge T, Baedorf-Kassis E, Banner-Goodspeed V, et al. Effect of Esophageal Pressure-guided Positive End-Expiratory Pressure on Survival from Acute Respiratory Distress Syndrome: A Risk-based and Mechanistic Reanalysis of the EPVent-2 Trial. Am J Respir Crit Care Med 2021;204:1153–63.

12. Zee P van der, Somhorst P, Endeman H, and Gommers D. Electrical Impedance Tomography for Positive End-Expiratory Pressure Titration in COVID-19-related Acute Respiratory Distress Syndrome. Case. 2020.

13. Somhorst P, Zee P van der, Endeman H, and Gommers D. PEEP-FiO2 table versus EIT to titrate PEEP in mechanically ventilated patients with COVID-19-related ARDS. Crit Care 2022;26:272.

14. Force ADT, Ranieri VM, Rubenfeld GD, et al. Acute respiratory distress syndrome: the Berlin Definition. JAMA 2012;307:2526–33.

15. Costa EL, Borges JB, Melo A, et al. Bedside estimation of recruitable alveolar collapse and hyperdistension by electrical impedance tomography. Intensive Care Med 2009;35:1132–7.

16. Mauri T, Yoshida T, Bellani G, et al. Esophageal and transpulmonary pressure in the clinical setting: meaning, usefulness and perspectives. Intensive Care Med 2016;42:1360–73.

17. Mughal MM, Culver DA, Minai OA, and Arroliga AC. Auto-positive end-expiratory pressure: mechanisms and treatment. Cleve Clin J Med 2005;72:801–9.

18. Natalini G, Tuzzo D, Rosano A, et al. Assessment of Factors Related to Auto-PEEP. Respir Care 2016;61:134–41.

19. Bellani G, Guerra L, Musch G, et al. Lung regional metabolic activity and gas volume changes induced by tidal ventilation in patients with acute lung injury. Am J Respir Crit Care Med 2011;183:1193–9.

20. Writing Group for the Alveolar Recruitment for Acute Respiratory Distress Syndrome Trial I, Cavalcanti AB, Suzumura EA, et al. Effect of Lung Recruitment and Titrated Positive End-Expiratory Pressure (PEEP) vs Low PEEP on Mortality in Patients With Acute Respiratory Distress Syndrome: A Randomized Clinical Trial. JAMA 2017;318:1335–45.

21. Gattinoni L, Quintel M, and Marini JJ. Volutrauma and atelectrauma: which is worse? Crit Care 2018;22:264.

22. Mojoli F, Iotti GA, Torriglia F, et al. In vivo calibration of esophageal pressure in the mechanically ventilated patient makes measurements reliable. Crit Care 2016;20:98.

23. Yoshida T, Amato MBP, Grieco DL, et al. Esophageal Manometry and Regional Transpulmonary Pressure in Lung Injury. Am J Respir Crit Care Med 2018;197:1018–26.

24. Cressoni M, Chiurazzi C, Gotti M, et al. Lung inhomogeneities and time course of ventilator-induced mechanical injuries. Anesthesiology 2015;123:618–27.

25. Scaramuzzo G, Spadaro S, Dalla Corte F, et al. Personalized Positive End-Expiratory Pressure in Acute Respiratory Distress Syndrome: Comparison Between Optimal Distribution of Regional Ventilation and Positive Transpulmonary Pressure. Crit Care Med 2020;48:1148–56.

26. Dargaville PA, Rimensberger PC, and Frerichs I. Regional tidal ventilation and compliance during a stepwise vital capacity manoeuvre. Intensive Care Med 2010;36:1953–61.

27. Fumagalli J, Santiago RRS, Teggia Droghi M, et al. Lung Recruitment in Obese Patients with Acute Respiratory Distress Syndrome. Anesthesiology 2019;130:791–803.

28. Victorino JA, Borges JB, Okamoto VN, et al. Imbalances in regional lung ventilation: a validation study on electrical impedance tomography. Am J Respir Crit Care Med 2004;169:791–800.

29. Haudebourg AF, Perier F, Tuffet S, et al. Respiratory Mechanics of COVID-19- versus Non-COVID-19-associated Acute Respiratory Distress Syndrome. Am J Respir Crit Care Med 2020;202:287–90.

Chapter 8

Mechanical ventilation guided by ventilation and circulation: a research proposal

Together with my medical supervisor Dr. H. Endeman, I have conceptualized a study on PEEP titration based on micro-circulatory and macro-circulatory indices. We have submitted different versions of the proposals to the European Society of Intensive Care Medicine (ESICM), the Society of Critical Care Medicine (SCCM) and the Erasmus MC innovation grant. This chapter includes the research proposal submitted to the SCCM.

Mechanical Ventilation Guided by Ventilation and Circulation

Research Proposal

***Arthur van Nieuw Amerongen, BSc**, Technical University Delft, The Netherlands*
***Dr. Henrik Endeman, MD, PhD**, Erasmus Medical Center, Rotterdam, The Netherlands*
***Prof. Jan Bakker, MD, PhD, FCCM**, New York University NYU Langone Medical Center and Columbia University Medical Center, New York, USA*

Study purpose and aims

The aim of the project is to develop and validate a novel method finding the optimal PEEP in ARDS patients by optimizing both ventilation and lung microcirculatory perfusion (LMP).

The LMP can be estimated using volumetric capnography which measures alveolar partial pressure of CO_2 and the mixed expired partial pressure of CO_2 enabling the determination of true Bohr dead space. However, several aspects require additional studies.

First, the effect of PEEP on the interaction between micro- and macro-circulation. A change in dead space due to increased PEEP could result from capillary compression or decreased cardiac output. We aim to study this by combining volumetric capnography with invasive hemodynamic monitoring.

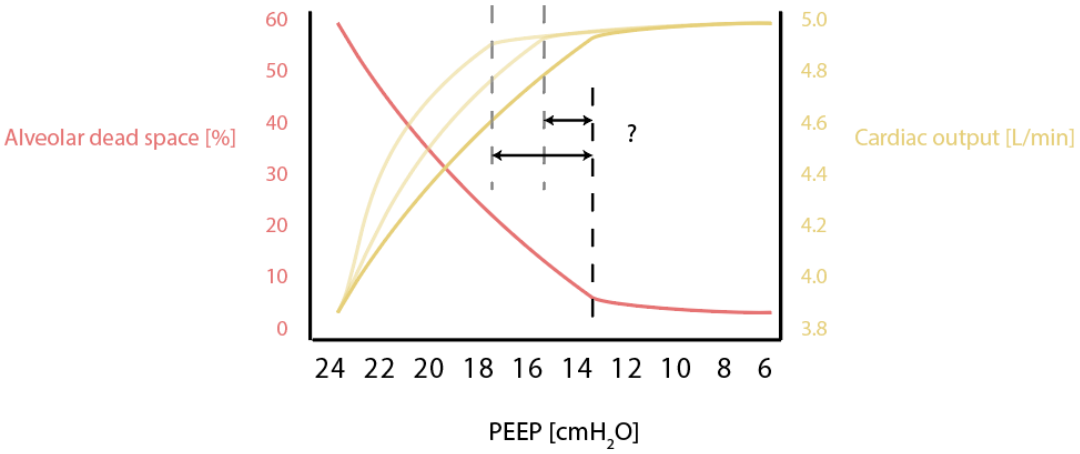

Figure 1 *Possible relationships between alveolar dead space and cardiac output during a decremental PEEP trial. Alveolar dead space can be caused by capillary compression and by reduced cardiac output. If alveolar dead space is increased but cardiac output remains stable, the alveolar dead space can likely be attributed to capillary compression.*

Second, the relationship between lung mechanics and alveolar dead space has not been fully explored. In PEEP trials, lung overdistention is often determined only by measuring compliance. We aim to study the relationship between capillary compression and mechanical overdistention by combining volumetric capnography with electrical impedance tomography measurements.

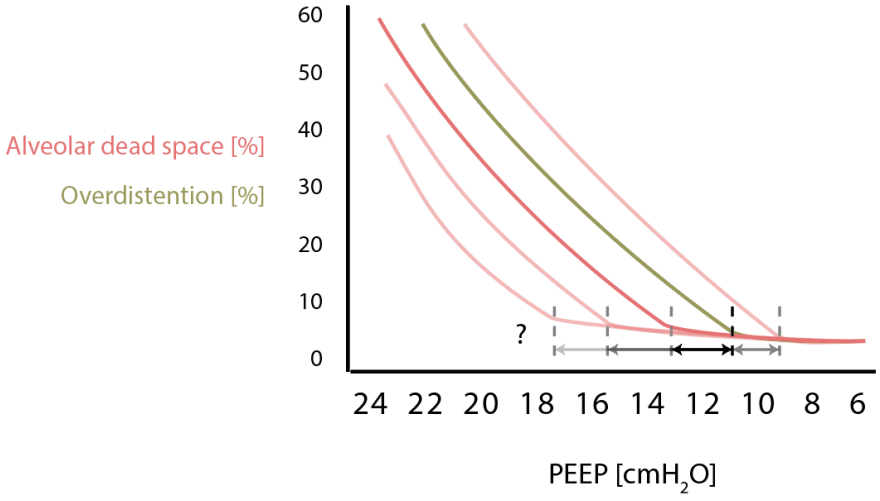

Figure 2 *Possible relationships between alveolar dead space and mechanical overdistention during a decremental PEEP trial. It is unknown whether these phenomena occur simultaneously or with a delay.*

From these results we will develop a novel method that optimizes PEEP for both its effect on ventilation and circulation. Ventilation will be optimized using electrical impedance tomography; the Costa method [1] finds the PEEP level with the lowest sum of relative overdistention and collapse (figure 3A). Circulation will be optimized by the addition of alveolar dead space as a measure of LMP (figure 3B). The model is aiming to find optimal PEEP defined as the lowest sum of relative overdistention, relative collapse and alveolar dead space fraction.

This novel method will then be validated in ARDS patients by comparing the differences in the initially set PEEP to the optimal-model PEEP and the effect on oxygenation status.

Summary

Primary objective: Define individual best PEEP that optimizes both ventilation and circulation in ARDS patients using a novel approach based on volumetric capnography

> **Sub-goal 1:** Assess the relationship between alveolar dead space and macro-circulatory hemodynamics
>
> **Sub-goal 2:** Assess the relationship between alveolar dead space and global and regional lung compliance

Secondary objective: Validate the novel method by comparing the differences in the initially set PEEP to the optimal-model PEEP and the effect on oxygenation status.

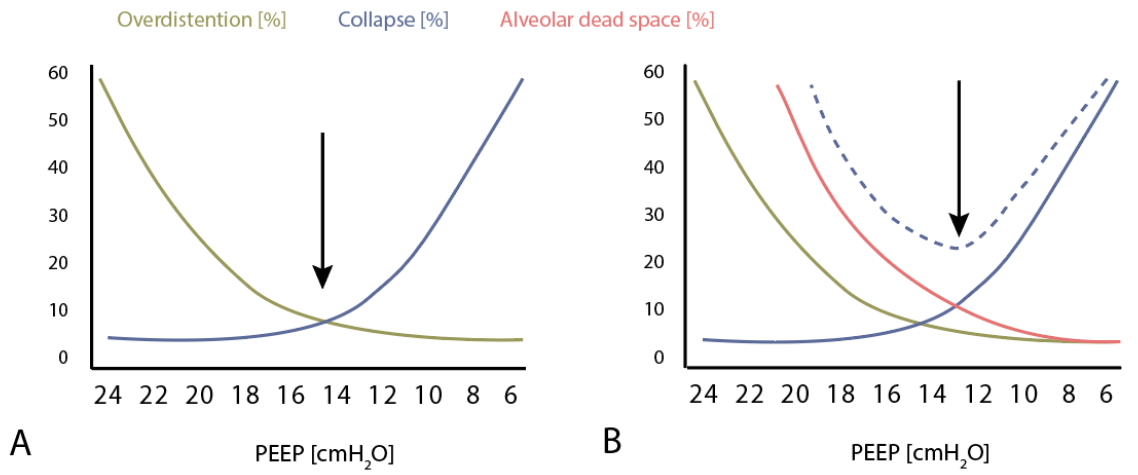

Figure 3 A) *Optimal PEEP based on the Costa method, which minimizes the sum of relative overdistention and collapse.* ***B)*** *Hypothetical course of alveolar dead space fraction along decremental PEEP steps, added to relative overdistention and collapse. The dashed line represents the sum of overdistention, collapse and alveolar dead space. The arrows suggest optimal PEEP.*

Background and Significance

Physiological dead space is an important predictor for mortality in acute respiratory distress syndrome (ARDS) [2]. Intrathoracic pressures induced by mechanical ventilation may increase dead space even more by reducing alveolar capillary perfusion through the compression of pulmonary capillaries and a reduction in cardiac output [3, 4]. However, ventilators are clinically set to limit mechanical lung injury [5], rather than optimizing the pulmonary microcirculation.

Dead space is commonly estimated using the arterial partial pressure of CO2 (Enghoff modification) which is valid only in the case of ideal gas exchange assuming that arterial CO2 and alveolar CO2 are equilibrated [6]. In mechanically ventilated patients with ARDS, this assumption is not valid. Hence, intrapulmonary shunt and diffusion impairments are brought into the Enghoff equation, leading to an overestimation of true dead space [7].

Volumetric capnography enables the estimation of alveolar partial pressure of CO2, permitting the calculation of true Bohr dead space [8]. Accordingly, the Bohr method allows us to discriminate between the effects of PEEP on dead space and pulmonary shunt. Moreover, volumetric capnography enables continuous bedside monitoring of dead space. Thus, it could be used to guide PEEP titration to optimize alveolar perfusion and thus gas exchange. Its value in finding optimal PEEP has been shown in an experimental model of lung injury [9, 10] and in healthy lungs [11-13], but not yet critically ill ARDS patients. At this moment, no bedside tool is available to guide mechanical ventilation settings based on pulmonary microcirculation.

To implement this technique clinically, a better understanding of the interplay of micro- and macro-circulatory changes due to PEEP is required. Also, a better understanding of the relationship between mechanical overdistention (reduced compliance) and ‘functional’ overdistention (capillary compression) is required. In this project we will determine how these changes interact, opening the door to clinical implementation.

Preliminary Data

We have created a measurement setup with a proximal flow sensor and a mainstream CO_2 sensor. Figure 4 shows a volumetric capnogram of a mechanically ventilated patient admitted to our intensive care unit. Alveolar partial pressure of CO2 ($PACO_2$) and mixed expired partial pressure of CO_2 ($PeCO_2$) are determined according to the method described by Tusman et al. [14]. Physiological dead space fraction was 0.37 and alveolar dead space volume was 4 mL. This demonstrates our ability to measure and analyze a volumetric capnogram.

We haven't measured CO_2 during a decremental PEEP trial yet, requiring IRB approval. The Discovery grant will facilitate the study after IRB approval.

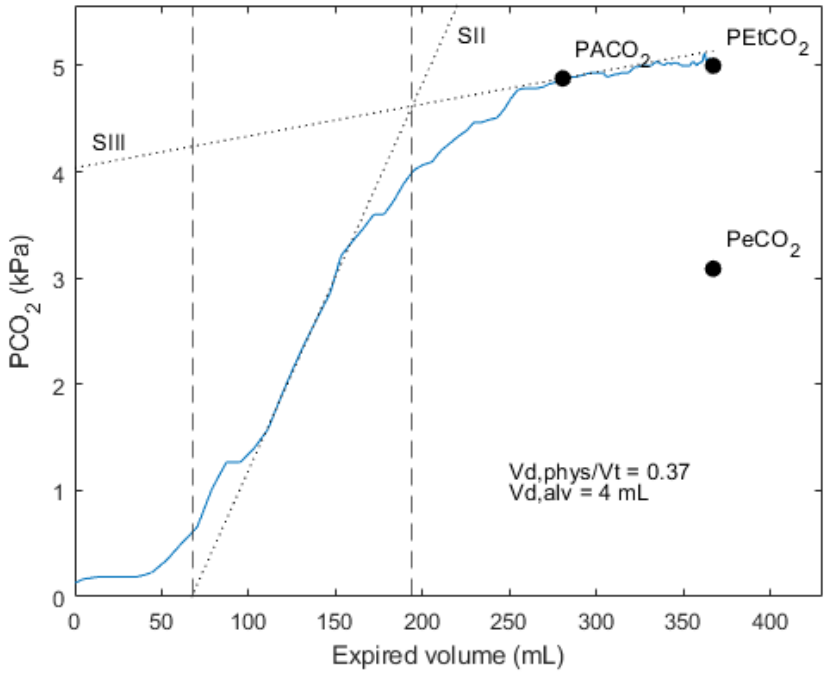

Figure 4 *Volumetric capnogram from a mechanically ventilated patient. Alveolar partial pressure of CO_2 ($PACO_2$) is determined by the midpoint between the intersection of SII and SII, and end-tidal CO_2. Mixed expired partial pressure of CO_2 ($PeCO_2$) is determined by the integral of the volumetric capnogram divided by the expired volume.*

Research Design

Design

This will be a multi-center prospective observational study recruiting 60 newly diagnosed moderate and severe ARDS patients following adequate consenting.

A decremental PEEP trial according to local clinical protocol will be executed: PEEP is gradually increased to a high level, with a minimum of 24 cmH_2O or up to 10 cmH_2O above the baseline clinically set PEEP, whichever is higher. Increases in PEEP will be made in steps of 3-4 cmH_2O to test the patient's tolerance. Starting at the highest level, every 5

minutes PEEP is lowered by 2 cmH_2O until -6 cmH_2O is reached. Driving pressure is kept constant. At the end of each step, an inspiratory and expiratory hold is performed. After the trial, PEEP is returned to the baseline level.

During PEEP titration, continuous recording of volumetric capnography, hemodynamics and ventilation distribution will be performed. Simultaneous measurement of CO_2 and flow at the airway opening will be performed with a Respironics NICO2 monitor. $PACO_2$, $PeCO_2$ and $PetCO_2$ will be derived from the capnogram with offline signal processing. PiCCO measurements will be executed at 24, 20, 16, 12 and 6 cmH_2O PEEP. Ventilation distribution will be monitored using a Dräger Pulmovista 500. This allows for quantification of lung overdistention and collapse.

Sample size

Given the lack of prior data in this area a meaningful power calculation can't be made. From this pilot study we expect to assess the possible clinical relevance of the method and to design follow-up studies with adequate power calculation.

For this study, we aim to recruit 60. The first 40 patients will be included for the explorative phase. The last 20 patients will be included for the validation phase.

Inclusion/Exclusion Criteria

Intubated mechanically ventilated patients will be considered for enrolment in the first 48 hours of ARDS diagnosis.

Inclusion criteria:

- Age ≥ 18 years
- Intubated moderate and severe ARDS according to the Berlin definition (PaO_2/FiO_2 ratio ≤ 200 mmHg)
- Receiving invasive hemodynamic monitoring (PiCCO)
- Under continuous sedation with or without paralysis
- Informed consent granted by legally representative

Exclusion criteria:

- Contraindication to EIT monitoring (e.g. burns, pacemaker, thoracic wounds limiting electrode placement)
- Hemodynamic instability (Systolic BP < 75 mmHg or MAP < 60 mmHg despite vasopressors and/or heart rate < 55 bpm)
- Attending physician deems the transient application of high airway pressures to be unsafe. If oxygen saturation drops below 88% or if MAP drops below 55 mmHg, the PEEP trial will be stopped.
- Severe COPD, lobectomy or other conditions which impact volumetric capnography considerably

Methods to Achieve Aims

We will collect the following outcome measures.

Development phase
During each PEEP step:

- **Alveolar dead space (Vd_{alv})** as assessed with volumetric capnography at 60 seconds and at 5 minutes after PEEP change
  What are the Vd_{alv} levels in our patient group?

Do the measurements remain stable after the first 60 seconds after PEEP change?

- **Global compliance** – $\Delta V/(P_{plat}-P_{PEEP,total})$
  How does global compliance relate to Vd_{alv}?
- **Regional compliance** as assessed with EIT
  How does anterior and posterior compliance relate to Vd_{alv}?
  With higher PEEP levels, how do the onset times of increasing overdistension and increasing Vd_{alv} relate to each other?
  How does the lowest relative percentage of collapse and overdistension relate to Vd_{alv}?

At 24, 20, 16, 12, 6 cmH_2O PEEP:

- **Cardiac output**, **extravascular lung water (EVLW)** and **global end-diastolic volume (GEDV)** as assessed with PiCCO
  How are capillary compression and impaired macro-circulation related as potential causes for reduced lung perfusion?
  - *How does cardiac output relate to Vd_{alv}?*
  - *How does hydrostatic pressure (EVLW) relate to Vd_{alv}?*
  - *How does cardiac preload relate to Vd_{alv}?*

Validation phase
At baseline and 2 hours and 24 hours after setting PEEP according to the novel method:

- **PaO_2** and **FiO_2**
  Does PaO_2/FiO_2 ratio improve? To what extent does PaO_2/FiO_2 ratio improve?

Descriptive statistical analysis will demonstrate distributions of measured alveolar dead space, lung mechanics and hemodynamics at different PEEP levels. Repeated-measure ANOVA followed by least significant difference for multiple comparisons will be applied to test which pairs of measurement means along the PEEP steps are significant ($p<0.05$). Linear regression analysis will be done to assess the relationships between alveolar dead space and hemodynamics, and between alveolar dead space and lung mechanics. Paired student's t-test will be done to test for differences in oxygenation status before and after the PEEP titration.

Evaluation Plan

After the inclusion of the first 10 patients, we will evaluate the data quality of the volumetric capnography measurements, the invasive hemodynamic measurements and the electrical impedance tomography measurements. We will also evaluate whether results are comparable between the participating centers and we will evaluate protocol compliance.
After the inclusion of the first 20 patients, we will evaluate the volumetric capnography measurement stability. We will compare whether metrics differ between the first 60 seconds and the first 5 minutes after PEEP change. If the alveolar dead space fraction differs more than 0.002 on average, we will consider this as clinically unstable and we will prolong the time per PEEP step.
At the end of the study, the potential impact of the newly developed method to titrate PEEP on clinical decision making will be evaluated. The method will be retrospectively applied to determine the PEEP that optimizes both ventilation and circulation. The resulting PEEP value will be compared to the PEEP initially set by the clinician and to the PEEP that minimizes the sum of overdistention and collapse.
Finally, an interventional follow-up study will be designed that evaluates the impact of the newly developed method on oxygenation status and ventilator-free days.

Status of IRB

We have not yet requested approval of the institutional review board for the study. The Discovery grant will enable us to request approval and set up the study.

Bibliography

[1] Costa EL, Borges JB, Melo A, Suarez-Sipmann F, Toufen C, Bohm SH, et al. Bedside estimation of recruitable alveolar collapse and hyperdistension by electrical impedance tomography. Intensive Care Med. 2009 Jun;35(6):1132-7.
[2] Nuckton TJ, Alonso JA, Kallet RH, Daniel BM, Pittet JF, Eisner MD, et al. Pulmonary dead-space fraction as a risk factor for death in the acute respiratory distress syndrome. N Engl J Med. 2002;346(17):1281-6.
[3] Suter PM, Fairley B, Isenberg MD. Optimum end-expiratory airway pressure in patients with acute pulmonary failure. N Engl J Med. 1975;292(6):284-9.
[4] Nieman GF, Paskanik AM, Bredenberg CE. Effect of positive end-expiratory pressure on alveolar capillary perfusion. J Thorac Cardiovasc Surg. 1988;95(4):712-6.
[5] Slutsky AS, Ranieri VM. Ventilator-induced lung injury. N Engl J Med. 2013;369(22):2126-36.
[6] Riley RL, Cournand A. Ideal alveolar air and the analysis of ventilation-perfusion relationships in the lungs. J Appl Physiol. 1949;1(12):825-47.
[7] Doorduin J, Nollet JL, Vugts MP, Roesthuis LH, Akankan F, van der Hoeven JG, et al. Assessment of dead-space ventilation in patients with acute respiratory distress syndrome: a prospective observational study. Crit Care. 2016;20(1):121.
[8] Tusman G, Suarez-Sipmann F, Bohm SH, Borges JB, Hedenstierna G. Capnography reflects ventilation/perfusion distribution in a model of acute lung injury. Acta Anaesthesiol Scand. 2011;55(5):597-606.
[9] Tusman G, Suarez-Sipmann F, Bohm SH, Pech T, Reissmann H, Meschino G, et al. Monitoring dead space during recruitment and PEEP titration in an experimental model. Intensive Care Med. 2006;32(11):1863-71.
[10] Tusman G, Gogniat E, Madorno M, Otero P, Dianti J, Ceballos IF, et al. Effect of PEEP on Dead Space in an Experimental Model of ARDS. Respir Care. 2020;65(1):11-20.
[11] Tusman G, Groisman I, Fiolo FE, Scandurra A, Arca JM, Krumrick G, et al. Noninvasive monitoring of lung recruitment maneuvers in morbidly obese patients: the role of pulse oximetry and volumetric capnography. Anesth Analg. 2014;118(1):137-44.
[12] Blankman P, Shono A, Hermans BJ, Wesselius T, Hasan D, Gommers D. Detection of optimal PEEP for equal distribution of tidal volume by volumetric capnography and electrical impedance tomography during decreasing levels of PEEP in post cardiac-surgery patients. Br J Anaesth. 2016;116(6):862-9.
[13] Tusman G, Wallin M, Acosta C, Santanera B, Portela F, Viotti F, et al. Positive end-expiratory pressure individualization guided by continuous end-expiratory lung volume monitoring during laparoscopic surgery. J Clin Monit Comput. 2021.
[14] Tusman G, Scandurra A, Böhm SH, Suarez-Sipmann F, Clara F. Model fitting of volumetric capnograms improves calculations of airway dead space and slope of phase III. J Clin Monit Comput. 2009 Aug;23(4):197-206.

Chapter 9

Conclusions

This thesis provided solutions for the filtering of undesired information from EIT and P_{es} recordings and elaborated on the differences of EIT and P_{es} with respect to the titration of PEEP.

In **chapter 2** and **3**, I described the technology behind EIT and P_{es} monitoring, as well as how these technologies can be used for PEEP titration. The most widely used EIT method for titrating PEEP aims at finding equal alveolar collapse and overdistention. P_{es} monitoring is most often used to ensure a positive end-expiratory transpulmonary pressure. Evidence on clinical outcome is limited for both methods.

In **chapter 4**, I proposed an algorithm for the suppression of circulatory information in EIT recordings. Empirical Mode Decomposition enables the separation of impedance traces into respiratory and circulatory activity, but requires masking of the signals to reach satisfactory results. The technology also proved to work for P_{es} recordings, albeit with several adjustments (**chapter 5**)

In **chapter 7**, I compared PEEP titration guided by EIT and P_{es} monitoring. EIT guided PEEP is higher than P_{es} guided PEEP and yielded less alveolar collapse and more alveolar overdistention. Zero end-expiratory transpulmonary pressure is associated with significant collapse dorsal to the esophageal level. Both technologies provide useful information for PEEP titration, but understanding the origin of the suggested PEEP level is important for their clinical use.

Appendices

Appendix A

Example of filtering P_{aw} and P_{tp}

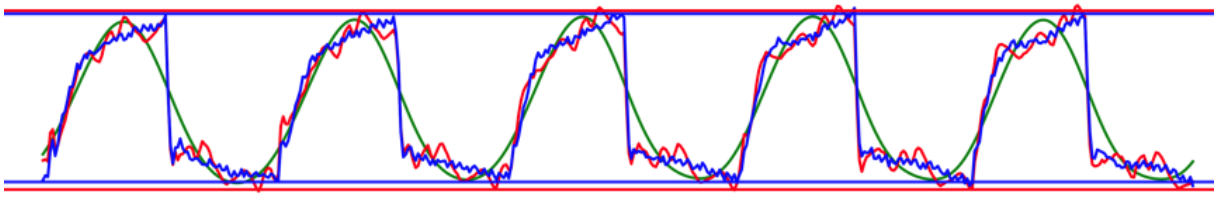

Figure A.1: Example of the effects of filtering P_{aw} and P_{tp}. The red trace shows the raw transpulmonary pressure, obtained by subtracting raw P_{es} from raw P_{aw}. The green trace reflects the filtered transpulmonary pressure by applying empirical mode decomposition to the raw transpulmonary pressure. A significant loss of detail can be observed. The blue trace reflects filtered transpulmonary pressure, obtained by only filtering P_{es} and subtracting it from raw P_{aw}. Cardiac oscillations have disappeared, while important ventilatory details are preserved. The horizontal lines reflect de obtained inspiratory and expiratory pressures. Especially the end-expiratory pressure is higher for the filtered trace compared to the unfiltered trace.

Appendix B

Evaluation of the effect of removing high PEEP levels on the calculation of optimal PEEP and collapse

Optimal EIT PEEP and relative alveolar collapse was assessed with and without removing all PEEP-steps above 24 cmH_2O. Table B.1 shows that the mean absolute difference between was 0.2 cmH_2O between PEEP levels was and 0.2% between collapse values. This can be considered not clinically relevant.

Patient	Best PEEP with cut-off	Best PEEP without cut-off	Absolute difference	CL without cut-off	CL with cut-off	Absolute difference
C014	18 cmH_2O	18 cmH_2O	0 cmH_2O	9.0%	8.0%	1.0%
C016	14 cmH_2O	14 cmH_2O	0 cmH_2O	5.6%	5.6%	0.0%
C017	14 cmH_2O	14 cmH_2O	0 cmH_2O	11.4%	10.9%	0.5%
C020	10 cmH_2O	10 cmH_2O	0 cmH_2O	5.9%	5.9%	0.0%
C024	12 cmH_2O	12 cmH_2O	0 cmH_2O	4.5%	4.5%	0.0%
C025	16 cmH_2O	16 cmH_2O	0 cmH_2O	9.9%	9.1%	0.9%
C027	12 cmH_2O	12 cmH_2O	0 cmH_2O	7.1%	7.1%	0.0%
C028	12 cmH_2O	12 cmH_2O	0 cmH_2O	10.1%	10.1%	0.0%
C031	14 cmH_2O	14 cmH_2O	0 cmH_2O	7.7%	7.7%	0.0%
C033	12 cmH_2O	12 cmH_2O	0 cmH_2O	4.6%	4.6%	0.0%
C034	14 cmH_2O	14 cmH_2O	0 cmH_2O	10.6%	10.6%	0.0%
C035	18 cmH_2O	18 cmH_2O	0 cmH_2O	10.0%	9.6%	0.4%
C038	16 cmH_2O	16 cmH_2O	0 cmH_2O	6.7%	6.7%	0.0%
C044	18 cmH_2O	18 cmH_2O	0 cmH_2O	9.0%	8.7%	0.3%
C045	12 cmH_2O	12 cmH_2O	0 cmH_2O	4.3%	4.3%	0.0%
C055	18 cmH_2O	16 cmH_2O	2 cmH_2O	9.1%	8.1%	1.0%
C057	20 cmH_2O	20 cmH_2O	0 cmH_2O	3.9%	3.4%	0.4%
C061	18 cmH_2O	18 cmH_2O	0 cmH_2O	7.1%	7.0%	0.0%
C066	14 cmH_2O	14 cmH_2O	0 cmH_2O	10.2%	10.2%	0.0%
C069	20 cmH_2O	18 cmH_2O	2 cmH_2O	12.1%	12.9%	0.8%
C071	8 cmH_2O	8 cmH_2O	0 cmH_2O	3.7%	3.7%	0.0%
C074	14 cmH_2O	14 cmH_2O	0 cmH_2O	5.2%	5.2%	0.0%
C077	10 cmH_2O	10 cmH_2O	0 cmH_2O	7.2%	6.9%	0.2%
C084	16 cmH_2O	16 cmH_2O	0 cmH_2O	9.1%	8.9%	0.2%
C086	20 cmH_2O	20 cmH_2O	0 cmH_2O	1.9%	1.9%	0.0%
C087	14 cmH_2O	14 cmH_2O	0 cmH_2O	4.3%	4.3%	0.0%
MAE			**0.2 cmH_2O**			**0.2%**

Table B.1: Abbreviations: *CL*: collapse; *MAE*: mean absolute error. *PEEP*: positive end-expiratory pressure